AL/EQ-TR-1994-0050

A R M S T R O N G   L A B O R A T O R Y

TRANSPORT EXPERIMENTS IN INTERMEDIATE-SCALE COLUMNS

E.P. Springer, M.H. Ebinger, B.D. Newman

Los Alamos National Laboratory
Environmental Science Group
Mail Stop J495
Los Alamos NM 87545

ENVIRONICS DIRECTORATE
139 Barnes Drive, Suite 2
Tyndall AFB FL 32403-5323

December 1994

Final Technical Report for Period February 1989 - February 1993

AIR FORCE MATERIEL COMMAND
TYNDALL AIR FORCE BASE, FLORIDA 32403-5323

DISCLAIMER NOTICE
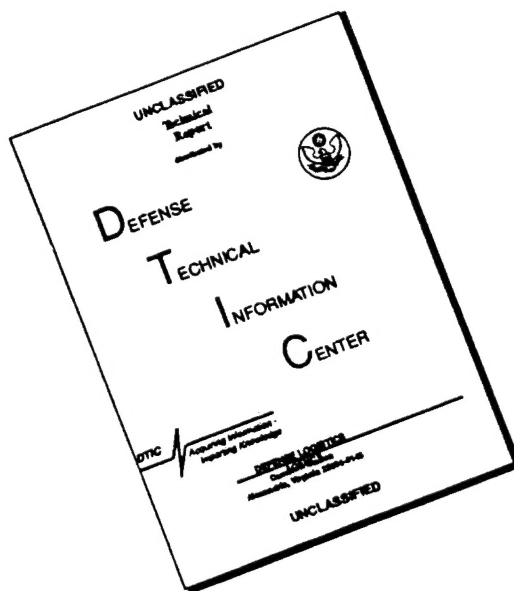
THIS DOCUMENT IS BEST QUALITY AVAILABLE. THE COPY FURNISHED TO DTIC CONTAINED A SIGNIFICANT NUMBER OF PAGES WHICH DO NOT REPRODUCE LEGIBLY.

NOTICES

This report was prepared as an account of work sponsored by an agency of the United States Government. Neither the United States Government nor any agency thereof, nor any employees, nor any of their contractors, subcontractors, or their employees, make any warranty, expressed or implied, completeness, or usefulness of any privately owned rights. Reference herein to any specific commercial product, process, or service by trade name, trademark, manufacturer, or otherwise, does not necessarily constitute or imply its endorsement, recommendation, or favoring by the United States Government or any agency , contractor, or subcontractor thereof. The views and opinions of the authors expressed herein do not necessarily state or reflect those of the United States Government or any agency , contractor, or subcontractor thereof.
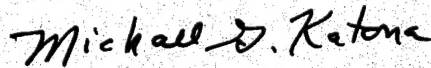
When Government drawings, specifications, or other data are used for any purpose other than in connection with a definitely Government-related procurement, the United States Government incurs no responsibility or any obligation whatsoever. The fact that the Government may have formulated or in any way supplied the said drawings, specifications, or other data is not to be regarded by implication, or otherwise in any manner construed, as licensing the holder or nay other person or corporation; or as conveying any rights or permission to manufacture, use, or sell any patented invention that may in any way be related thereto.

This technical report has been reviewed by the Public Affairs Office (PA) and is releasable to the National Technical Information Service (NTIS) where it will be available to the general public, including foreign nationals.

This report has been reviewed and is approved for publication.

BRENT C. ROBERTS, 1Lt, USAF
Project Manager

MICHAEL G. KATONA, PhD
Chief Scientist, Environics Directorate

MARK H. SMITH, Major, USAF, BSC
Chief, Site Remediation Division

NEIL J. LAMB, Colonel, USAF, BSC
Director, Environics Directorate

REPORT DOCUMENTATION PAGE

1. AGENCY USE ONLY (Leave blank)	2. REPORT DATE December 1994	3. REPORT TYPE AND DATES COVERED Final Report - Feb 89 - Feb 93

4. TITLE AND SUBTITLE
Transport Experiments in
Intermediate-Scale Columns

5. FUNDING NUMBERS
LA-UR-94-2514

6. AUTHOR(S)

E.P. Springer, M.H. Ebinger, B. D. Newman

7. PERFORMING ORGANIZATION NAME(S) AND ADDRESS(ES)

Los Alamos National Laboratory
Environmental Science Group
Mail Stop J495
Los Alamos, NM 87545

8. PERFORMING ORGANIZATION REPORT NUMBER

9. SPONSORING / MONITORING AGENCY NAME(S) AND ADDRESS(ES)

AL/EQW-OL
139 Barnes Drive, Suite 2
Tyndall AFB, Florida 32403-5323

10. SPONSORING / MONITORING AGENCY REPORT NUMBER

AL/EQ-TR-1994-0050

11. SUPPLEMENTARY NOTES

Lt. Brent C. Roberts, Project Manager
(904) 283-6290; FAX # (904) 283-6286

12a. DISTRIBUTION / AVAILABILITY STATEMENT

Approved for public release. Distribution Unlimited.

12b. DISTRIBUTION CODE

13. ABSTRACT *(Maximum 200 words)*

The objective of the research presented in this report was to analyze subsurface contaminant transport by water at different experimental scales to provide information for moving from the laboratory experiments to field applications. The scale-dependent behavior of subsurface hydrologic and transport processes has been recognized as one of the key issues in assessing contaminant behavior for either compliance or remedial actions. Scale-dependent behavior means that the magnitude of parameters implications of scale dependency are apparent when using parameter values from laboratory columns to describe transport in a field setting, contaminant arrival times in aquifers were underestimated. The obvious solution is to conduct field experiments to obtain critical transport parameters, but field experiments are expensive, time intensive and have possible environmental ramifications (permitting requirements) compared to laboratory efforts.

14. SUBJECT TERMS

Transport, scale-dependent, columns

15. NUMBER OF PAGES

16. PRICE CODE

17. SECURITY CLASSIFICATION OF REPORT UNCLASSIFIED	18. SECURITY CLASSIFICATION OF THIS PAGE UNCLASSIFIED	19. SECURITY CLASSIFICATION OF ABSTRACT UNCLASSIFIED	20. LIMITATION OF ABSTRACT UL

PREFACE

This report was prepared by the Environmental Science Group, MS J495, P.O. Box 1663, Los Alamos National Laboratory, Los Alamos, MN 87545, for the Armstrong Laboratory Environics Directorate (AL/EQ), Suite 2, 139 Barnes Drive, Tyndall Air Force Base, Florida 32403-5319.

This final report describes experiments conducted at Los Alamos to examine subsurface transport of contaminants by water. Design and construction of small glass columns and a large stainless steel column; measurement and sampling techniques; data collected from each experiment; and analyses to examine the effects of experimental scale are given in this report.

The work was performed between February 1989 and February 1993. The AL/EQS project officer was Dr. Thomas B. Stauffer.

EXECUTIVE SUMMARY

The objective of the research presented in this report was to analyze subsurface contaminant transport by water at different experimental scales to provide information for moving from the laboratory experiments to field applications. The scale-dependent behavior of subsurface hydrologic and transport processes has been recognized as one of the key issues in assessing contaminant behavior for either compliance or remedial actions. Scale-dependent behavior means that the magnitude of parameters governing processes increases with the length or scale of an experiment. The implications of scale dependency are apparent when using parameter values from laboratory columns to describe transport in a field setting, contaminant arrival times in aquifers were underestimated. The obvious solution is to conduct field experiments to obtain critical transport parameters, but field experiments are expensive, time intensive and have possible environmental ramifications (permitting requirements) compared to laboratory efforts.

Los Alamos National Laboratory performed a number of intermediate-scale experiments to bridge the gap between the laboratory and field settings. Intermediate-scale experiments include features found in the field such as three-dimensional flow and transport and heterogeneous properties that can be measured using the same techniques as a field study. Concurrently, control of initial and boundary conditions similar to that found in laboratory experiments is possible. For this project, a series of experiments was conducted at the laboratory scale in columns that were 1-meter long and at an intermediate scale in a column that was 3-meters long. Both organic and inorganic tracers were used to compare physical and chemical mechanisms controlling transport.

The tests used aquifer material from Columbus Air Force Base in Mississippi. The Air Force is conducting a field-scale aquifer test at this site so an opportunity was available for further comparisons. The Los Alamos experimental program used two different columns. The laboratory-scale column was a 1-meter long glass column. The larger column was stainless steel with dimensions of 1-meter in diameter and 3-meters in length. In the laboratory column both sieved (< 2 millimeter) and unsieved aquifer material was used. In the large column only unsieved aquifer material was used. For all tests, a steady-state flow was established before the tracer pulse was injected. The inorganic tracer was bromide which is expected to trace the movement of water. Naphthalene and p-xylene were the organic tracers which were expected to chemically interact with the aquifer material or be retarded relative to water movement.

Tracer concentrations were measured only at the outlet of the glass column. The steel column had twenty-four porous stainless steel samplers located in groups of four at six depths and a single outlet. Following injection of a tracer pulse, samples were collected at regular intervals to define the tracer distribution in space and time. Bromide concentrations were measured with an ion specific electrode, and organic concentrations were obtained using a gas chromatograph. Data analysis used the method of moments and nonlinear least-squares fitting to the one-dimensional, advection-dispersion equation. The method of moments does not assume any underlying conceptual model governing tracer transport, so the moments can be compared directly. The nonlinear fitting routine employs the advection-dispersion

equation as the underlying conceptual model. The velocity and dispersion coefficient were the parameters that were estimated.

Data from two glass column experiments revealed the effects of sieving on the tracer breakthrough curves. For the sieved material, the breakthrough curves were relatively symmetrical and unimodal. The curves from the unsieved material exhibited an extended tail on the bromide breakthrough curve and a multipeaked response for p-xylene. Estimated bromide recovery for both sieved and unsieved cases was greater than actual input, but only 14 percent of the p-xylene was collected in the unsieved experiment. The low recovery of the p-xylene was attributed to difficulties mixing the influent solution and analytical technique.

Analysis of the glass column data used two conceptual models to describe the behavior. The conventional advection dispersion equation and the mobile/ immobile models were employed because the response of the two columns was much different. The long tail exhibited by the column with the unsieved material suggested that the mobile/immobile or two-region model was appropriate. Criteria such as the sum of squares of observed minus predicted values, statistics of the parameters, and the parameter values themselves were used to discriminate between the models to determine if one of the models was better than the other. For the column with the less than 2-mm material, the advection dispersion equation appeared to be the most appropriate. The results were not as obvious for the column with the greater than 2-mm material because both models exhibited favorable attributes. A simulation was made with both models to resolve the effects of distance on the breakthrough curves of these models indicated that at 5 meters differences in the breakthrough curves would be difficult to discern between the mobile/immobile and advection dispersion models for the parameters derived from the glass column with the greater than 2-mm material. Both models were used to analyze results of the large column.

The results of three large column experiments were reported. Mass balance, velocities, and dispersion coefficients calculated by the method of moments for each sampling location showed large variations for each experiment. Bromide breakthrough curves at a given location were compared between experiments by defining dimensionless time and concentration variables and plotting all three experiments on the same graph, and essentially no consistency was found.

Breakthrough curves for the four samplers at each of the six sampling depths were averaged to carry out a one-dimensional analysis. Some consistency was found in terms of the magnitude of the dispersion coefficients between the glass and large columns, but the effluent data from the large column were not represented by the data from the samplers. Fitting the mobile/immobile model to the data revealed the same inconsistencies between effluent and sampler concentrations and did not provide any additional insight into the behavior of the steel columns. Some of the discrepancy between the range of sampler values and the overall behavior as defined by the effluent concentrations can be attributed to the design of the outlet of the large column that brings all the flow lines together and may induce additional mixing.

This research demonstrated some of the problems with extrapolating between experimental scales when describing contaminant transport. The inability of 24 point measurements to bound the effluent response is critical in the design of sampling

networks for environmental assessment. One possible explanation may be the design of the lower boundary on the large column, and future experiments using this approach should consider this feature. This research can be used by personnel who are responsible for environmental compliance to illustrate problems of scale and sampling effectiveness when dealing with contaminant transport issues.

This research can be used by the Air Force to support the field-scale experiments being conducted at Columbus AFB.

This research is pertinent to agencies, firms, and organizations that make environmental assessments of groundwater pollution.

(The reverse of this page is blank.)

TABLE OF CONTENTS

TABLE OF CONTENTS (CONCLUDED)

LIST OF FIGURES

LIST OF FIGURES (CONTINUED)

LIST OF FIGURES (CONCLUDED)

LIST OF TABLES

LIST OF TABLES (CONTINUED)

LIST OF TABLES (CONTINUED)

LIST OF TABLES (CONCLUDED)

SECTION I

INTRODUCTION

A. OBJECTIVE

The objective of this research was to conduct experiments using small-scale (1 meter x 0.15 meter diameter) and intermediate-scale (3 meter x 1 meter diameter) columns to study the migration and retardation of selected organic compounds in geologic material from the aquifer at Columbus Air Force Base, Mississippi.

B. BACKGROUND

Transport of organic compounds such as fuel oils and solvents is one of many potential insults to surface and subsurface groundwater. The knowledge base of organic transport, however, is considerably smaller than for transport of inorganic contaminants. The experiments described in this report were designed to provide data so that models of the behavior of organic compounds in surface and subsurface waters can be evaluated and refined to predict the effects of organic fuels and solvents on the environment.

Retardation depends on interactions between the organic of interest and organic matter and inorganic solid phases in the aquifer. Sorption of organics depends on their hydrophobicity, or insolubility, and the amount of organic matter in the porous medium (Reference 1). Organic compounds that have some ionic character can sorb to inorganic materials in the medium by electrostatic interactions, whereas organics with little ionic character tend to be repelled by water and can form globules or are forced near mineral surfaces as a result of repulsive interactions with water. Media with high organic matter composition, such as surface soils, tend to sorb organic compounds because of the high affinity of the organic matter for the compound. The aqueous/nonaqueous partition coefficient, K_p, is related to the octanol/water partition coefficient, K_{ow}, and to the fraction of organic carbon in the media:

$$\log K_p = a \log K_{ow} + \log f_{oc} + b \qquad (1)$$

where a and b are coefficients. Large values of K_p can be due to high organic matter content, large K_{ow}, or both (Reference 2).

Inorganic minerals also affect the retardation of organics. Experiments with different clay minerals (References 3, 4, and 5) demonstrated that aluminosilicates commonly found in soils sorb significant amounts of organic solvents in some cases. Other researchers (Reference 6) showed that iron oxides sorbed more organics than low organic matter aquifer material, and both sorbed more than aluminum oxides. Tests to determine sorption coefficients (K_d) and/or coefficients using different soil and inorganic materials demonstrate small but significant sorption of fuel components and solvents, thus slight retardation of organics compared to unretained water is expected in aquifers.

Extrapolation of retardation effects from batch sorption tests to dynamic systems is compounded by uncertainty. The uncertainty derives from geochemical differences in the field and the laboratory, greater heterogeneity of physical and chemical properties in the field media compared to the media used in batch studies, and variations in groundwater flow rate in the

1

field compared to the thoroughly mixed solution and solid in the laboratory studies. Extrapolation of Sr batch sorption data to column studies is difficult (Reference 7), but good agreement was found between K_d's measured from batch, column, and box tests for naphthalene (Reference 8).

Transport parameters, such as the dispersion coefficient, depend on the size of the systems from which they are determined. As the size of a system increases, so does the dispersion of a solute in a given medium (Reference 9). Thus, transport times can be underestimated if dispersion determined from small column experiments is used to estimate transport on a larger scale system such as a watershed or a caisson. Field-scale experiments can be difficult and expensive to perform. Control of initial and boundary conditions is often impractical, adverse environmental effects can result by introducing hazardous or toxic solutes into an aquifer, and sampling the solute plume to resolve tracer behavior requires an extensive network of wells. An alternative is to conduct tests in experimental apparatus that are large enough to produce large-scale flow and transport behavior. These intermediate-scale tests have inherent advantages and disadvantages over field and laboratory studies. The remainder of this report describes procedures and results of intermediate-scale column tests involving bromide (Br⁻), p-xylene, 1-methylnaphthalene, and naphthalene. Two sizes of columns were used, 1-meter x 0.15-meter diameter glass columns and a 3-meter x 1-meter diameter stainless steel column.

C. APPROACH

Several tests at two scales were conducted during this study. The smaller-scale tests used glass columns 1 meter in length and 0.15 meter in diameter. One column was filled with fine material that passed a 2 mm sieve, one contained unsieved material. These columns allowed testing the effects of > 2 mm particles on transport. The larger-scale apparatus was a single 3 meter by 1 meter diameter column that was filled with unsieved material. Sampling ports were installed at six different vertical positions to extract water flowing through the column. All columns were designed so that the effluent could be sampled.

The geologic material used for all experiments was obtained from the saturated zone near Columbus Air Force Base, Mississippi, and represents a Pleistocene terrace deposit. The glass columns enabled testing of the aquifer material with and without the >2 mm component. The large amount of material needed to fill the steel column precluded using sieved material in the larger-scale tests. The presence of the greater than 2 mm component significantly altered transport through the steel and glass columns. The fuel components used for the tests were p-xylene, 1-methylnaphthalene, and naphthalene, each obtained from commercial sources. Br⁻ from lithium bromide (LiBr) was used as a conservative tracer. Lithium concentrations were not measured. Water for all column studies was formulated from deionized water and was based on the chemical analysis of water from the Mississippi aquifer.

Each of the fuel components was tested individually in the glass columns with sieved material; 1-methylnaphthalene and p-xylene were tested in the glass column that contained unsieved aquifer material; and p-xylene and naphthalene were tested in the steel column. Br⁻ was used in each test as a conservative tracer so that the water velocity and hydrodynamic characteristics of the column could be estimated. Data collected during each test included Br⁻ concentration, organic concentration, flow rates, and time. Concentrations of Br⁻ and organics were used to determine mass balance as well as the transport properties of interest. Overall,

the organics were slightly retarded with respect to Br, and this will be discussed in detail below.

SECTION II

EXPERIMENTAL

A. NATURAL AND SYNTHETIC GROUNDWATER CHARACTERISTICS

1. Mississippi Aquifer Water

Column tests were designed to contact the aquifer material with water representative of groundwater from the site. The large volume of water required for each test precluded use of actual water from the aquifer. The aquifer water was analyzed in order to formulate synthetic water for each test. The water analyses also suggested possible geochemical processes that controlled water chemistry and affected contaminant transport.

Water composition data form the Columbus AFB aquifer showed a low ionic strength solution that is dominated by calcium (Ca^{2+}), chloride (Cl^-) and nitrate (NO_3^-). $CO_{2(g)}$ evolved when samples were collected and indicated excess CO_2 at depth. The Ca^{2+}, Cl^-, and pH values are explained in part by the dissolution of carbonates from the aquifer. The relatively high NO_3^- concentration may be the result of fertilizer use or other additions to the aquifer. Since large volumes of water were required for the column tests, different soluble salts were dissolved in deionized water to approximate the actual groundwater. The synthetic formulation is discussed below and given in Appendix A. Dry sieving significantly affected water composition. Deionized water that contacted dry-sieved aquifer material had higher Ca^{2+}, magnesium (Mg^{2+}), carbonate, and sulfate (SO_4^{2-}) which indicates dissolution of dolomite, calcite, and gypsum after short time contact with water.

Geochemical calculations using PHREEQE (Reference 10) and EQ3/6 (Reference 11) programs found that the aquifer water was of low ionic strength and contained small amounts of dissolved solids. Mineral solubility indexes based on solution data were computed for several minerals. According to the saturation indexes, the solution is undersaturated with respect to calcite and dolomite and should dissolve these minerals if they exist in the aquifer material. Reactions involving calcite and dolomite probably control Ca^{2+} and Mg^{2+} concentrations and contribute to the pH and P_{CO_2} of the water. The solution appears in equilibrium with chalcedony or quartz, and Si is controlled by the reaction with a small contribution from dissolution of aluminosilicates. The solution is saturated with respect to both goethite and hematite, but the yellow-brown color indicates that goethite is the dominant phase and controls the Fe concentration in the water.

Low pH and dissolution of carbonates from the aquifer suggest the identity and source for the bubbles observed in the water. Carbonate dissolution produces CO_3^{2-} that is readily converted into H_2CO_3 and $CO_{2(g)}$ when pH is acidic. Carbonate dissolution in waters of higher pH, such as the water used for wet sieving, would dissolve less carbonate material producing less CO_2. Abrasion of Ca^{2+} and Mg^{2+} minerals during dry sieving resulted in higher concentrations of the basic cations in solution keeping pH at high values. Synthetic aquifer water was used for both column tests and sample preparation to minimize potential alteration of the aquifer material so that material representative of the aquifer can be tested.

2. Synthetic Groundwater

Reagent grade salts and concentrated acids were added to deionized water in the laboratory to approximate the aquifer water. Salts of KNO_3, $CaCl_2$, $NaCl$, and $NaHCO_3$ were dissolved in the deionized water, and concentrated HNO_3 and H_2SO_4 were diluted to match the pH of water sampled in the field. The exact specifications for the synthetic groundwater and for pre-mixed concentrates are given in Appendix A. Approximately 100 liters were prepared for the glass column and 1000 liters for the large column of synthetic water for each test. The solutions were sparged with nitrogen ($N_{2(g)}$) to minimize the amount of degassing that occurs inside the column during the test.

B. MISSISSIPPI AQUIFER MATERIAL

Material from the aquifer at Columbus AFB, Mississippi was loaded and shipped to Los Alamos in 1989 with no further treatment. The material was covered by a tarp and stored outdoors at TA-51 after delivery until used in glass and steel column tests.

Geomorphic information from the Air Force described the area as a river terrace deposited in the Pleistocene. The texture of the aquifer material and the abundance of gravel and sand reinforced the origin and suggested that the aquifer may have high transmissivity. Over 55 percent by weight of the material is > 2 mm, and the < 2 mm fraction is 89.9 percent sand, 2.1 percent silt, and 8 percent clay. The clay fraction consisted of smectite, kaolinite, and trace amounts of iron oxides and chlorite. The presence of smectite and chlorite was expected because they are commonly found in large cemented masses. Goethite and lepidocrocite were identified by X-ray diffraction and produced the 10YR 5/6 Munsell color in most aquatic material samples. Hematite would be expected in more basic and drier environments and would shift the color of a moist sample to redder hues. The iron oxides appear as coatings on the > 2 mm gravel as well as dispersed throughout the < 2 mm matrix. Few gray mottles that distinguish alternating oxidizing and reducing conditions were found in the material. The low organic matter content (<< 1 percent) and the homogeneous yellow-brown color indicate oxidizing conditions are dominant. Trace amounts of lepidocrocite indicate that reduced iron was probably quickly oxidized and precipitated.

Abundant fossils were found in the aquifer material from both > 2 mm gravels and in the < 2 mm fraction. No effervescence was observed when 10 percent HCl was applied to the material. Effervescence indicates the presence of $CaCO_3$, thus, the fossiliferous material was largely dolomite and/or shell material that had been replaced by Si. The fossils suggests one source of carbonate that could be released as the aquifer material contacts groundwater. Carbonates derived from the aquifer material could explain both the increase in pH during dry sieving and the evolution of gas bubbles when water is sampled from depth. Increased carbonate and/or bicarbonate from dolomite dissolution could result in a pH shift as well as evolution of $CO_{2(g)}$.

Wet aquifer material could be easily compacted to a density that inhibited water flow. An ultrasonic concrete vibrator was used to pack a test column. Vibration of only a few seconds was sufficient to seal the material and prevent water movement except under high applied pressure. Compacted material that was allowed to dry was extremely stable and resembled building material. The dry material could be broken only with a hammer. This propensity of the aquifer material to form dense blocks meant that care was taken to minimize excess compaction when packing the glass or steel columns.

The Air Force requested 0.2 m^3 of < 2 mm aquifer material for tests at Columbus AFB. Wet sieving with water of approximately the composition of the aquifer groundwater was used because dry sieving resulted in water composition significantly different from water in the aquifer. The effects of wet and dry sieving on the solution pH are shown in Figure 1. The composition of the water used for the wet sieving is given in Appendix A.

C. TRACER AND ORGANICS

LiBr from EM Science was the source of the conservative Br⁻ tracer for all tests. A solution of 1000 ppm Br⁻ was prepared by weighing the appropriate amount of LiBr into the volume of water to be injected as the contaminant pulse. For glass column tests the injection volume was 1 L, for steel column tests the volume was 10 to 15 liters. LiBr is readily soluble in water and required little mixing after addition to the reservoir.

Three organic fuel components were used individual in the tests. Naphthalene (J. T. Baker), 1-methylnaphthalene (Aldrich Chemical), and p-xylene (EM Science) were used as the injected contaminants and in analytical standards. Aqueous solubilities of the organics were 25 mg/L for 1-methylnaphthalene, 30 mg/L for naphthalene, and 180 mg/L for p-xylene.

All tests were preceded by flushing the column with 0.02 percent sodium azide (NaN$_3$). This treatment inhibited microbial activity and minimized loss of the organics due to biological degradation. Copper sulfate (CuSO$_4$) and NaN$_3$ have been used in combination by other researchers (Reference 8). CuSO$_4$ was not used in order to preserve the natural clay mineralogy.

D. ANALYTICAL METHODS

1. Bromide

Bromide concentration was measured by an Orion 94-35A Br⁻ specific electrode and single junction reference electrode with an Orion EA 940 Ion Analyzer. Samples of 7 to 10 mL for Br⁻ analysis were collected at specific intervals from the effluent port of the glass columns and from the side ports and effluent port of the steel column throughout the duration of a given test. Originally, a Br⁻ electrode was installed in the effluent port of the steel column to enable continuous Br⁻ measurements. The data from the electrode measurements, however, were extremely variable due to power fluctuations and instrument drift (Figure 2). In addition, calibration of the electrode was cumbersome. More useful data were obtained when 7 to 10 mL samples were collected at specific times and the electrode could be calibrated several times during analysis.

Samples were collected from the effluent ports or the side ports with a 10mL glass syringe. Samples were immediately transferred to plastic scintillation vials. The vials were capped and stored in a refrigerator at about 4°C until they were analyzed, usually within one week of the end of a test. Samples were discarded after analysis and the vials were washed and reused.

Calibration standards were prepared from certified 1000 ppm Br⁻ solutions and ranged from 0 to 1000 ppm. Exponential or polynomial regression was used to obtain a

calibration curve for the standard data. This curve was used to convert the measured mV values to Br⁻ concentrations. Frequent calibration was required to adjust for instrumental drift.

2. Organics

Organic concentrations were measured using a Perkin Elmer Model 8500 gas chromatograph (GC). The GC was equipped with a 30 m x 50 mm diameter column, FID detector, head space analyzer and auto sample changer, and data were collected with Perkin-Elmer's OMEGA software. Head space GC was used because a large number of analyses were required for a test (up to 700) and automation of the analysis was relatively simple. Up to 100 samples could be analyzed automatically, freeing the operator to begin preparations for the next test.

An analytical method for each organic was developed by analyzing aliquots of the organic of interest in deionized water (Appendix B). Methods included information on GC parameters (oven temperature, etc.), auto-sampler temperature control and sample identification. The methods were stored in the GC and were used for appropriate analysis when needed.

Samples were collected from the effluent port or side ports using a 10 ml glass syringe. The samples were transferred immediately from the syringe to tared head space vials capped with Teflon/aluminum septa, then weighed again. The samples were never in contact with the atmosphere. The septa were used with the aluminum side in contact with the solution to minimize loss of sample by sorption to the Teflon®. Samples were stored in a refrigerator at about 4°C after collection and analyzed as soon as possible after collection. Glass vials were washed and used again, the caps and septa were discarded after a single use. Loss of samples because of leakage through the septa during storage and/or analysis was one source of error in the organic analyses and will be discussed below.

Calibration standards were prepared using the organics of interest for a particular test. A stock solution of the organic of interest was prepared at or near the solubility limit. The desired amount of organic was placed in a 1 liter volumetric flask partially filled with deionized water then diluted to volume with water. The flask was stoppered and the solution were stirred with a magnetic stirrer slowly for at least 24 hours. Aliquots of the stock solution were analyzed by head space GC to evaluate the uniformity of mixing. The stock solution was considered well-mixed and ready to use for standards when triplicate analyses were reproducible within about 5 percent of previous values and with each other. Replicates often showed considerable variability in measured concentrations after 24 to 48 hours of slow mixing. One possible source for the variability was the formation of droplets of organic suspended in the water instead of being truly dissolved. Light scattering measurements on solutions with and without organics present suggested that there were droplets in the solutions with organics. However, this observation could not be quantified due to instrumental difficulties. A solution generator (Reference 12) was used in an attempt to eliminate the variability in the stock solutions, but the stock solutions had as much or more variability as stock solutions made without the generator. One reason for highly variable solution concentrations from the solution generator was that only single-component organics were mixed with water, whereas other researchers (Reference 12) successfully mixed binary organic phases in water. The presence of the second organic component in the mixture may have prevented droplet formation (Reference 12). The original method was used because less
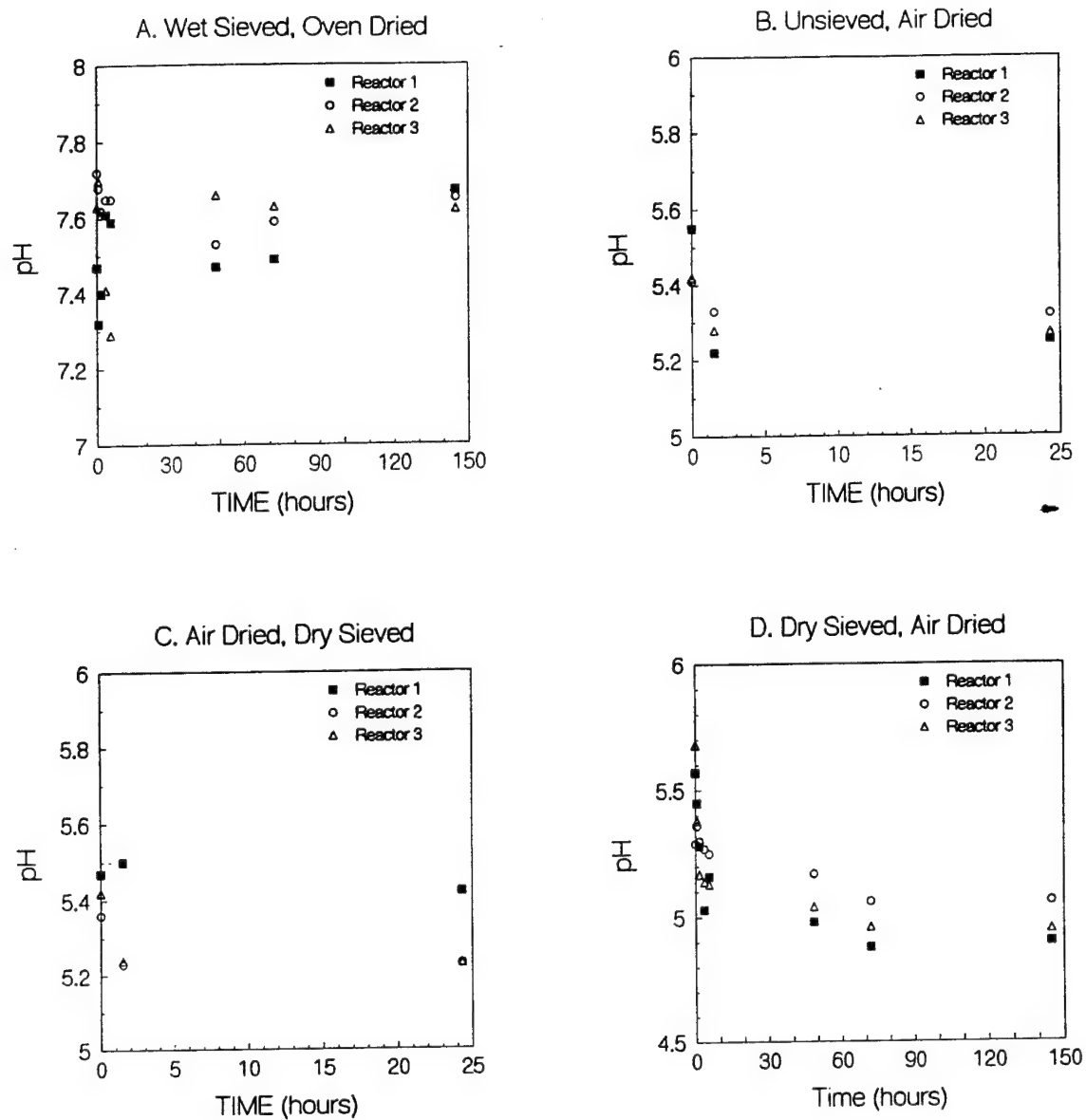
Figure 1. Sieving and effects on pH. Wet sieved, oven dried (upper left), unsieved, air dried (upper right), air dried, dry sieved (lower left), dry sieved, air dried (lower right).
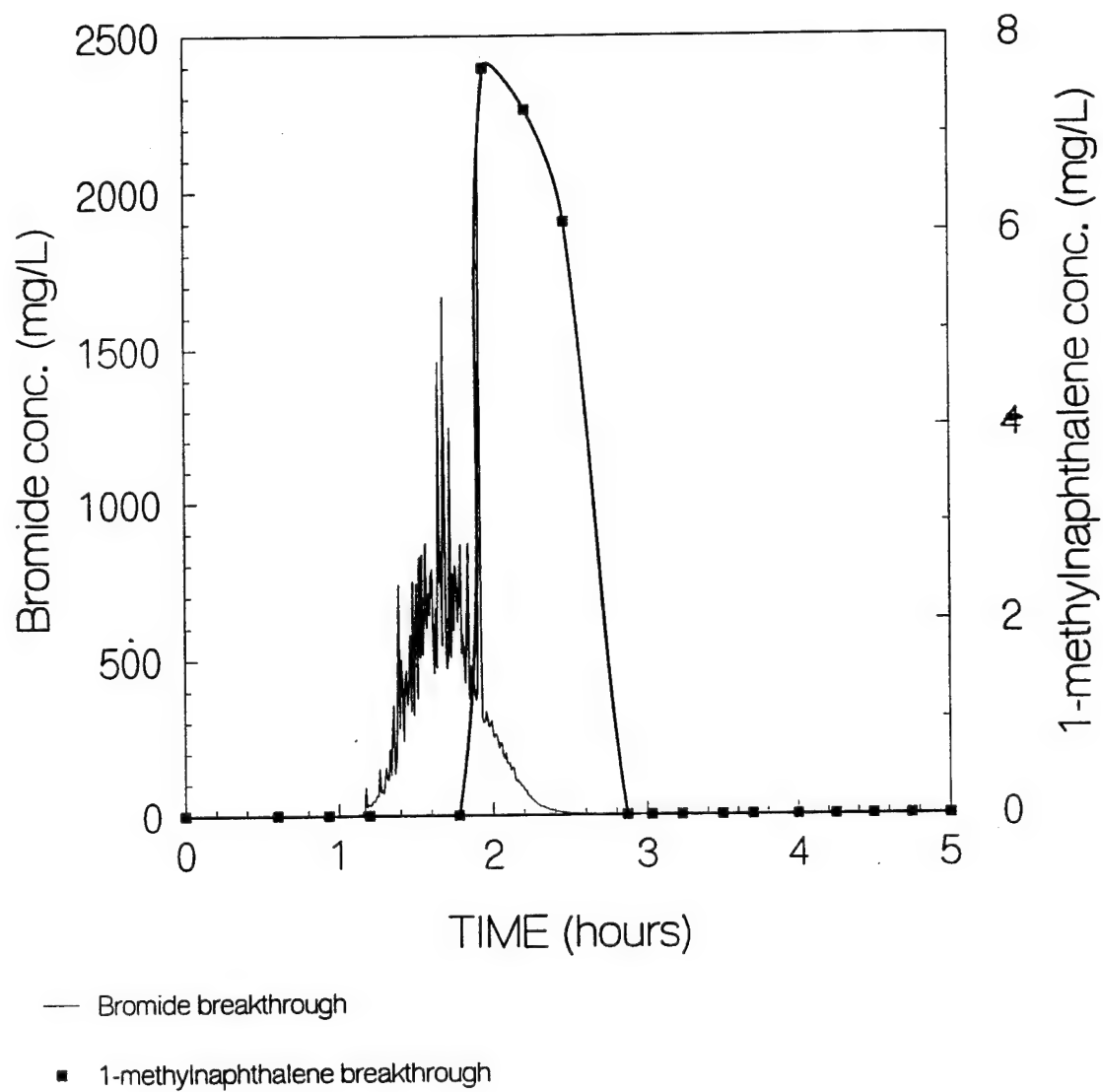
Figure 2. Bromide and 1-methylnaphthalene breakthrough, glass column. Bromide curve (no points) shows noisy electrical line, organic line (with data points) shows smoother data.

variability in the measured concentrations was observed using the original method compared to the solution generation method.

Calibration standards were diluted from the stock solutions in concentrations of 0 to 5 mg/L or 0 to 10 mg/L. The desired volume of a stock solution was pipetted into a 100 mL volumetric flask, diluted to volume with deionized water, then the flask was tightly stoppered. Aliquots of the standards were collected with 10 mL glass syringes and transferred to GC vials identical to the ones used for samples. The volume of standard used was the same as the sample volume in all cases. Triplicates of each standard were run with the samples to ensure that adequate calibration data were obtained. Linear or polynomial regression of the GC data from the standards were used as calibration curves and programmed in to the GC data analysis software. Peak areas from the organics of interest were converted to concentrations for each sample.

Relatively large variations in the organic analyses were observed throughout this study. Loss of organic components from the sample due to different causes would explain the observed variation. Leakage of organic chemicals from the GC vials prior to analysis was the largest single error in the determination of organic concentrations. Volatilization could have occurred at three points between extraction and analysis. First, organics could have been lost during sample extraction on either the glass or steel columns. Transfer from sampling port to GC vial was done as quickly as possible to minimize losses. We believe this error is minor. Second, volatilization of the organic could have occurred during sample storage. Volatilization at this step was unlikely because samples were stored at 4°C immediately after extraction. Volatilization most likely occurred as the samples cycled through the GC auto sampler. Vials at the end of a cycle were at or slightly above room temperature because of their proximity to the vial heater. Prolonged exposure (up to several hours, depending on the number of samples in the queue) could have caused loss of the organic before the samples were analyzed. Another possibility related to the auto sampler is loss of the organic during the heating segment of the head space analysis. The most volatile organic, p-xylene, was the most susceptible to organic loss of this type. To minimize organic loss due to sample heating, short heating times were used. However, sample leakage caused by heating was still the largest single source of error in the organic analyses.

3. Water Flow Rate

Volumetric flow rates were measured several times during a test by diverting effluent flows to a 1 liter graduated cylinder and measuring the time required to obtain a given volume. Flow rate data were important in the analysis of moments, and to ensure that all effluent was collected in proper containers for disposal. Water flow rates were also a check to ensure the columns performed as it had in previous tests.

E. GLASS COLUMNS AND STEEL COLUMNS

1. Glass Columns

Two columns were fabricated from glass cylinders of 0.15 meter diameter and 1 meter length (Figure 3). Stainless steel retaining plates were fitted to the top and bottom of the column and held in place by four threaded compression rods. The top plate was fitted with an influent port through which water carrying the Br⁻ tracer and the organic of interest were introduced. A purge tube was also fitted to the top plate to facilitate the removal of trapped air

in the column. A porous stainless steel plate at the bottom supported the aquifer material and allowed water to flow out of the column. An effluent port was fitted into the bottom plate, and a sampling port was affixed to one side of the effluent port. A septum from a head space vial was attached to the sampling port so that a glass syringe could be used to draw samples at the effluent. O-rings between the steel plates and the glass were used to seal the column.

Aquifer material was wetted to near saturation then loaded into the columns. One column was prepared with < 2 mm material, the second column was prepared with unsieved material. Wetted material was placed in the columns in 10 cm depths then lightly compacted in an attempt to establish a homogeneous column. The unsieved material was initially packed with a vibrator for settling concrete. The result was an almost impermeable mass of aquifer material. Very little water flowed through the column even with 12 - 15 psi applied pressure. The column was repacked without vibration and used for several tests.

Each column was saturated with $CO_{2(g)}$ from the bottom after the retainer plates were secured. The $CO_{2(g)}$ displaced air trapped in the column and then dissolved as the column was filled with water. Initially, synthetic aquifer water was introduced from the bottom of the column and flowed out the top. This procedure forced the trapped $CO_{2(g)}$ to move with the water and ensured that trapped gas was minimized for each test. The water flow was reversed after saturation of the aquifer material was complete, then several liters of 0.02 percent NaN_3 was pumped through to inhibit microbial activity. Synthetic aquifer water was used to flush the residual NaN_3 out of the column. At this point, the column was considered ready for a test.

Synthetic water was prepared and stored in a 150-liter Nalgene tank. A peristaltic pump was used to deliver the water from the reservoir to the column. The pump rate (volume/min) was calibrated before each test and checked periodically during a given test. All tubing from the reservoir to the influent port was stainless steel except for about 20 cm of Si tubing around the pump head. Samples collected before and after contact with the Si tubing showed no measurable difference in organic concentration due to adsorption on the Si tubing walls. LiBr and the organic of interest were mixed together and stored in a stainless steel reservoir plumbed separately into the delivery line. At injection time, the water reservoir was closed and the contents of the steel reservoir were pumped into the column. Reservoir flow resumed after the organic reservoir was emptied. Relatively constant flow rates were maintained in this manner. Effluent flow rates (vol/min) were measured to ensure that steady-state flow was maintained and as a required parameter for the analysis of the data. Effluent was collected in 55-gallon drums for proper disposal.

Br$^-$ was measured continuously in the initial tests by mounting the electrode in a holder and placing the assembly in the effluent stream. Fluctuations in the power supply, however, caused significant variation in the data with time (Figure 2). Better data were collected by withdrawing a sample from the sampling port at the base of the column and analyzing it off-line. This procedure allowed frequent and simple calibration of the Br$^-$ electrode.

The effluent was also used to collect samples for GC analysis. Samples of 3 to 4 mL were extracted and analyzed by head space GC. An Al-coated butyl rubber septum was used to seal the port, and only the Al side of the septum contacted the solution. The rubber septum was convenient and easily maintained between tests.
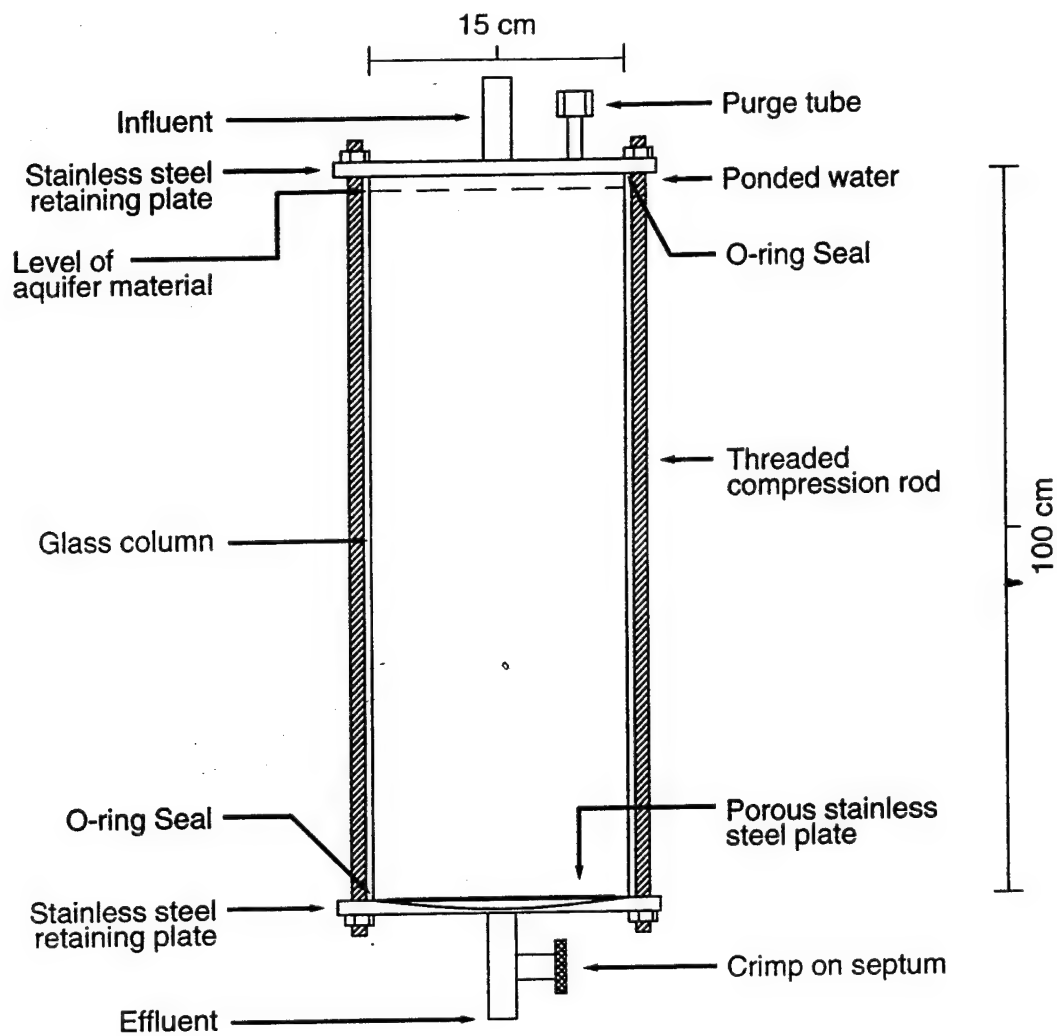
Figure 3. Schematic diagram of the glass column.

12

Samples for Br⁻ and organic analysis were collected in immediate succession with the Br⁻ sample coming first. Br⁻ samples were placed in plastic scintillation vials and organic samples were injected directly into tared head space vials. Samples were collected at predetermined intervals to capture the maximum Br⁻ and organic concentrations and to determine the behavior of the concentration peak during the tests. Background Br⁻ concentrations were measured at several times before tracer injection. Synthetic water was pumped constantly during and after the tests to keep the aquifer material in its most natural state.

2. Steel Column

The 3 meter x 1 meter diameter column was fabricated from #316 stainless steel (Figure 4). The column was designed to provide large scale conditions but was small enough for use in a laboratory. Twenty-four sampling ports were installed on six levels so that transport of the Br⁻ tracer and organic of interest could be followed vertically during a test. The samplers were made from porous stainless steel to minimize sorption of the organics, and each port extended about 30 cm into the aquifer material. The samplers were filled with glass beads to minimize the dead volume and to facilitate sampling. Samples were extracted using a head space septum that was attached to the end of each sampler. Each sampler had a valve through which water could be drained if necessary. The ports were spaced evenly along the vertical axis of the column (Figure 4.).

The bottom cone was constructed so that the effluent could be collected and easily sampled and to minimize back pressure at the top. The cone held a porous stainless steel disk in place, and the stainless steel nipple was fitted with an assembly to hold the Br⁻ and reference electrodes for continuous measurement of Br⁻ concentrations. A three-way valve was also installed so that effluent flow could be momentarily diverted for sampling and flow rate measurements. The effluent port served as the 25th sampling port for each of the steel column tests.

The stainless steel cover was bolted directly to a flange on top of the column. An influent port was affixed to the center of the cover and functioned as a dispersed source for the tests. Two purge ports were placed off-center in order to remove trapped air. Synthetic water with Br⁻ tracer and the organic of interest were introduced through the influent port. The aquifer material filled all but about 11 cm of the 3 m length of the column. The remaining head space was filled with water, and care was taken to remove trapped air before a test was started. A mixing device rotated within the head space to ensure even distribution of the tracers during injection.

A stainless steel point source delivery port was installed about 4 cm below the surface of the aquifer material. This device provided an alternate method for introducing tracers and reduces the effects of tracer storage in the ponded water at the surface. A computer-controlled peristaltic pump supplied water to the top of the column. Water was delivered at a nearly constant rate for a given test, and delivery rates were easily changed. The volume of water pumped through the column was recorded automatically and a detailed account was given of how much water was used for a test.

Approximately 1100 liters of water was prepared and stored in three plastic tanks. The tanks were connected in series to the pump, and each tank could be refilled without interrupting the water flow to the column. The tanks were connected to the pump with tygon
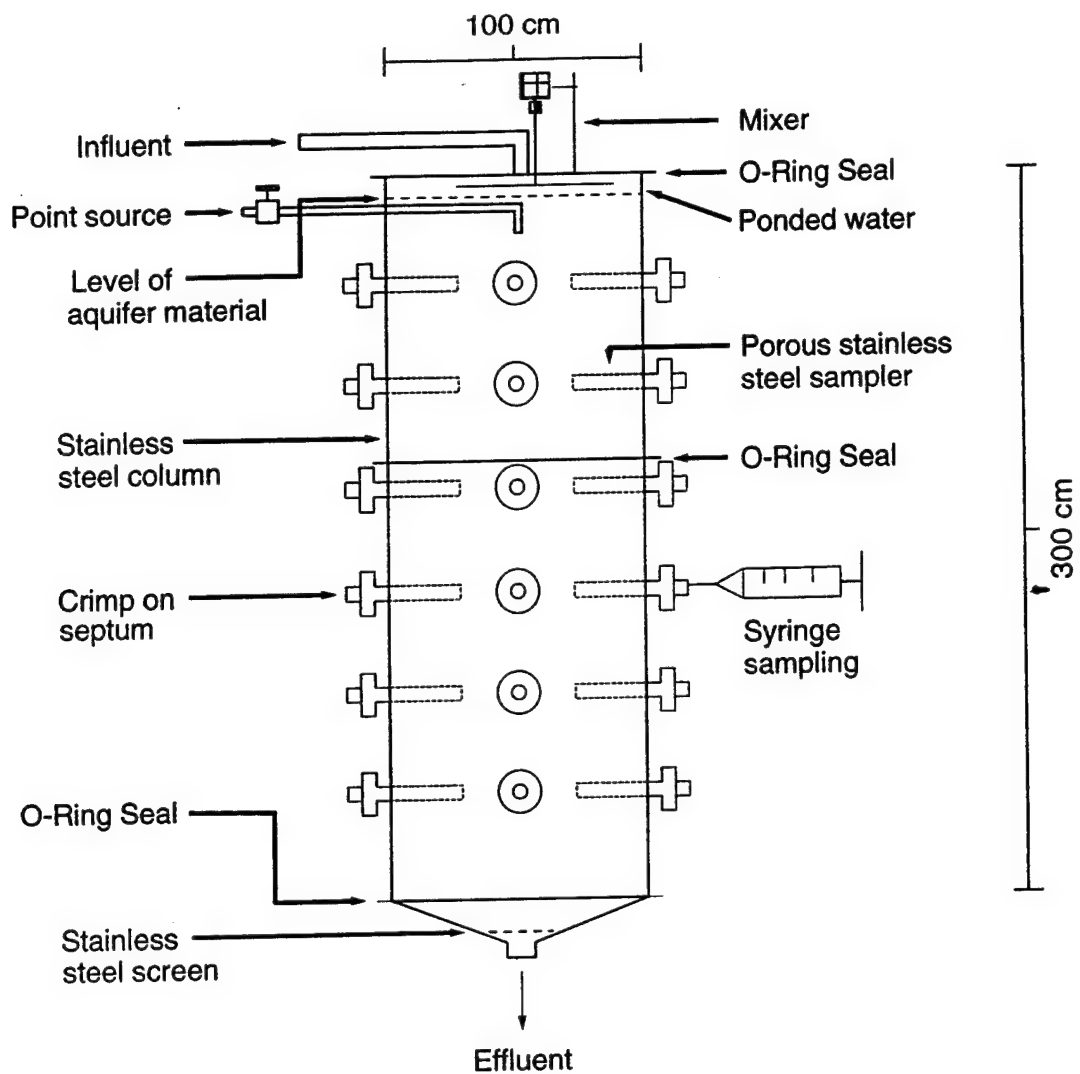
Figure 4. Schematic of steel column.

14

tubing. A 50-liter stainless steel reservoir was plumbed into the pump and isolated by a valve, and only stainless steel tubing was used from the reservoir to the pump. LiBr and the organic of interest were mixed in the stainless steel reservoir and then injected into the column. A magnetic stirrer mixed the solution in the reservoir until it was delivered to the column. The solution flowed through stainless steel tubing from the pump to the point of injection, to minimize sorption of the organics to tygon tubing or other plastic parts. Check valves were installed in the delivery line to guard against back flow from the column.

Effluent was collected in 55-gallon drums after it left the column. Several drums plumbed in series provided effluent collection for several days of operation. The drums were used inside the laboratory initially, but were replumbed to collect effluent and stored remotely in the waste collection area. All waste was collected and disposed of according to LANL ES&H policies.

The column was attached to a unistrut frame that secured the apparatus. Wheels were attached to the bottom of the frame so that the column could be moved around the laboratory until it was filled. The frame ensured that the column would not tip when it was positioned in the laboratory or during testing. An OSHA-approved scaffold was used to access the top of the column and the upper sampling ports.

The column was packed with unsieved aquifer material in 10 cm lifts using a cement conveyor. The upper half of the column was bolted in place after the lower half was filled, then the remaining volume was filled. The material was wetted first to eliminate dust and accommodate packing. Each lift of material was compacted by lightly tamping.

F.   DATA REDUCTION METHODS

1.   Method of Moments

Several methods are available to analyze the response of the column experiments (Reference 13). The method of moments was applied because it is relatively simple and interpretation of the moments is possible without assuming a conceptual model. If a particular model is assumed, then parameter estimates can be made from the moments. Temporal moments were used to examine the effluent and sampler data from the glass and steel columns.

Temporal moments are defined by Turner (Reference 14). The nth temporal moment

$$M_n = \int_o^t \tau^n C(x,\tau) Q(\tau) d\tau \qquad (2)$$

where M_n is the nth moment; τ^n is time raised to the nth power; $C(x,\tau)$ is the concentration at location x for time τ; $Q(\tau)$ is the flow rate at time τ; and t is the time. Generally, the zero, first, and second moments are derived. The zero moment defines the total mass of tracer in the breakthrough curve. The first moment is related to the center of mass, and the second moment describes the spread of the breakthrough curve. The integration of Equation (1) was numerically evaluated using a two-point Gauss-Legendre formula (Reference 15).

The moments provide useful information on the behavior of a solute in the system under study and can also be used to determine parameters of a conceptual model. If the

advection-dispersion equation is considered appropriate, then the pore water velocity (v) and dispersion coefficient (D) can be estimated using methods from Reference 14. The pore water velocity is estimated by

$$v = \frac{L}{\dfrac{M_1}{M_0} - \dfrac{T_0}{2}}$$

(3)

where v is the velocity; L is the length of the zone over which the measurements are made (in this case column length); M_1 is the first temporal moment; M_0 is the zero temporal moment; and T_0 is the duration of the input pulse. The first term in the denominator on the right-hand side of Equation (3) is the normalizing of the first moment by the zero moment. The second term in the denominator is a correction due to the input which is assumed to be a square wave that started at time zero with duration equal to T_0. The dispersion coefficient is estimated by

$$D = \frac{v^3 \left[\dfrac{M_2 M_0 - M_1^2}{M_0^2} - \dfrac{T_0^2}{12} \right]}{2L}$$

(4)

where D is the dispersion coefficient; M_2 is the second temporal moment; and all other terms are as previously defined. Again, the moments are normalized by the zero moment, and a correction factor ($T_0^2/12$) is made for the square wave input.

Equations (3) and (4) were used to make estimates for both the glass and steel column experiments. The retardation factor, R, was estimated by comparing the first moments or velocities for reactive and nonreactive tracers.

2.   Nonlinear Least Squares Analysis

The least squares approach to parameter estimation was also employed. For one-dimensional systems, the program CXTFIT can estimate parameters for the advection-dispersion equation, the mobile-immobile or two site adsorption equation, and a field transport equation that assumes a stochastic velocity distribution (Reference 16). The CXTFIT program has the capability to address various boundary conditions, solute production and/or decay, linear sorption, and resident or flux concentrations (Reference 17) depending on the experimental conditions. An extension of this program adds degradation in both the sorbed and solution phases (Reference 18).

Details of the mathematical development of this approach to parameter estimation will not be given in this report. References 16 and 18 show the mathematical development. CXTFIT was not modified for this study.

SECTION III

RESULTS

A. GLASS COLUMN EXPERIMENTS

The glass column tests were performed to compare the effects of sieved and unsieved aquifer material on tracer behavior. 1-methylnaphthalene, p-xylene, and Br⁻ were used as tracers in these experiments.

The breakthrough curves of the organics from the glass column tests were asymmetric and multipeaked (Figure 5 and Appendix C). One reason for the multipeaked breakthroughs was that the organics were introduced as emulsions rather than a dissolved phase. This mode of input not only caused multipeaked breakthrough curves, but also made mass balance difficult to achieve. Bromide curves were generally more symmetrical, and much of the asymmetry could be attributed to electrode drift. This is especially true for the continuously monitored experiments (Figure 2).

The aquifer materials that were used in the columns have a large influence on the behavior of the tracers. Unsieved aquifer material caused a multipeaked p-xylene curve (Figure 5) and a bromide breakthrough with an extremely long tail (Figure 6). More symmetrical curves with shorter total breakthrough times for p-xylene and bromide were observed for the sieved materials (Figure 7). These differences in tracer response between these two experiments (Figures 6 and 7) demonstrated the effects of the heterogeneities of the unsieved material. Conceptually, instead of a uniform solute front, the tracer pulse was split into different flow paths by the gravel and low permeability lenses that are postulated to occur in the unsieved material. These heterogeneities in the unsieved material produced a highly dispersed breakthrough curve. The heterogeneous nature of flow in the columns also has important consequences for analyzing results by the method of moments.

Temporal moments were used to estimate mass balances, tracer velocities and dispersion coefficients. Temporal moment data for Column 9 are given in Table 1. Predicted mass was determined by multiplying the zero moment by the average flow rate of the column. By comparing the predicted mass to the actual injected mass, one can see that mass balance was poor for these experiments. The predicted Br⁻ mass balance was 14 percent to 29 percent higher than the actual mass injected, and the predicted p-xylene mass was about 85 percent lower than the actual injected. Errors in the Br⁻ concentration measurements and in the flow rate determinations were hypothesized to account for most of the discrepancy between actual- and predicted Br⁻ mass. Power supply fluctuations to the Br⁻ electrode altered measured Br⁻ concentrations. Frequent calibration of the Br⁻ electrode was required due to the power fluctuations and because of the analysis of a large number of samples; error in Br⁻ concentrations could have been introduced as a result of measurements made with the Br⁻ electrode slightly out of calibration. A small change in the mass error was achieved by smoothing the Br⁻ concentration values. Thus, the analytical error for Br⁻ was not significant and indicated that the flow rate was largely responsible for the higher predicted mass estimates compared to the actual masses injected. The minimum and maximum flow rates from one test were used to estimate the effect of fluctuations in flow rate. For the Column 9 test, measured flow rates ranged from 0.234 L/hr to 0.256 L/hr, and the corresponding
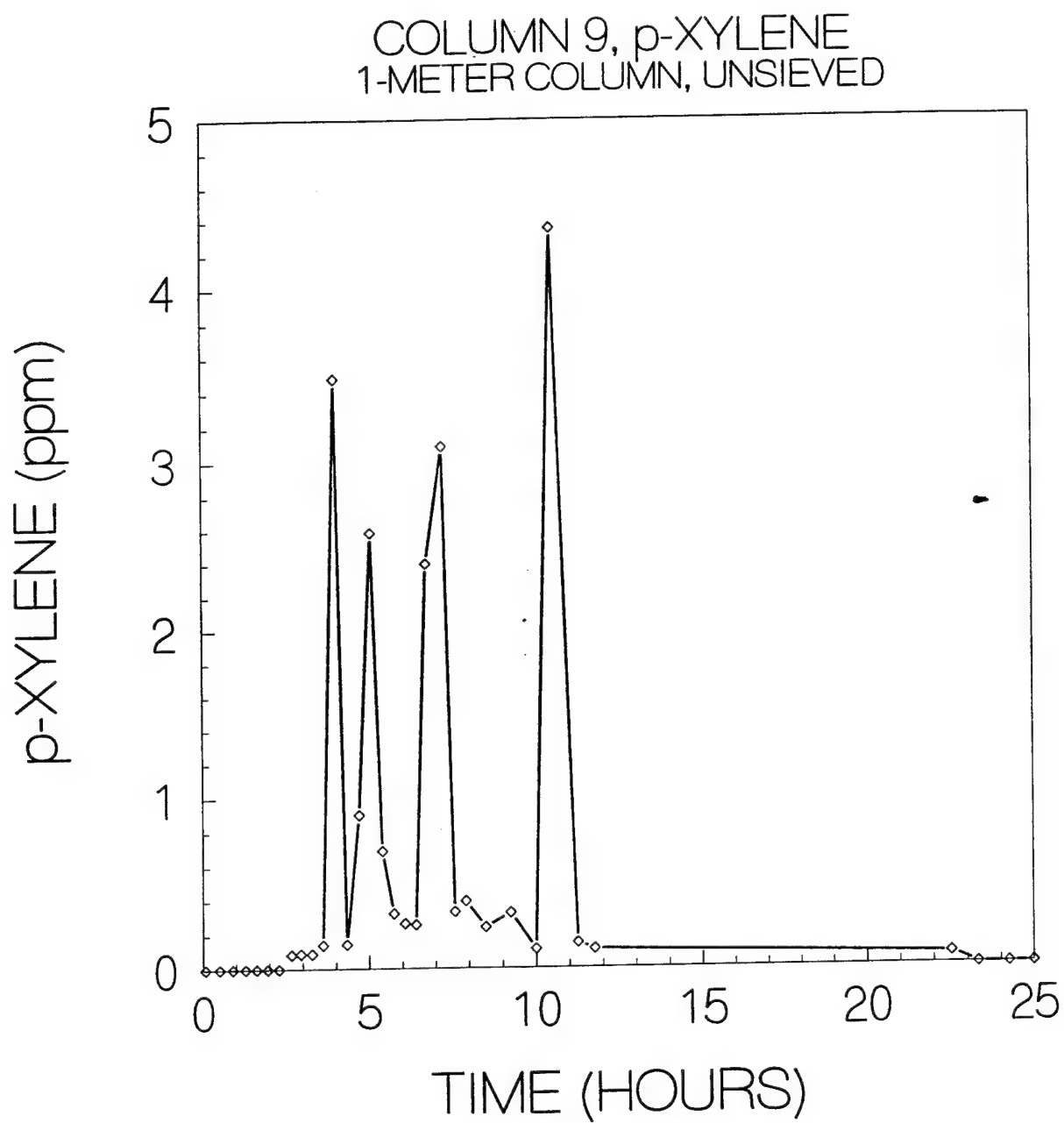
Figure 5. Asymmetric p-xylene peaks in glass column experiment.

COLUMN 9 BROMIDE
1-METER COLUMN, UNSIEVED
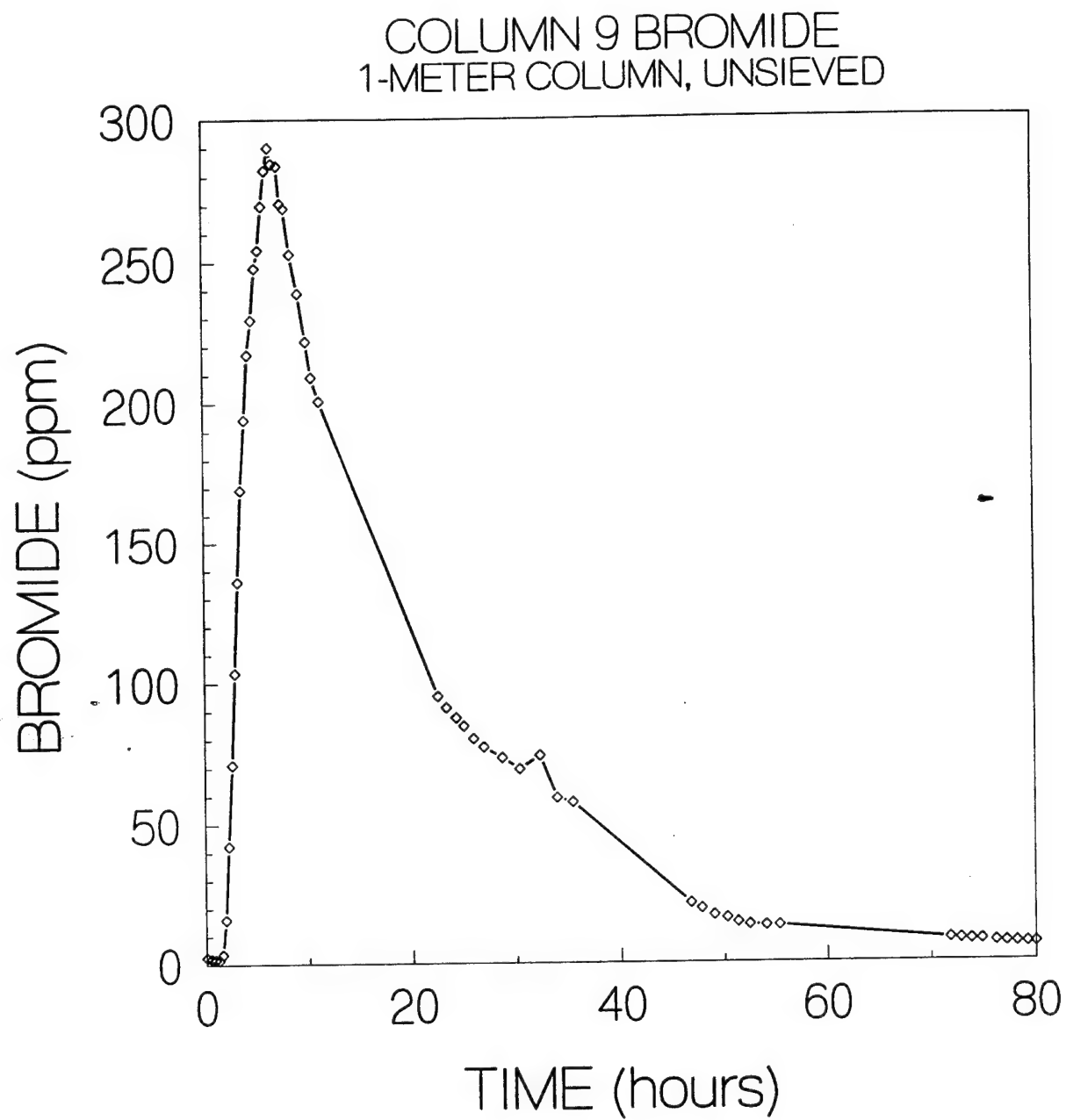
Figure 6. Bromide breakthrough curve for Column 9 test.
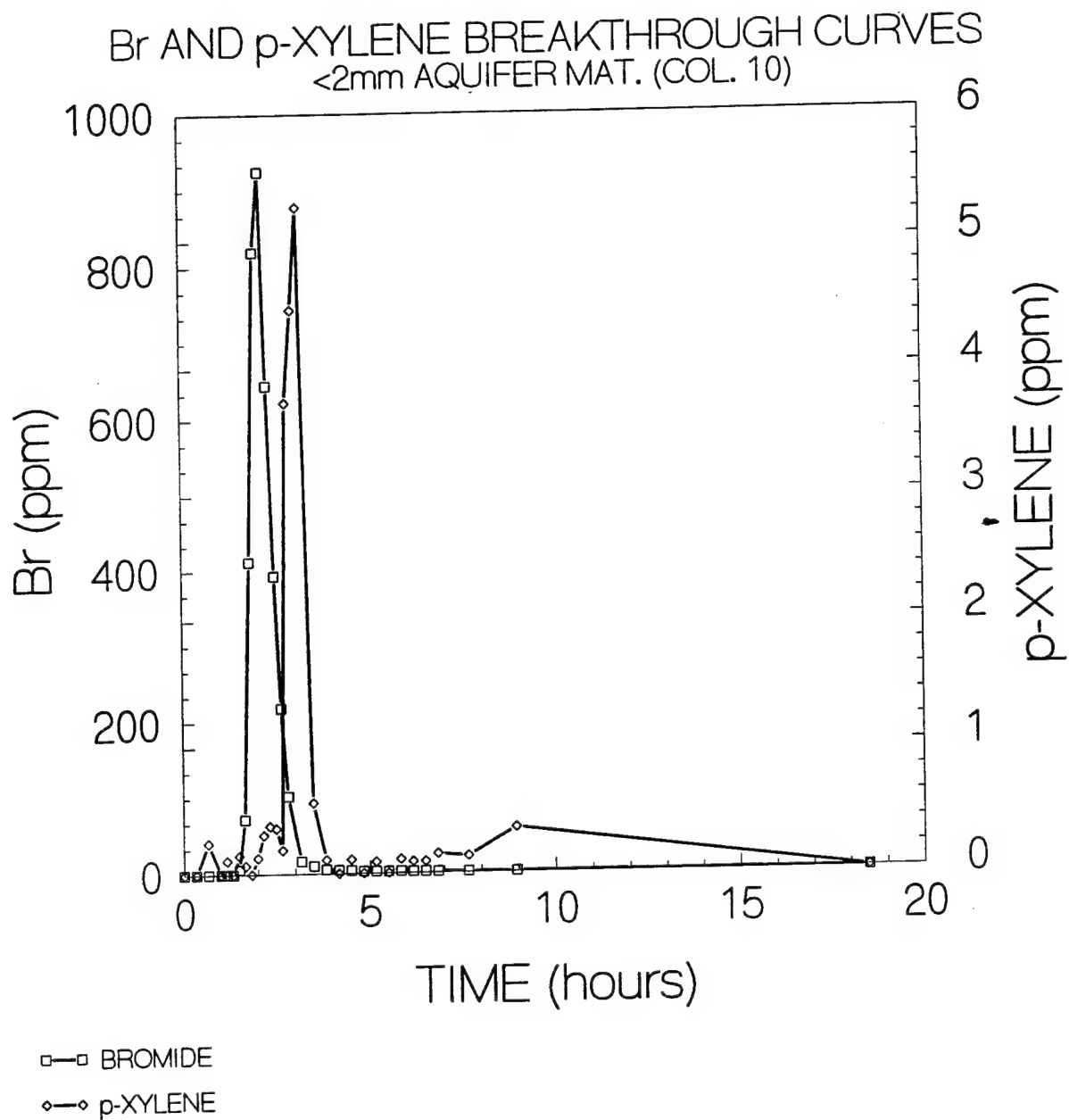
Figure 7. Bromide breakthrough curve for Column 10 test.

predicted Br⁻ masses were 1243 mg Br⁻ to 1361 mg Br⁻ or a predicted mass balance error of 24 to 35 percent greater than the actual injected mass. Flow rate variation does not bracket the injected mass, but a question remains as to the representativeness of an average rate for a column. Only a single flow rate was measured for Column 10, so no range of predicted masses can be calculated.

TABLE 1. TEMPORAL MOMENTS, COLUMN 9 (UNSIEVED), BROMIDE AND P-XYLENE

Tracer	Zero Moment (mg-hr/L)	First Moment (mg-hr^2/L)	Second Moment (mg-hr^3/L)	Corrected Velocity (cm/hr)	Corrected Dispersion Coefficient (cm^2/hr)	Predicted Mass (mg)	Injected Mass (mg)
Bromide	0.531E+04	0.105E+06	0.32E+07	5.65	198.59	1296.6	1007
p-Xylene	0.100E+02	0.840E+02	0.851E+03	15.72	261.40	2.45	15.08

Errors in the mass balance for p-xylene in both Column 9 and Column 10 (Table 2) tests were due to the same two causes as the Br⁻ error and the uncertainty in whether a true p-xylene + water solution or a p-xylene emulsion was injected. The actual mass of organic injected does not depend on the solution being a true solution or an emulsion, but determining the p-xylene concentration and the transport properties are different for an emulsion or a solution. Emulsion "particles" could sequester in pores and thus be removed from water moving through the column. The "particles" would not necessarily be sampled in a representative manner, thereby altering the concentration vs. time data and the moments analysis. Loss of p-xylene during sample preparation and analysis would also decrease the apparent p-xylene concentrations and affect the mass balance calculations. Analytical difficulties discussed previously suggest that sample loss could have been significant and is probably the cause for the large discrepancy between predicted and actual mass of p-xylene.

A comparison of the error in predicted mass of Br⁻ between the sieved and unsieved columns reveals a 14 percent error for the sieved column and a 29 percent error for the unsieved column. The larger error for the unsieved column suggests that the more heterogeneous flow is not as well represented by the average flow rate. The 14 percent error for the sieved column is within the analytical precision given the conditions that prevailed during the test.

The glass column experiments also allowed comparison of the transport behavior of the organics and bromide. We have assumed that bromide is conservative (nonreactive), and its behavior is analogous to water. Therefore, bromide provides a baseline to which the behavior of the organics can be compared. The amount of time between the peak in the bromide concentration and the peak of the p-xylene concentration gives an indication of how much interaction occurred between the organic and the porous medium. The breakthrough behavior of p-xylene relative to bromide is shown in Figure 7. The organics were only slightly retarded indicating that adsorption of the organics was limited. The small amount of retardation observed for the organics is consistent with the low amount of organic carbon in the aquifer material.

TABLE 2. TEMPORAL MOMENTS, COLUMN 10 (SIEVED), BROMIDE AND P-XYLENE

Tracer	Zero Moment (mg-hr/L)	First Moment (mg-hr^2/L)	Second Moment (mg-hr^3/L)	Corrected Velocity (cm/hr)	Corrected Dispersion Coefficent (cm^2/hr)	Predicted Mass (mg)	Injected Mass (mg)
Bromide	0.634E+03	0.151E+04	0.445E+04	47.70	729.91	1902.5	1670
p-Xylene	0.556E+01	0.372E+02	0.391E+03	15.65	486.95	16.68	104

The glass column experiments provided an opportunity to examine solute behavior for both the composite and < 2mm fraction Columbus AFB aquifer material. The physical components of the solute transport, velocity and dispersion, were expected to be different because of the large differences in particle size distribution. It was not apparent that the sorption behavior would be different because the dominant reactive component was anticipated to be in the smaller size fraction.

Breakthrough curves for bromide from columns with the composite material revealed extended tailing when compared to that from the columns with the < 2mm material. To account for this difference in behavior, different conceptual models were proposed for these columns. Definition of the underlying conceptual model is an important first step in applying computer models to the resolution of environmental problems.

As used here, a conceptual model consists of the following: the geologic structure including stratigraphy and lithology of a site, boundary conditions, initial conditions, parameter heterogeneities in space and time, physical, chemical and biological processes, and temporal conditions (transient versus steady state) for state variables.

The scale of the glass columns and the fact that only the effluent was sampled means the parameters are considered homogeneous. Steady-state flow conditions were established and solute was introduced through the top boundary. Sampling at the effluent end and the small width to length ratio also lead to a one-dimensional system. The structure is assumed to be uniform, but there are clearly differences in particle size distributions between the two columns. Different particle size distributions along with the observed long tail behavior of the breakthrough curve leads to two conceptual models being proposed for the columns. The advection dispersion equation (ADE) is proposed for the column with the < 2mm material and the mobile/immobile or two region model for the column with unsieved material.

For contaminant transport in porous media, the ADE has been the traditional conceptual model (Reference 20). The physical processes are advection and dispersion for the bromide. For the organic tracer, linear equilibrium sorption is added as a chemical process. The governing equation for these conditions is

$$R\frac{\partial C}{\partial t} = D\frac{\partial^2 C}{\partial x^2} - v\frac{\partial C}{\partial x} \tag{5}$$

where C is the concentration; D is the dispersion coefficient; v is the pore water velocity; R is the retardation factor defined below; x is the space coordinate; and t is the time coordinate.

Two terms need further definition. The pore water velocity, v, is the Darcy flux (q) divided by the volumetric water content (θ). The retardation factor, R, is

$$R = 1 + \frac{K_d \rho_b}{\theta} \qquad (6)$$

where K_d is the linear equilibrium sorption coefficient and ρ_b is the bulk density. For saturated conditions, the porosity, ϕ, is used for θ.

Initial and boundary conditions must be specified in order to complete the model. These are

$$C(x,0) = C_i \qquad (7)$$

$$\left(C - \frac{D}{v} \frac{\partial C}{\partial x} \right)\Big|_{x=0} = \begin{cases} C_o & 0 < t \le T_o \\ \\ 0 & t > T_o \end{cases} \qquad (8)$$

$$\frac{\partial C}{\partial x}(L,t) = 0 \qquad (9)$$

where T_0 is the input duration; C_i is the initial concentration (assumed to be zero for all columns); and C_0 is the input concentration. This completes specification for the ADE equation used to analyze the column experiments.

A characteristic of the ADE is the Gaussian breakthrough curve that retains a symmetric shape throughout the transport domain. However, asymmetric breakthrough curves were observed for all tests using the glass or steel column. Data from petroleum recovery cores also displayed asymmetry, and the mobile/immobile or capacitance model was formulated to describe the behavior of the breakthrough curve (Reference 21). The resulting equation has been used to characterize asymmetric curves from columns due to physical effects such as dead-end pores or exclusion volumes and chemical effects such as two-site sorption (Reference 22). The equation is formulated the same whether the effect is physical or chemical. For the analysis of the column experiments, the mobile/immobile transport equation is

$$(\theta_m + f\rho_b K_d)\frac{\partial C_m}{\partial t} + \left[\theta_{im} + (1-f)\rho_b K_d\right]\frac{\partial C_{im}}{\partial t} = \theta_m D_m \frac{\partial^2 C_m}{\partial x^2} - q\frac{\partial C_m}{\partial x} \qquad (10)$$

where θ_m is the volumetric water content of the mobile region; θ_{im} is the volumetric water content of the immobile region; C_m is the concentration of solute in the mobile region; C_{im} is the concentration of solute in the immobile region; f is the fraction of sites in the mobile region; ρ_b is the bulk density; K_d is the linear equilibrium sorption coefficient; D_m is the dispersion coefficient; q is the Darcy flux; x is the space coordinate; and t is the time coordinate. Also, if a first order exchange model is assumed to govern the transfer of solutes between the mobile and immobile regions. The relationship is

$$\left[\theta_{im} + (1-f)\rho_b K_d\right]\frac{\partial C_{im}}{\partial t} = \alpha^* (C_m - C_{im}) \tag{11}$$

where α^* is the first order rate constant that governs the exchange of solute between the mobile and immobile regions.

In using the computer program CXTFIT (Reference 16) to fit the mobile/immobile model, two dimensionless parameters are introduced. The parameter, β, is calculated as

$$\beta = \frac{\theta_m + f\rho_b K_d}{\theta + \rho_b K_d} \tag{12}$$

where all parameters have been previously defined. In equation 12, β describes the volumetric relationship between the mobile region and the total system. The second dimensionless parameter used by CXTFIT is defined by

$$\omega = \frac{\alpha^* L}{q} \tag{13}$$

where L is the total column length and q is the Darcy flux. ω compares the rate of interaction between the mobile and immobile zones to the rate of water movement through the column.

Boundary and initial conditions for the mobile/immobile model are the same as for the ADE (Equations (7) - (9) except that these conditions are applied to C_m and an initial condition is required for Equation (11). For these analyses, this initial condition is

$$C_{im}(x,0) = 0 \tag{14}$$

Analysis will focus on the glass column experiments numbers 9 and 10. Breakthrough curves for bromide from these columns are given in Figures 6 and 7, respectively. These two experiments represent different matrix compositions with column 10 using the < 2mm material only, and bulk aquifer material comprised Column 9. This sequence of experiments presented an opportunity to determine the behavior of porous materials at a smaller scale before moving on to the larger column experiments.

The moments for the two breakthrough curves are given in Tables 1 and 2. Other pertinent values for these experiments are input fluxes of 0.244 and 3.0 L/hr and input durations of 4.0 and 0.557 hours for Columns 9 and 10, respectively. Column 9 exhibited a skewed breakthrough curve with a long tail (Figure 6). Analyses of the moments assuming that the ADE is the correct model and correcting for the input pulse duration are given in Table 1. The long tail exhibited by column 9 and low flux rate are expected to lead to a large dispersion coefficient.

Model discrimination is an important step in field application of computer codes. An algorithm was developed (Reference 23) for model discrimination using one-dimensional forms of the ADE. The approach was predicated on a two-tiered sampling scheme. An initial sampling would allow predictions of system response by proposed models, and a second sampling would be conducted based on results of the predictions from the initial data set.

These predictions allowed sampling points to be identified in both space and time so that an experimental design can be implemented to test differences in the various models. This approach was demonstrated on the Cape Cod aquifer experiment (Reference 24). In the present study, data were available for the initial round of sampling and the experimental design was fixed with sampling only occurring at the effluent. For the initial round of sampling, Reference 23 indicated that the error or residual term from fitting the equations to the data and analysis of the residuals were criteria to discriminate among models. These criteria are reported in Table 3 and Figures 8-11. Although limitations in sampling only the effluent do not allow us to take the glass columns any further, the steel column may provide a better test bed.

In an *a priori* sense, the results are expected to reveal a better fit for the mobile/immobile equation to the data from Column 9 because of the long tail and asymmetric breakthrough curve. Both models would fit the data from Column 10 due to the relatively symmetric breakthrough curve. The principle of parameter parsimony is expected to govern in the case of Column 10 and the ADE equation would be selected because it has fewer parameters.

The results of fitting the two data sets to both models are presented in Table 3. Column 10 is considered first because it is assumed to represent a simpler system. One of the first comparisons is the residual sums of squares (SSQ) from fitting. For Column 10, there is a slight decrease in the SSQ value for the mobile/immobile model suggesting a better fit. This decrease in SSQ was expected even if the mobile/immobile model is not conceptually correct because there were four fitted parameters in the mobile/immobile model versus two in the ADE. Conceptually, the mobile/immobile model can collapse to the ADE if the values for β and ω are one and zero, respectively. In fitting the Column 10 bromide pulse with the mobile/immobile model, the value for ω is zero, but the value for β is 0.21. The value for β is meaningless in this case because there is no exchange occurring between the mobile and immobile regions. If the velocity and dispersion coefficient for the mobile/immobile model are divided by 0.21, then their value are essentially the same as the velocity and dispersion coefficient for the ADE. This demonstration indicates the importance of selecting the correct conceptual model or at least the testing of alternative conceptual models. Fitting routines will attempt to fit the data as specified, and the result can be meaningless parameters which in this case was a mobile fraction of 21 percent. Using the model with the parameters, disparate predictions of system behavior can be model that lead to the wrong conclusion in terms of compliance or proposed action.

Values for the t-statistic for the fitted parameters are also provided in Table 3. The nonlinear least-squares method does not necessarily meet the assumptions required to use this statistic for statistical significance testing, but these statistics can provide some insight into interpretation of the fit (Reference 25). It is assumed that a t value greater than 2 is indicative of statistical significance. For column 10, the t values for the parameters of the mobile/immobile model are all less than 1, suggesting that these parameters are not statistically significant. Table 3 clearly shows that both parameters for the ADE from Column 10 have relatively large t values. These results support the ADE as the model to describe the bromide data from Column 10 even without imposing parsimony. The low t values for the mobile/immobile model parameters must be scrutinized in the same way as the parameter values themselves. Dependencies between parameters spreads variation among the parameters. Therefore, uniformly low t statistics were observed for the parameters from the mobile/immobile model.

25

TABLE 3. CXTFIT SUMS OF SQUARES (SSQ), PARAMETER ESTIMATES, AND T-STATISTICS FOR BROMIDE FROM COLUMNS 9 AND 10.

Model	Column 9	Column 10
	------------------ SSQ ---------------------	
ADE	20081.1	32596.6
MIM	16918.1	32171.7

	Parameters							
	----------- Column 9 --------------				------------- Column 10 ------------			
Model	V (cm/hr)	D (cm^2/hr)	β	ω	V (cm/hr)	D (cm^2/hr)	β	ω
ADE	6.64	420.17			53.30	25.94		
MIM	7.25	300.75	0.76	0.63	11.51	5.17	0.21	0.0

	t-Statistics							
	----------- Column 9 --------------				----------- Column 10 ------------			
Model	V	D	β	ω	V	D	β	ω
ADE	21.4	23.3			220.1	9.5		
MIM	10.3	1.7	2.3	0.6	0.7	0.6	0.7	0.0

Column 9 was analyzed the same way. A larger difference in SSQ between the ADE and mobile/immobile models is seen, but the significance of this difference is not apparent. Intuitively, the lower SSQ for the mobile/immobile model represents the better description for the long tail of the breakthrough curve, and this is assumed to be the appropriate conceptual model. The t-statistics for the dispersion coefficient and ω (Table 4) confound this issue because as with Column 10 the t-statistics for parameters from the mobile/immobile model are less than the value of 2 suggested as a level of significance. The magnitudes of the velocities and dispersion coefficients are more consistent between the two models than was the case for column 10.

Plots of the residuals (defined as observed concentration -predicted concentration) for each model from the two columns are given in Figures 8 - 11. The behavior of the residuals between the models for a given column are consistent and do not support selection of one model over the other. Figures 8 and 9 (Column 9) indicate that a period of low predictions occurred beginning approximately ten hours after the tracer was introduced and continuing until the end of the experiment. For Column 10, the residuals (Figures 10 and 11) were somewhat better behaved. The period 2-4 hours after bromide injection corresponded to the period where breakthrough occurred (Figure 7). During this time, the residuals revealed a pattern of overprediction on the rising limb and underprediction on the falling limb of the breakthrough curves for both models. The residuals approach zero as the breakthrough diminishes. The residuals provide little insight into the selection of one model over another even for Column 9.

A final analysis of the glass column data involves the use of a single statistic. The possibility that a single statistic can be used to distinguish between models has much appeal. A relatively simple index can be used to make decisions about different models on a

quantitative basis. Four different criteria are presented that could be used to distinguish between various conceptual models in an inverse problem (Reference 26). One discrimination statistic (Reference 27) is

$$AIC(B) = S(B) + 2M \qquad (15)$$

where AIC(B)is the Akaike Information Criteria; S(B)is the logarithm of the likelihood function; B is the vector of estimated parameters; and M is the dimension of B. The minimum value for the AIC indicates the most appropriate model. The AIC formulation also has the concept of parsimony imbedded. Transforming the SSQ for each model to the log of the likelihood function, the AIC values for each model from column 9 are 8.3 for the ADE and 12.2 for the mobile/immobile model, and for Column 10 the AIC values are 8.5 for the ADE and 12.5 for the mobile/immobile model. Using this statistic, the ADE would be selected over the mobile/immobile model for both columns. This result is a function of the parsimony component of the AIC. The penalty for the four estimated parameters from the mobile/immobile model is substantial using Equation (15). If the mobile/immobile model were to be selected, the value for S(B) would have to be essentially zero given the number of fitted parameters (2 for ADE and 4 for mobile/immobile) and the value for S(B) from the ADE fit.

Additional interpretations of these data are possible. The use of the mobile/immobile model is one approach to describe long-tailed or skewed breakthroughs. Other research has shown that the effect of heterogeneities and their scale relative to the overall experimental scale is important (Reference 28). Breakthrough curves became more Gaussian as transport distances increased, and the researchers were able to show this by measuring concentrations at ten locations within a 30 cm sample (Reference 28). They also noted that the number of samples allowed an unique estimation of the parameters as opposed to mathematical fitting of an effluent curve that does not provide unique estimates for these parameters. Data were not available from the glass columns to characterize concentrations at locations other than the effluent. Further analyses are not justified given the available data.

Using estimated parameters for making predictions, a Stage 2 sampling scheme (Reference 23) was generated to determine if the large column could be used to discriminate between the models. The parameters in Table 3 from Column 9 were used with the appropriate model and simulations were made for 500 cm and 1000 cm distances. The results of this exercise are shown in Figure 12. At 500 cm, the two curves appear to be close and measurement errors would make it difficult to distinguish between the ADE and mobile/immobile models. The simulations at 1000 cm reveal the more delayed response of the ADE. The length of the large column is approximately 300 cm which means the differences between the models are even less distinguishable. This example further illustrates the difficulty in deciding which model should be used.

The organic tracer, p-xylene, was analyzed using the parameters determined by fitting the bromide for the velocity, dispersion, β, and ω. Column 9 was analyzed because the injection method used for Column 10 was different. As indicated in previous discussion, the p-xylene breakthrough curves were erratic and mass conservation was inadequate. For both the ADE and mobile/immobile models, the fit was very poor for the retardation factor, R, when parameter values from the bromide and the input concentration were fixed. The R values were 4.82 for the ADE and 4.11 for the mobile/immobile mode.

From a quantitative standpoint, either model can be selected for either column. This reveals the art in groundwater transport modeling in terms of model selection. In a regulatory arena, a temporal frame must be established, then the most conservative model (in terms of violating a limit) can be selected.

B. STEEL COLUMN EXPERIMENTS

1. Column C

Column C was run for 142 hours with the Br and p-xylene. The Br tracer and p-xylene were mixed and injected into the ponded water on top of the column, and the injected solution was stirred by the mixing device for several hours. Time 0 for this test was when the pump was started. Total of 11,735 mg of Br and 2750 mg of p-xylene were injected.

Both the p-xylene and Br data obtained maximum concentrations within 30 hours after injection (Figure 13, Tables C5-C29). Measured flow rates averaged 0.51 L/min (30.6 L/hour).

Analysis of the Br and p-xylene breakthrough data from port 25 (effluent port) show uncorrected velocities of 14.2 cm/hr and 23.4 cm/hr, respectively and uncorrected dispersion coefficients of 4262 cm^2/hr for Br and 13747 cm^2/hr for p-xylene. Storage and analytical difficulties precluded p-xylene measurements in samples extracted from Ports 1-24. Br measurements exhibited considerable variation in uncorrected velocities, uncorrected dispersions, and mass balance. Predicted mass from Ports 2, 21, 24, and 25 are within 10 percent of the actual mass injected, but the remaining predictions range from 10 percent to 155 percent of the input mass. Little correlation exists between uncorrected dispersion and uncorrected velocity or uncorrected dispersion and predicted mass when compared port by port. Uncorrected velocity and predicted mass show slight correlation (linear r^2 = 0.36, polynomial r^2 = 0.5). Uncorrected dispersion, velocity and predicted mass calculated from Ports 21 and 24 are in relatively close agreement. Uncorrected velocities for Br from the upper four ports (21-24) range from 1.4 cm/hr to 2 cm/hr. Average uncorrected velocity and predicted mass computed for each vertical level (i.e., four ports) were correlated (r^2=0.68). The predicted mass from the top four ports is 2270 over the actual mass, 20 percent under for the bottom 4 ports. Mass balances for the middle ports were consistently under estimated, ranging from 15 percent to 70 percent. Uncorrected dispersion by vertical level does not appear to be correlated with velocity or predicted mass.

2. Column D

Br and 1-methylnaphthalene (MNAP) were injected in this test with total masses of 11,000 mg and 450 mg, respectively. The average flow rate was 0.29 L/min or 17.5 L/hr, and the contents of the reservoir (Br and MNAP) were pumped into the column in 38 minutes. The Br and naphthalene concentration maxima occurred within 30 hours of injection (Tables C30-C57). This result was similar to that in Column C, even though the flow rate for Column D was nearly one-third the value from Column C. Large variations in both the Br and the
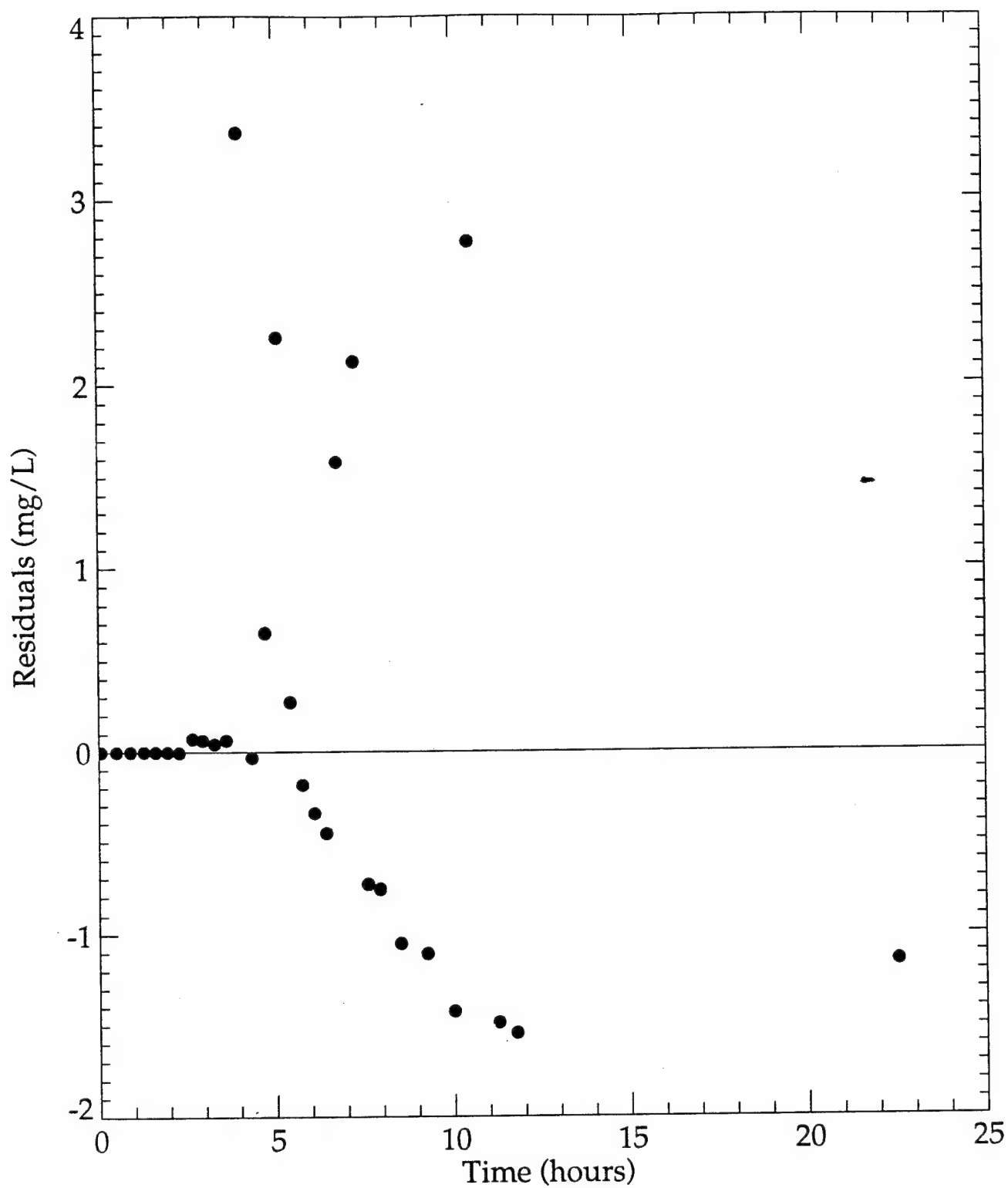
Figure 8. Residuals plot, Column Test 9, using ADE model.
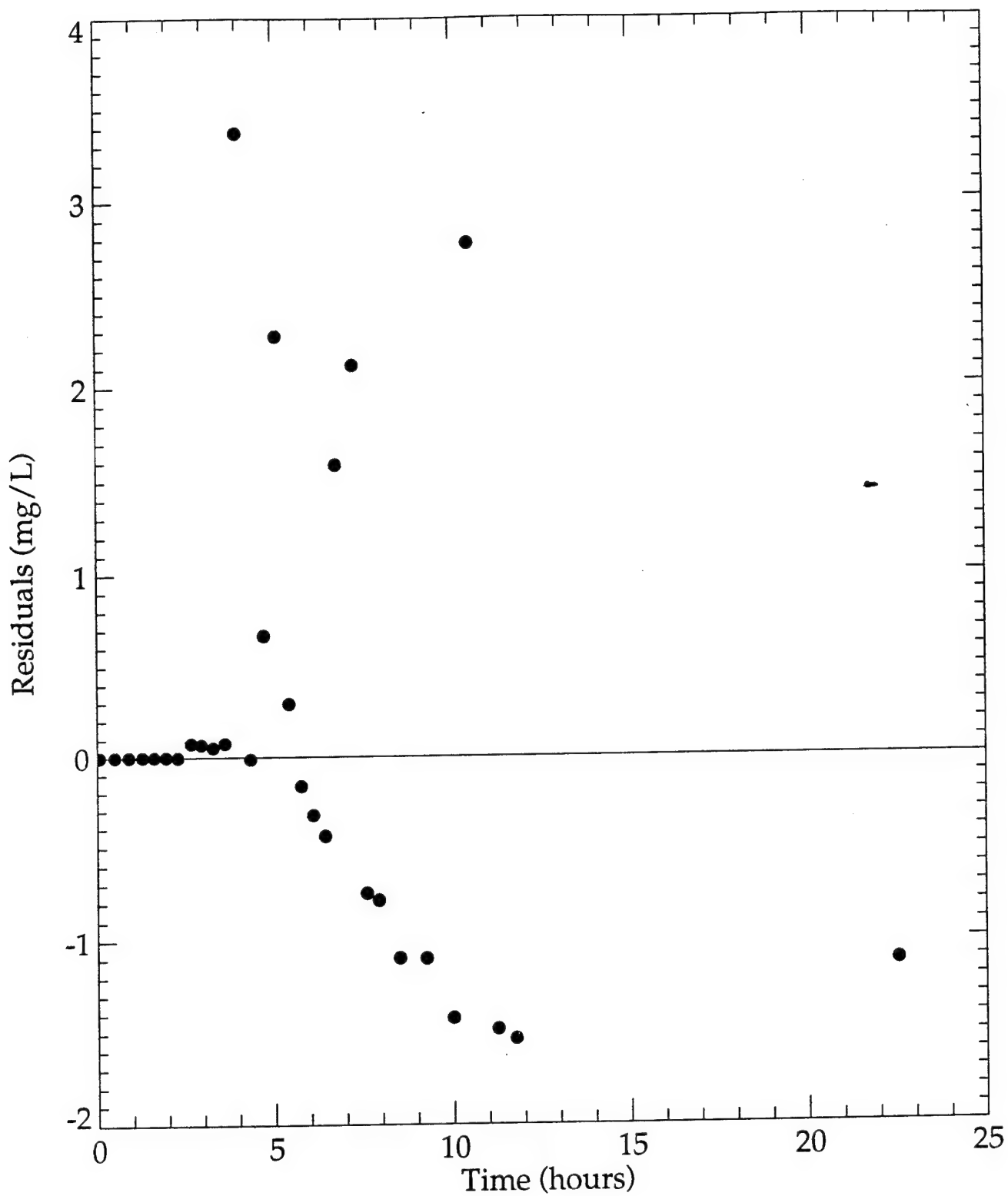
Figure 9. Residuals plot, Column Test 9, using mobile/immobile model.
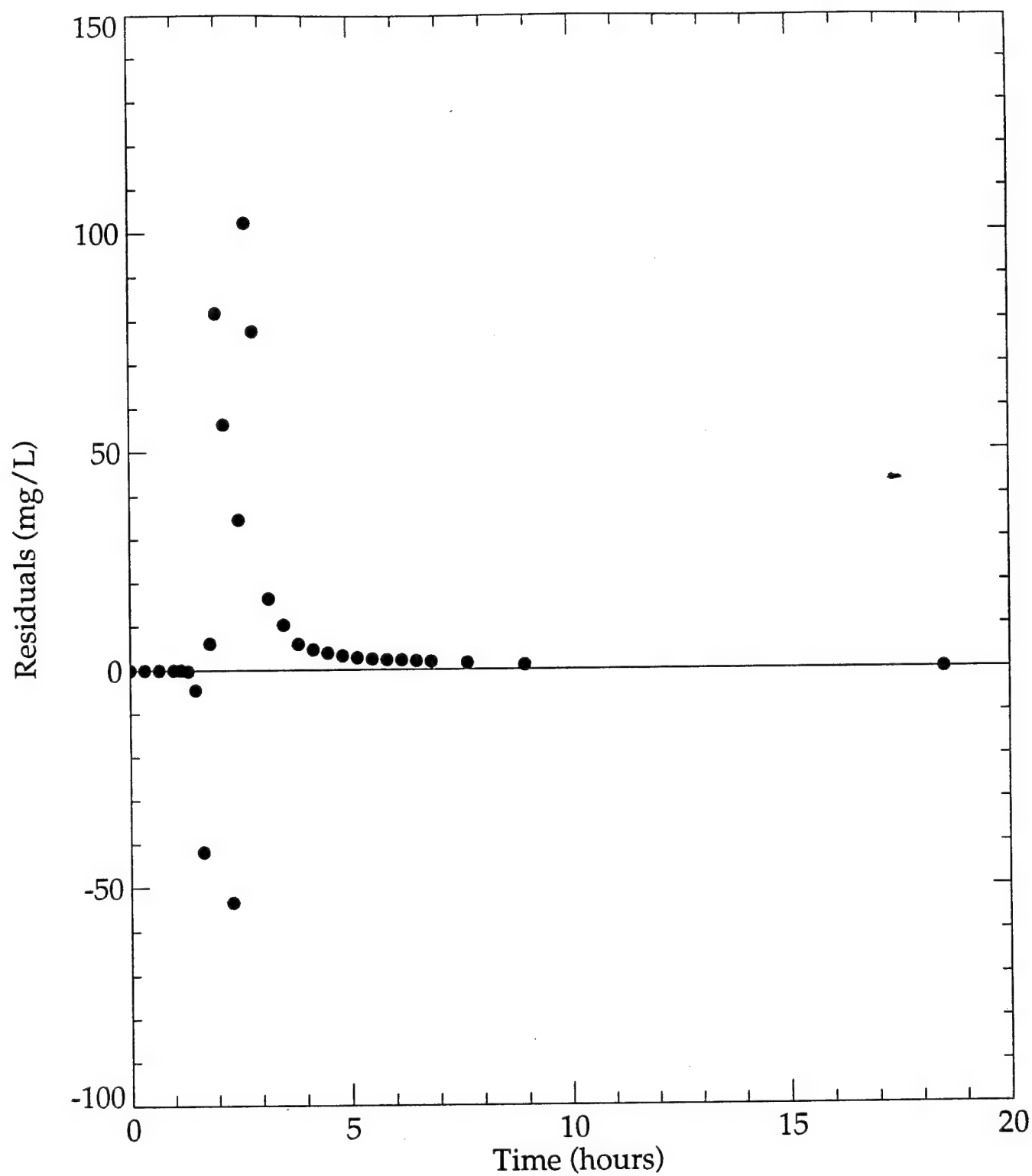
Figure 10. Residuals plot, Column Test 10, using ADE model.
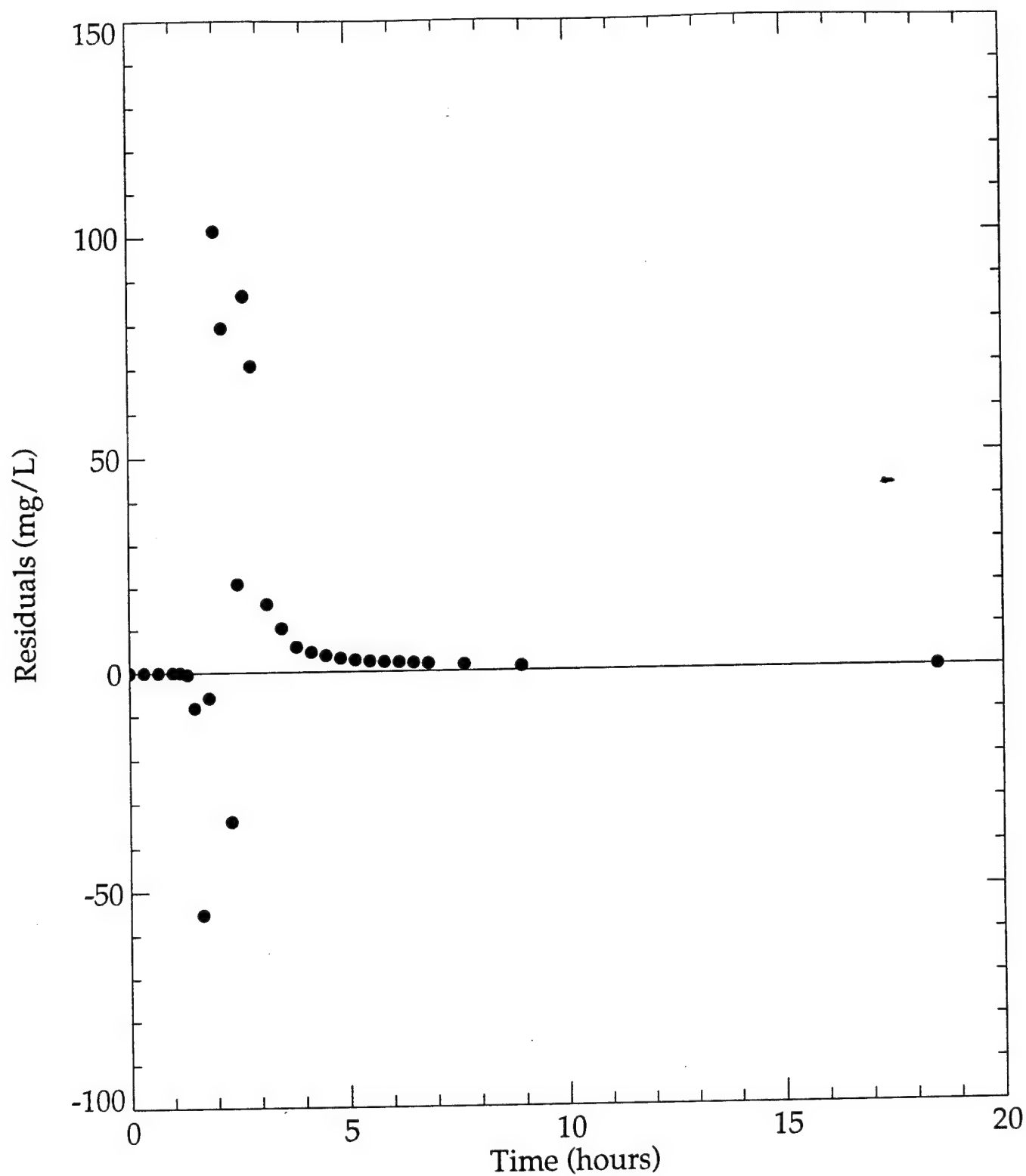
Figure 11. Residuals plot, Column Test 10, using mobile/immobile model.
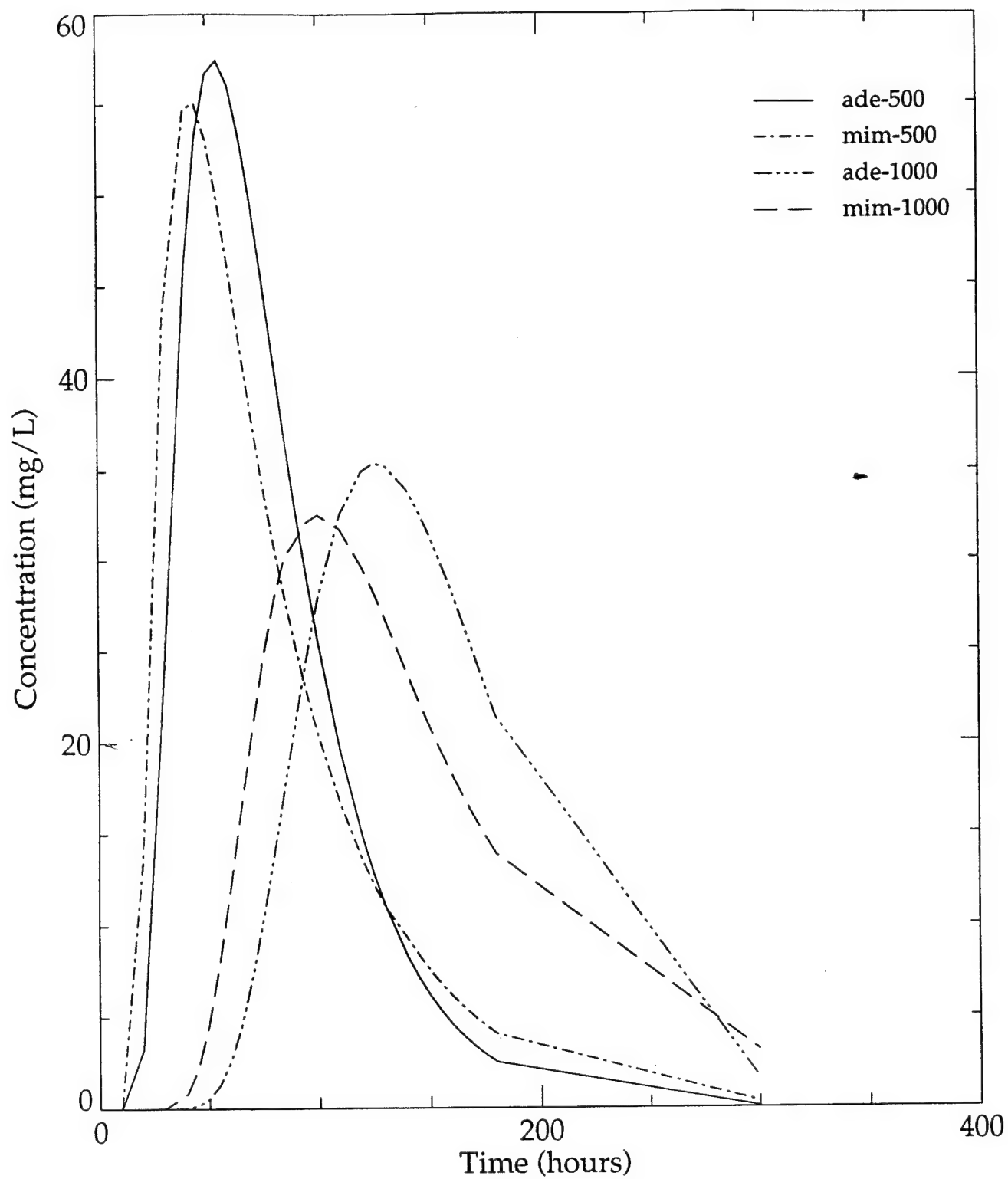
Figure 12. Model comparisons at 500 cm and 1000 cm from source.
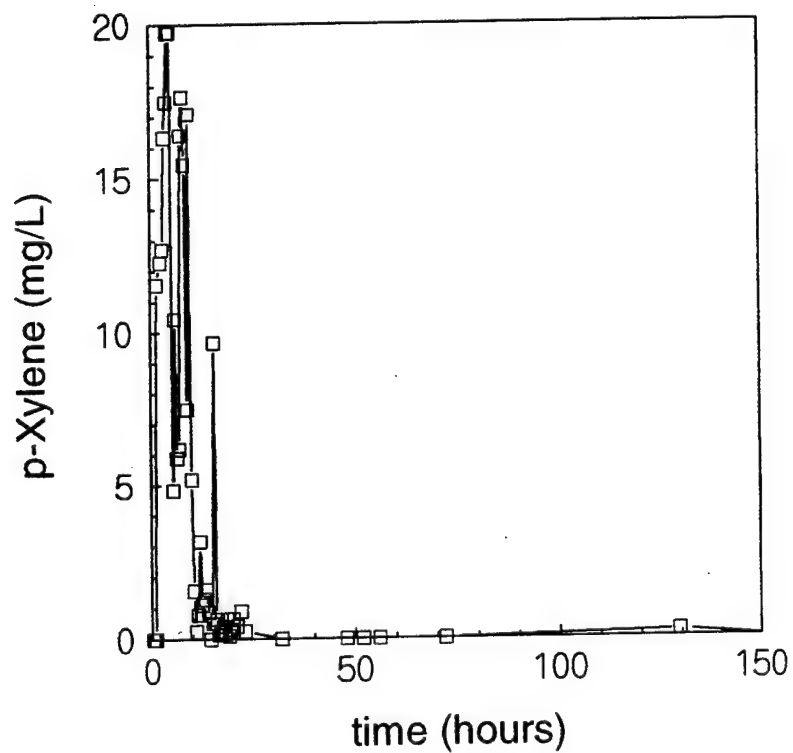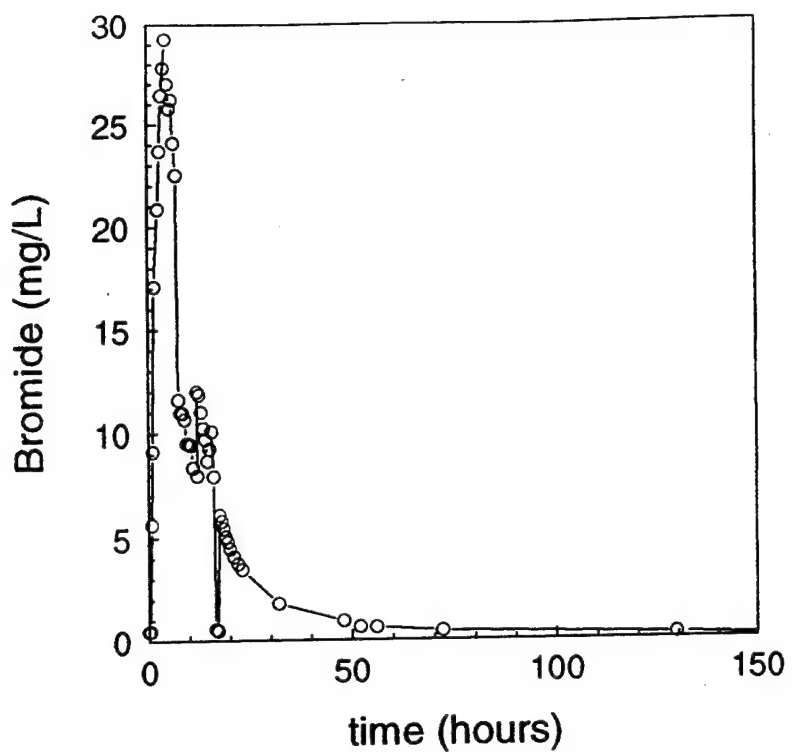
Figure 13. Bromide breakthrough (upper) and organic breakthrough (lower), Steel Column Test C.

Corrected velocities-ranging from 0.81 cm/hr to 15.03 cm/hr, corrected dispersions ranging from 4 cm^2/hr to 217 cm^2/hr, and predicted masses from 726 mg to over 40,000 mg were calculated from the Br data for each port. The data from one port are not highly correlated to data from other ports, and do not show the relation between calculated value and the level from which the data were collected. Port 1 is the only port that approximates the injected Br mass, and most of the other ports gave predicted masses that were greater than the input concentration.

The MNAP data show large variation in corrected velocities, dispersions, and predicted masses. Corrected velocities ranged from 0.72 cm/hr to 11.4 cm/hr; corrected dispersions ranged from 4.4 cm^2/hr to over 1100 cm^2/hr, and the predicted mass ranged from 17 mg to 1168 mg. Velocity, dispersion, and predicted mass are slightly correlated. There is no additional correlation if the data from a given level are pooled and averaged. This observation could result from data variability. MNAP data from several ports were not collected due to loss of naphthalene in sampling, storage, and/or analysis.

3. Column E

Br and naphthalene were used in Column E with total injected masses of 14,077 mg and 450 mg, respectively. Average flow rate was 34 L/hr (0.58 L/min), and the Br and naphthalene solution was pumped in over 40 minutes. The point-source delivery port was used for injection in this experiment. Thus, all of the tracer solution was in the column when injection was completed. Most of naphthalene and Br passed through the column within 30 hours of injection as in previous tests (Appendix D). Variation in the naphthalene analysis obscured the tail of the naphthalene curve some, but the trend with time was clear (Tables C58-C84).

The Br data varied considerably, therefore the parameters calculated from the moments analysis also varied. The corrected velocity from Ports 1 to 24 ranged from 0.77 cm/hr to 33 cm/hr, the corrected dispersion ranged from 2 cm^2/hr to 325 cm^2/hr, and the predicted mass ranged from 201 mg to over 49,000 mg. The highest velocity of 33 cm/hr and largest dispersion of 2499 cm^2/hr were calculated for Port 25. The data showed little correlation when averages from each level were compared.

Naphthalene data from only four ports were recovered due to difficulties in sample storage and analysis. Corrected velocities ranged from 5.7 cm/hr to 24 cm/hr, corrected dispersion ranged from 74 cm^2/hr to almost 3000 cm^2/hr, and predicted mass was 85 to 944 mg. The predicted masses calculated from data obtained in this test were in better agreement than any data sets reported above. There were not enough data to compare averages of each level to the other levels.

4. Discussion and Analysis

The steel column experiments offer the advantage of making point measurements at intermediate distances between the source and outlet and compare the results at these intermediate distances with the outlet and the glass column experiments. The opportunity to examine point behavior in conjunction with system behavior as manifested in the effluent concentrations is an advantage of the steel column experiment.

As with the glass column experiments, data on the hydrologic properties were not collected on the steel column. Also, this column was filled with the composite Columbus AFB aquifer material. All analyses rely on interpretation of the breakthrough curves from each experiment. Discussion from Section 2B indicated that data on the organic tracers were limited, so the analysis of the steel column experiments will focus on the bromide results.

a.   Comparison Between Experiments

Three experiments Columns C, D and E, were compared for the reproducibility in breakthrough curves between locations. Caisson experiments reported by Fuentes (Reference 29) revealed consistent behavior between breakthrough curves for a given location for unsaturated flow conditions. For our comparison dimensionless time and concentration were defined as

$$T^* = \frac{q \cdot t}{L} \qquad (16)$$

and

$$C^* = \frac{C(t) - C_i}{C_o - C_i} \qquad (17)$$

where T^* is the dimensionless time; q is the Darcy flux, t is time; L is the distance from the surface to the sampling location; C^* is the dimensionless concentration; $C(t)$ is the concentration measured at time t; C_i is the initial concentration; and C_o is the initial concentration for the input.

The curves for each sampling port from the three steel column experiments are plotted on a single figure allowing a graphical comparison (Figures D-1 to D-25). Rapid dilution of the initial input can be observed in these figures. The four ports nearest the surface, are located approximately 30 cm below the surface. Their peak concentrations are approximately 10 percent of the initial concentration (Figures D-21 to D-24). In comparison, Fuentes (Reference 30) observed relative peak concentrations of 90 percent at 36 cm below the surface for the saturated caisson experiment. For the steel column, concentration at the effluent has decreased another order of magnitude (Figure D-25). Partial explanation for the large dilution may be the short duration of the input pulse. In the experiments reported by Fuentes (References 29 and 30) input durations were six days. In the experiments reported here, they were less than one hour and with higher input concentrations.

In comparing the breakthrough curves in Figures D-1 to D-25, there does not appear to be much consistency between experiments for the port concentration behavior, but the effluent curves behave in a similar manner. This could be due to a combination of the sampling interval and the mixing that occurs in the outlet that smoothes the response. For the point samples, the peak relative concentrations were higher for the two later experiments (D and E) compared to Column C. These analyses indicate that consistency between the steel column experiments for a given point did not exist except for the effluent concentrations.

36

b. Mean Breakthrough Curves

The variability in the breakthrough curves in Figures D-1 to D-25 makes interpretation difficult if one compares to the effluent. The uncertainty that is associated with predicting the concentration at a single point is large, therefore moments of the concentration distribution in either space or time are used. Four samplers were located at six levels in the large column (Figure 4). Sampling was usually conducted at the same time for each of the levels (Tables C1 to C25). To smooth these data, the arithmetic average for each level was calculated by editing the breakthrough data for each sampler so that the time values were consistent at a level and then summing and dividing the concentrations by 4. These breakthrough curves are termed the mean breakthrough curves for a given set of ports. Figures D-26 to D-43 are the mean breakthrough curves for Columns C, D, and E. These breakthrough curves appear to be smoother than individual curves, and the effect of the lower flux rate for Column D is seen through the higher peak concentrations at all levels.

The mean breakthrough curves were treated as a one-dimensional representation of the steel column experiments. Temporal moments assuming a one-dimensional ADE are given in Tables 4 to 6. The moments for the effluent breakthrough from the same test are also supplied for comparison. From these tables, one can see that the velocities and dispersion coefficients are about 10 times greater for the effluent than for the mean breakthrough curves. This difference in the behavior between the effluent and point values was observed in previous caisson experiments (Reference 29). In Column C the velocities appear to fluctuate with distance from the surface, but in Columns D and E, a trend of increasing velocity with depth (except for level 3 in Column D) is obtained.

Treating the mean breakthrough curves as a one-dimensional ADE allows calculation of the dispersivity length scale from the temporal moment data in Tables 4 to 6. These dispersivities are given in Table 7. Again, the effluent values were greater than those from the mean curves. Columns D and E appear to be more consistent in terms of magnitude and trend when compared with Column C. Values for velocity and dispersion from the moments analysis for glass Column 9 were 5.65 cm/hr and 198.59 cm^2/hr which gives a dispersivity of 35.1 cm, or 63.3 cm if the best fit values using the fitting procedure (Reference 16) for Column 9 from Table 3 are used. Both the moments and least-squares fitting procedures have their limitations, but the magnitudes of the dispersivities from the glass column are consistent with those observed in the large column except for the effluent dispersivity from Column C. These results support the contention that additional mixing induced by the single outlet creates additional dispersion which is an artifact of experimental design.

As a final comparison, the mean breakthrough curves were fitted with the procedure used on the glass columns (Reference 16). These results are given in Table 8. Column C was omitted because the input pulse duration (T_0) was not known. Also, it should be remembered that the boundary condition imposed on the ADE by the fitting routine for Column E does not correspond to the point source condition that was used in this experiment. The parameters were estimated for the sampling ports using resident concentrations. Column effluent concentrations were treated as flux concentrations. One of the more anomalous results from this fitting was the difference in velocities for the outlet between Columns D and E.

Given that the input flux rate for Column E was twice that for Column D, there is no apparent reason for the calculated velocity to be a factor of four smaller for Column E. The moment-estimated velocities (Tables 5 and 6) exhibited the expected response. Another fit

37

was made using the resident concentration model for the effluent breakthrough curve, and these results are included in Table 8. The difference in the estimated velocity using the resident concentrations for Column E is a factor of seven greater than the flux concentration fit and more consistent with expectations. Column D exhibits the type of behavior that is more generally observed between fits using resident and flux concentrations. This exercise points to the problems that can be encountered when fitting data and interpreting results. It is critical to scrutinize the results from any fitting exercise and ensure that they are physically plausible.

TABLE 4: MOMENTS FROM MEAN BREAKTHROUGH CURVE FROM EACH LEVEL FOR BROMIDE PULSE FROM COLUMN C.

Port	Depth (cm)	Zero (mg-hr/L)	First (mg-hr^2/L)	Second (mg-hr^3/L)	V (cm/hr)	V' (cm/hr)	D (cm^2/hr)	D' (cm^2/hr)
6	34	0.468E+03	0.100E+05	0.478E+06	1.59	1.59	32.99	32.99
5	68	0.762E+02	0.846E+03	0.117E+05	6.12	6.12	50.37	50.37
4	102	0.973E+02	0.827E+03	0.865E+04	12.00	12.00	140.93	140.93
3	136	0.265E+03	0.117E+05	0.960E+06	3.08	3.08	178.43	178.43
2	170	0.566E+02	0.567E+03	0.687E+04	16.97	16.97	302.25	302.25
1	204	0.299E+03	0.118E+05	0.721E+06	5.17	5.17	288.30	288.30
Outlet	274	0.350E+03	0.739E+04	0.468E+06	12.97	12.97	3555.79	3555.79

V' and D' are values corrected for the input pulse.

TABLE 5: MOMENTS FROM MEAN BREAKTHROUGH CURVE FROM EACH LEVEL FOR BROMIDE PULSE FROM COLUMN D.

Port	Depth (cm)	Zero (mg-hr/L)	First (mg-hr^2/L)	Second (mg-hr^3/L)	V (cm/hr)	V' (cm/hr)	D (cm^2/hr)	D' (cm^2/hr)
6	34	0.171E+04	0.528E+05	0.249E+07	1.10	1.11	9.91	10.22
5	68	0.147E+04	0.595E+05	0.365E+07	1.68	1.69	29.14	29.83
4	102	0.142E+04	0.407E+05	0.164E+07	3.56	3.60	74.42	76.93
3	136	0.174E+04	0.882E+05	0.574E+07	2.69	2.71	52.42	53.41
2	170	0.863E+03	0.406E+05	0.242E+07	3.62	3.62	81.90	83.58
1	204	0.765E+03	0.380E+05	0.238E+07	4.11	4.14	110.88	113.02
Outlet	274	0.709E+03	0.144E+05	0.393E+06	13.52	13.73	645.43	676.47

V' and D' are values corrected for the input pulse.

TABLE 6: MOMENTS FROM MEAN BREAKTHROUGH CURVE FROM EACH LEVEL FOR BROMIDE PULSE FROM COLUMN E.

Port	Depth (cm)	Zero (mg-hr/L)	First (mg-hr^2/L)	Second (mg-hr^3/L)	V (cm/hr)	V' (cm/hr)	D (cm^2/hr)	D' (cm^2/hr)
6	34	0.110E+04	0.255E+05	0.805E+06	1.46	1.48	8.89	9.28
5	68	0.362E+03	0.858E+04	0.276E+06	2.87	2.91	35.27	36.80
4	102	0.382E+03	0.788E+04	0.226E+06	4.95	5.03	98.18	103.08
3	136	0.251E+03	0.569E+04	0.176E+06	6.00	6.09	148.47	155.19
2	170	0.165E+03	0.415E+04	0.139E+06	6.74	6.83	185.35	192.86
1	204	0.217E+03	0.599E+04	0.207E+06	7.37	7.46	185.69	192.53
Outlet	274	0.226E+03	0.206E+04	0.278E+05	30.01	31.15	1954.58	2183.27

V' and D' are values corrected for the input pulse.

TABLE 7. DISPERSIVITIES (CM) FOR MEAN EFFLUENT BREAKTHROUGH CURVES FROM COLUMNS C, D AND E.

Level	Depth (cm)	Column C	Column D	Column E
6	34	20.79	9.17	6.25
5	68	8.23	17.67	12.63
4	102	11.75	21.40	20.51
3	136	58.00	19.73	25.48
2	170	17.81	23.11	28.24
1	204	55.81	27.33	25.80
Outlet	274	274.13	49.27	70.09

TABLE 8. VELOCITY AND DISPERSION COEFFICIENT ESTIMATED BY NONLINEAR LEAST SQUARES METHOD FOR MEAN BREAKTHROUGH CURVES AT EACH DEPTH.

Ports	Depth (cm)	Column D — V (cm/hr)	Column D — D (cm^2/hr)	Column E — V (cm/hr)	Column E — D (cm^2/hr)
6	34	3.21	18.80	2.69	10.22
5	68	34.35	50.32	43.29	38.28
4	102	6.45	46.67	6.22	220.17
3	136	6.30	125.89	4.88	702.65
2	170	4.64	176.46	26.35	25.19
1	204	5.51	257.11	4.64	1032.19
Outlet	274	14.17	916.17	3.04	3915.69
Outlet res	274	18.03	1198.37	23.32	7746.09

From Table 8, a general increase in the dispersivities with distance from the source can be observed. At 102 cm from the surface, the dispersivities for Columns D and E were 7.2 cm and 35.4 cm, respectively. The dispersivity value at 102 cm for Column E was essentially the same as that for glass Column 9.

The effect of the fitting method is further demonstrated by the calculation of effective porosities using the input flux and velocities for each layer. In Table 9, the porosities for the moment-calculated velocities and reported input rate are given, and some values are greater than 1.0 which is physically impossible. Effective porosities estimated using the velocities derived by the nonlinear least squares method are given in Table 10. No consistency for Column E exists between the moment and least-squares estimated porosities.

The correct conceptual model for the larger column represents another source of uncertainty in the analysis. One weakness in this experiment is the lack of physical parameters to determine the flow field. This same weakness can be found in the caisson experiments (References 30 and 31). Both the magnitude and spatial distribution of the saturated hydraulic conductivity and porosity are required with the hydraulic conductivity term being the most sensitive for transport calculations. The glass columns were more representative of a one-dimensional system and made analysis more amendable to the equations (Reference 16). The problem with obtaining a priori measurements of these parameters is that the packing of the column will affect both their magnitude and spatial distribution. Packing the column, then sampling with a coring tool before any tracer experiments are conducted is another possibility, but the potential impact on the flow field if 30 or 40 samples are removed is expected to be substantial. Currently, the best approach is a post-mortem in which samples are collected after the experiments are completed. This approach was not possible here because of the limited resources available at the completion of the tracer experiments. In retrospect, Column E should have been eliminated and the effort used for a post-mortem.

Analysis of the glass column experiments used a two-region conceptual model [Equations (10) to (14)] to characterize the non-Gaussian breakthrough curves. This approach was also conducted using the mean curves as a comparison and to complement the data from the glass column experiments. These results are given in Tables 11 and 12 for Columns D and E, respectively.

TABLE 9. EFFECTIVE POROSITIES CALCULATED FROM MOMENT ESTIMATES OF VELOCITY AND AVERAGE DARCY FLUX FOR EACH COLUMN.

Ports	Depth (cm)	Column C	Column D	Column E
6	34	2.45	2.00	2.92
5	68	0.64	1.32	1.49
4	102	0.32	0.62	0.86
3	136	1.27	0.82	0.71
2	170	0.23	0.62	0.63
1	204	0.75	0.54	− 0.58
Outlet	274	0.30	0.16	0.14

TABLE 10. EFFECTIVE POROSITIES CALCULATED FROM NONLINEAR LEAST-SQUARES
ESTIMATES FOR VELOCITY AND AVERAGE DARCY FLUX FOR COLUMNS D
AND E.

Ports	Depth (cm)	Column D	Column E
6	34	0.69	1.61
5	68	0.06	0.10
4	102	0.35	0.70
3	136	0.35	0.89
2	170	0.48	0.16
1	2047	0.40	0.93
Outlet flux	274	0.16	1.42
Outlet res	274	0.12	0.19

The fitting routine experienced convergence problems for two levels from each column (Tables 11 and 12), and a number of the parameters had a t-statistic below a value of 2.0 which is used as an indicator of significance. Again, the velocities from the outlet flux concentrations do not reflect known differences in flux rates between the columns. An additional analysis using resident concentrations for the mobile/immobile model on the outlet was not conducted because the value of this analysis is limited given the available information.

In discussing the fitting of the mobile-immobile model to the glass column data, it was indicated that scale effects such as column length affect the magnitude of the parameters. By having intermediate values from the large column experiments, some indication of the dispersion behavior of the aquifer material may be obtained. Bacri et al. (Reference 28) provided a formula to calculate the asymptotic Gaussian dispersion given the fit to the mobile-immobile model. This equation is

$$D_\infty = D + (1-f)v^2(\alpha^*)^{-1} \tag{18}$$

where D_∞ is the asymptotic dispersion coefficient; D is the dispersion coefficient estimated from the data; v is the pore water velocity; and f and α^* are as defined for Equations (10) and (11). Using the estimated parameters from Table 3 for glass column 9, the asymptotic dispersion coefficient is calculated to be 1702.42 cm2/hr with a dispersivity length of 234.8 cm. Bacri et al. (Reference 28) indicate that distances of at least 10 dispersivity lengths are needed to recover Gaussian behavior which for these values is a length of 23.5 meter. These results are for a one-dimensional medium, but they indicate the heterogeneous nature of the material that was used in the experiment. Applying Equation 18 to the estimated parameters for the effluent from Column D (Table 11), the asymptotic dispersivity is 424.5 cm. Velocities differed between the glass and steel column by a factor of two for the calculations presented here.

The difference between the results of the glass column versus the steel columns were also observed for unsaturated flow experiments in the caisson. Small, 30 cm long columns were filled with crushed Bandelier Tuff, and unsaturated flow tracer experiments were carried out. Analysis of these data indicated that the dispersivity was from 0.5 to 1.0 cm. In the caisson tracer experiment, analysis of the breakthrough curves collected by solution samplers

(point measurements) provided a dispersivity of essentially 1 cm which was in good agreement with the small columns. The effluent from the caisson experiment that revealed the magnitude of the heterogeneity. The same results hold true for the experiments reported here. The variability exhibited by the effluent breakthrough curves is greater than that obtained by analyzing the point data.

TABLE 11. RESULTS OF FITTING MOBILE/IMMOBILE MODEL TO MEAN BREAKTHROUGH CURVES FOR COLUMN D.

Level	Depth (cm)	V (cm/hr)	D (cm^2/hr)	Beta	Omega
6	34	2.92	0.0	0.22	5.06
5	68	4.66	40.45	1.0	284.46
4	102	6.25	0.0	0.16	11.34
3	136	6.38	76.96	0.0	← 31.1
2	170	0.19	6.43	0.04	0.0
1	204	0.16	59.16	0.06	0.01
Outlet	274	14.95	199.89	0.45	2.49

[1]Indicates that convergence was not achieved after 99 iterations.
*Indicates that t statistic was less than 2.0.

TABLE 12. RESULTS OF FITTING MOBILE/IMMOBILE MODEL TO MEAN BREAKTHROUGH CURVES FOR COLUMN E.

Level	Depth (cm)	V (cm/hr)	D (cm^2/hr)	Beta	Omega
6	34	9.14*	1186.12*	0.0*	2.08*
5[1]	68	0.05	2.44*	0.02*	0.0
3	136	3.95	267.97	0.54	1.33*
2[1]	170	2.77	0.11*	0.02*	2.40*
1	204	4.38	207.78	0.29	4.38
Outlet	274	6.25	495.41	0.20	1.20

[1]Indicates that convergence was not achieved after 99 iterations.
*Indicates that t statistic was less than 2.0.

SECTION IV

CONCLUSIONS

Intermediate-scale experiments provide an opportunity to observe point and system behavior simultaneously. This feature is not readily available in other experimental designs because of restrictions in the flow domain as in the case of bench-scale laboratory experiments or sampling difficulties as in the case of field experiments. A basis can be formulated for using the point behavior to predict the system response by conducting intermediate-scale experiments. This approach may provide some insight into making the correct measurements in the field.

In this study, bench-scale and intermediate-scale experiments were conducted. Tracer experiments were conducted with an inorganic, nonreactive tracer (bromide) and an organic chemical, as a reactive constituent, either 1-methylnaphthalene or xylene. All experiments used saturated flow conditions. For the bench-scale laboratory column experiments, a 1-m long glass column was used and all measurements were made at the effluent end. The intermediate-scale experiment used a 3-m long by 1-m diameter stainless steel column with 24 individual sampling ports along with a single point discharge for effluent sampling.

The porous medium used in the experiments was an aquifer material from Columbus AFB in Mississippi. In the laboratory experiments, both the bulk material and a sieved (<2mm) component was used. Only the bulk material was used in the intermediate-scale experiments. The pH of the influent solution was adjusted to reflect conditions at the site where the aquifer material was collected.

The following conclusions can be made from these experiments and subsequent analyses.

1. The glass column experiments did not provide an analogue for the intermediate-scale experiment. This can be expected given the one-dimensional nature of the glass column experiments as opposed to the three-dimensional response for the intermediate-scale experiments. Parameters derived from the glass column were not reproduced in the larger-scale setting. This result is consistent with previous caisson tests. When the porous media for a column or field setting is packed, a structure is created that transmits fluids in a certain manner. It is difficult to reproduce this structure even in a laboratory setting. Even with the same mean and variance for the hydraulic conductivity for two different settings, one may not obtain the same flow field because of differences in the relative locations of the high and low conductivity values. The glass column experiments provided experience in using the aquifer material, and the value to the overall study was positive for that reason. In the future, the laboratory phase should be directed towards characterizing those processes and parameters that are independent of the flow regime, e.g. retardation or degradation processes.

2. Point data collected during the intermediate-scale experiments did not bracket the total system behavior represented by the effluent breakthrough curve. This has been listed as one of the principal advantages of the intermediate-scale experimental design concept because of the ability to control initial and boundary conditions along with a relatively high proportion of the volume that is sampled at a point. In this case, 24 stainless steel samplers were located at six levels in the large column.

43

The inability of point behavior to describe the effluent curve was not unique to this experiment. Point samples in the unsaturated flow caisson experiments (Reference 31) did not represent the behavior observed in the effluent. In the saturated flow caisson experiment (Reference 29), velocities estimated from the point breakthrough curves were less than the velocity estimated from the effluent breakthrough curve. These results demonstrate the difficulty in locating fast paths in a porous medium. More problematic is using the point estimates in a statistical description, because it is not obvious what the effluent represents in terms of the expected values of the distribution of velocities. This has significant ramifications for field sampling whether in a research or compliance setting becuase of the greater volumes involved versus the smaller percentage of this volume sampled.

3. The design of the lower boundary must be improved before any further experiments are conducted. The single effluent point concept used in the caisson experiments was maintained in these experiments. It offers ease of sample collection and on location of an automated measuring device. The problem is that all flowlines will converge, and mixing of tracer signals occurs. The current design was selected because experience had been gained through the caisson experiments. Unfortunately, more detailed analysis of the caisson experiments (References 32, 33, 34) had not been completed prior to this experiment. A new design based on a manifold concept is needed, to preserve the three-dimensional nature of the flow field and to provide more information on the fast-flow velocities. A source of porous stainless steel is now available which is needed for a manifold boundary condition. The disadvantage of the manifold design is the increased number of samples that will be generated.

4. The lack of characterization of the physical properties of the porous medium hinder the analyses. The difficulties of a priori characterization have been discussed. The most logical approach is to use a post-mortem. The Columbus AFB aquifer material contained clay rich lenses that did not readily disintegrate. These lenses of relatively low permeability could give rise to stagnant flow conditions or mobile/immobile regions. Evidence of this was demonstrated by some samplers flowing rather freely while other samplers just dripped. Movement of the fine fraction and subsequent caking around the samplers during and just after filling may have also contributed to the apparent heterogeneity of the system.

In simulating flow and transport, one often starts with the physical parameters or a statistical description of them to make predictions. Based on the results of this study and the caisson experiments, it is difficult to support the position of using tracer data collected at various locations in the field to develop parameters for models. Much depends on the selection of a conceptual model. The conceptual model for this study was simplified from a three-dimensional to a one-dimensional system. This step adds uncertainty which cannot be quantified without further information on the physical properties and parameters of the column. It is not evident that after obtaining the physical data a better prediction of the response of the large column can be made, but given the lack of this information the question is currently open and provides a lack of completeness for the analyses presented herein.

5. One of the keys to this study was to examine the behavior of an organic tracer as compared to a nonreactive inorganic tracer. There was difficulty maintaining mass balance for the large column experiments for both the organic and inorganic tracers. The analytical techniques using the nonlinear least-squares procedure (Reference 16) are sensitive to the

44

mass balance particularly when constraints such as no sorption, or sources or sinks are included. The method of moments is somewhat less sensitive.

Mass balance problems for the bromide from the steel columns could be due to transfer and retention of the tracer in stagnant regions of the column. Sampling may not have occurred frequently enough, particularly of the effluent, to catch the tracer breakthrough. Loss of bromide mass for a field test conducted at Columbus AFB (Reference 35) suggested that sorption was responsible because the minerals present and the low pH of the water were conducive to anionic sorption. Our experience with the glass column experiments was that mass was not lost even though mass balance in the glass column experiments was not maintained. The result from the glass column experiment does not support an anionic sorption mechanism for the Columbus-AFB material.

6. The results of this study should temper expectations when making field assessments of contaminant transport. Despite some shortcomings that have been noted, there was a considerable amount of information available for analysis and interpretation. The situation examined here is more controlled and contained more information on contaminant distribution was available than essentially any condition found in the field. Those responsible for compliance with regulations must focus on the uncertainty associated with these results when comtemplating potential actions for compliance.

REFERENCES

1.   McKay, D. M., Roberts, P. V., Cherry, J. A., "Transport of Organic Contaminants in Groundwater," Environ. Sci. Technol., 19, 384-392, 1985.

2.   Westall, J. C . "Adsorption Mechanisms in Aquatic Surface Chemistry," in Aquatic Surface Chemistry, W. Stumm, ed., John Wiley and Sons, NY, pp. 3-32, 1987.

3.   Boyd, S. A., Lee, J. F., and Mortland, M. M., "Attenuating Organic Contaminant Mobility by Soil Modification," Nature, 333, 345-347, 1988.

4.   Boyd, S. A., Mortland, M. M., and Chiou, C. T., "Sorption Characteristics of Organic Compounds on Hexadecyltrimethylammonium-Smectite," Soil Sci. Soc. Amer. Jour., 52, 652-657, 1988.

5.   Srinivasan, K. R. and Fogler, H. S., "Use of Inorgano-organo Clays in the Removal of Prioirity Pollutants from Industrial Waste Waters: Adsorption of Benzo(a)pyrene and Chlorophenols from Aqueous Solutions," Clays and Clay Miner., 38, 287-293, 1990.

6.   Stauffer, T. B. and MacIntyre, W. G., "Sorption of Low-Polarity Organic Compounds on Oxide Minerals and Aquifer Material," Environ. Toxicology and Chem., 5, 949-955, 1986.

7.   Reynolds, W. D., Gilham, R. W., and Cherry, J. A., "Evaluation of Distribution Coefficients for the Prediction of Strontium and Cesium Migration in a Uniform Sand," Can. Geotch. J., 19, 92-102, 1982.

8.   MacIntyre, W. G, Stauffer, T. B., and Antworth, C. P., "A Comparison of Sorption Coefficients Determined by Batch, Column, and Box Methods on a Low Organic Carbon Aquifer Material," Ground Water, 29, 908-913, 1991.

9.   Gelhar, L. W., Mantoglou, C. Welty, and Rehfelt, K. R., A Review of Field-Scale Physical Solute Transport Processes in Saturated and Unsaturated Porus Media, Electric Power Research Institute Report EA-4190, Palo Alto, CA, 1985.

10. Parkhurst, D. L., Thorstenson, D. C., and Plummer, L. N., PHREEQE--A Computer Program for Geochemical Calculations, U. S. Geological Survey Water-Resources Investigations Report 80-96, Reston, VA, 1980.

11. Wolery, T. J., EQ3NR--A Computer Program for Geochemical Aqueous Speciation-Solubility Calculations: User's Guide and Documentation, Lawrence Livermore National Laboratory Report UCRL-53414, Livermore, CA, 1983.

12. Burris, D. R. and MacIntyre, W. G., "Water Solubility Behavior of Binary Hydrocarbon Mixtures," Environ. Toxicology and Chem., 4, 371-377.

13. Jury, W.A., and Sposito, G., "Field Calibration and Validation of Solute Transport Models for the Unsaturated Zone," Soil Science Soc. Am. J., 49, 1331-1341, 1985.

14. Turner, G.A. Heat and Concentration Waves, p. 62, Academic Press, NY, 1972.

15. Carnahan, B., Luther, H.A., and Wilkes, J.O., Applied Numerical Methods, pp 101-105, John Wiley and Sons, New York, 1969.

16. Parker, J.C. and M. Th. van Genuchten, Determining Transport Parameters from Laboratory and Field Tracer Experiments, Virginia Agricultural Exp. Stn. Bulletin 84-3, 1984.

17. Parker, J. C., and van Genuchten, M. Th. "Flux-Averaged and Volume-Averaged Concentrations in Continuum Approaches to Solute Transport," Water Resour. Res., 20, 866-872, 1984.

18. van Genuchten, M.T. and Wagenet, R. J., "Two-Site/Two-Region Models for Pesticide Transport and Degradation: Theoretical Development and Analytical Solutions," Soil Sci. Soc. Am. J., 53,1303-1310, 1989.

19. Springer, E. P., Stauffer, T. B., MacIntyre, W. G., Newman, B. D., and Antworth, C. A., "Analysis of Contaminant Movement at Different Scales," HAZTECH International '90, Pittsburgh, PN, 1990.

20. Bear, J., Dynamics of Fluids in Porous Media, pp. 579-626, Am. Elsevier, NY, 1972.

21. Coats, K.H., and B.D. Smith, "Dead-end Pore Volume and Dispersion in Porous Median," Trans. AIME Soc. Petroleum Eng. J., 231,73-84, 1984.

22. van Genuchten, M.T. and P.J. Weirenga, "Mass Transfer Studies in Sorbing Porous Media: Analytical Solutions," Soil Sci. Soc. Am. J., 40, 473-479, 1976.

23. Knopman, D.S. and Voss, C.I., "Discrimination among One-Dimensional Models of Solute Transport in Porous Media: Implications for Sampling Design," Water Resour. Res., 24, 1859-1876, 1988.

24. Knopman, D.S., Voss, C.I., and Garabedian, S.P., "Sampling Design for Groundwater Solute Transport: Tests of Methods and Analysis of Cape Cod Tracer Test Data," Water Resour. Res., 27, 925-949, 1991.

25. Draper, N.R. and Smith, H., Applied Regression Analysis, John Wiley and Sons, NY, 19

26. Carrera, J. and Neuman, S.P., "Estimation of Aquifer Parameters under Transient and Steady State Conditions, 1, Maximum Likelihood Method Incorporating Prior Information, Water Resour. Res., 22, 199-210, 1986.

27. Akaike, H., "A New Look at Statistical Model Identification," IEEE Trans. Automat. Contr., AC-19, 716-722, 1974.

28. Bacri, J.-C., Rakotomalala, N. , and Salin, D., "Anomalous Dispersion and Finite-Size Effects in Hydrodynamic Dispersion, Phys. Fluids A, 2, 674-680, 1990.

29. Fuentes, H.R., and W.L. Polzer. 1986. Interpretative analysis of data for solute transport in the unsaturated zone. U.S. Nuclear Regulatory Comm., NUREG/CR-4737, 227pp.

30. Fuentes, H. R., Polzer, W. L., and Springer, E. P., <u>Effects from Influence Boundary Conditions on Tracer Migration and Spatial Variability Features in Intermediate-Scale Experiments</u>, U. S. Nuclear Regulatory Commission NUREG/CR-4901, 1987.

31. Polzer, W.L., E.H. Essington, H.R. Fuentes, and J.W. Nyhan. 1986. <u>Compilation of field scale caisson data on solute transport in the unsaturated zone</u>. U.S. Nuclear Regulatory Comm., NUREG/CR-4720, 184pp.

32. Dagan, G., V. Nguyen, and E. P. Springer. 1989. "Analyses of transport in the upper soil layer and interpretation of caisson experiments," Pages 233-240 in <u>Focus '89 Nuclear Waste Isolation in the Unsaturated Zone</u>, Sept 17-21, 1989,Las Vegas, NV.

33. Nguyen, V., G. Dagan, and E.P. Springer. 1989. "Analysis of caisson transport experiments by the travel time approach," <u>Workshop on Field- Scale Water and Solute Flux in Soils</u>, Sept. 25-29, 1989, Monte Verita, Switzerland.

34. Dagan, G., E.P. Springer, and V. Nguyen .1991. "Analyses of solute transport in an intermediate-scale unsaturated flow experiment," Pages 837-844 in <u>High Level Radioactive Waste Management</u>, Proc. 2nd Annual International Conf., April 28- May 3, 1991,Las Vegas, NV., Amer. Nuclear Soc., LaGrange Park, Il.

35. Boggs, J.M. and E.E. Adams. 1992. "Field study of dispersion in a heterogeneous aquifer: 4. Investigation of adsorption and sampling bias," Abstract. Geophysical abstracts in press, American Geophys. Union, 2(9):8.

APPENDIX A
COMPOSITION OF SYNTHETIC GROUNDWATER

The table below gives the amounts of salts added to deionized water to make 1 L of synthetic groundwater or 20 L of concentrate. Salts used were reagent grade. To use the concentrate for any desired volume, divide the volume of deionized water dispensed into the container by 750. The result is the number of liters of concentrate to add to the dispensed volume to make the synthetic groundwater. For example, 100 L of groundwater is required. Since 100/750 = 0.1333, add 133 ml of concentrate to 100 L to make approximately 100 L of groundwater.

Salt	to make 1 L, add to 1L H_2O	to make 20 L of concentrate add to 20 L H_2O
KNO_3	0.0059 g	88.98
CaCl	0.007 g	104.86
NaCl	0.0135 g	202.23
$NaHCO_3$	0.00138 g	20.672
HNO_3 (conc)	0.0095 ml	142.3 ml
H_2SO_4 (conc)	0.0006 ml	9 ml

APPENDIX B

GAS CHROMATOGRAPH METHODS

Analyses for p-xylene, 1-methylnaphthalene and naphthalene were conducted via the following chromatographic methods on a Perkin-Elmer Model 8500 GC and Model HS-101 automated head space analyzer. Sample volume was 10 ml, and glass vials with Al/Teflon septa were crimped onto vials to seal samples.

Naphthalene and 1-methylnaphthalene method:

Auto sampler:
Sample temperature: 90°C
Isothermal time: 3 minutes
Single injection into chromatograph

Chromatograph:
Oven temperature: 120° C for 2 minutes, ramp to 180°C at 30°/min, held at 180° C for 5 minutes.
Injection oven temperature: 180°C
FID Detector temperature: 275°C
Carrier gas: He, 15 ml/min
Column: 20 meters x 0.32 mm (ID) DB-5, 1.0 µm film tickness (J&W Scientific)

p-xylene method:

Auto sampler:
Sample temperature: 40°C
Isothermal time: 5 minutes
Single injection into chromatograph

Chromatograph:
Oven temperature: 150° C for 6 minutes (isothermal)
Injection oven temperature: 180°C
FID Detector temperature: 275°C
Carrier gas: He, 15 ml/min
Column: Same (DB-5)

(The reverse of this page is blank.)

APPENDIX C

DATA FOR GLASS COLUMN AND STEEL COLUMN TESTS

Attached are the raw data for the glass column tests (Column 9 and Column 10) and the steel column tests (Column C, Column D, and Column E).

TABLE C-1. TIME AND CONCENTRATION VALUES, COLUMN 9.

Time (hr.)	Bromide (ppm)	p-Xylene (ppm)
6.700E-02	2.603E+00	0.000E+00
5.000E-01	2.091E+00	0.000E+00
9.000E-01	1.818E+00	0.000E+00
1.283E+00	1.687E+00	0.000E+00
1.616E+00	3.663E+00	0.000E+00
1.949E+00	1.607E+01	0.000E+00
2.282E+00	4.244E+01	0.000E+00
2.665E+00	7.117E+01	8.590E-02
2.948E+00	1.036E+02	8.947E-02
3.281E+00	1.360E+02	8.989E-02
3.614E+00	1.693E+02	1.407E-01
3.997E+00	1.943E+02	3.485E+00
4.330E+00	2.172E+02	1.445E-01
4.713E+00	2.295E+02	9.005E-01
5.080E+00	2.479E+02	2.586E+00
5.413E+00	2.544E+02	6.904E-01
5.746E+00	2.699E+02	3.249E-01
6.079E+00	2.823E+02	2.656E-01
6.412E+00	2.902E+02	2.579E-01
6.745E+00	2.846E+02	2.397E+00
7.245E+00	2.838E+02	3.091E+00
7.578E+00	2.707E+02	3.331E-01
7.911E+00	2.691E+02	3.954E-01
8.494E+00	2.529E+02	2.405E-01
9.244E+00	2.389E+02	3.253E-01
9.994E+00	2.217E+02	1.097E-01
1.049E+01	2.091E+02	4.357E+00
1.124E+01	2.007E+02	1.460E-01
2.252E+01	9.507E+01	1.082E-01
2.332E+01	9.103E+01	6.736E-02
2.425E+01	8.743E+01	
2.500E+01	8.453E+01	
2.592E+01	8.004E+01	
2.692E+01	7.708E+01	
2.867E+01	7.318E+01	
3.033E+01	6.921E+01	
3.227E+01	7.395E+01	
3.392E+01	5.899E+01	
3.542E+01	5.734E+01	
4.675E+01	2.120E+01	
4.778E+01	1.926E+01	
4.900E+01	1.678E+01	
5.025E+01	1.581E+01	
5.130E+01	1.422E+01	
5.242E+01	1.329E+01	
5.400E+01	1.295E+01	
5.530E+01	1.294E+01	
7.183E+01	8.033E+00	
7.283E+01	7.742E+00	
7.383E+01	7.497E+00	
7.483E+01	7.375E+00	
7.617E+01	6.816E+00	
7.717E+01	6.640E+00	
7.817E+01	6.485E+00	
7.917E+01	6.236E+00	
8.000E+01	6.198E+00	

TABLE C-2. TIME AND CONCENTRATION VALUES, COLUMN 10.

Time (hr.)	Bromide (ppm)	p-Xylene (ppm)
0.000E+00	0.000E+00	0.000E+00
3.333E-01	0.000E+00	0.000E+00
6.667E-01	0.000E+00	2.500E-01
1.000E+00	0.000E+00	0.000E+00
1.167E+00	0.000E+00	1.100E-01
1.333E+00	0.000E+00	0.000E+00
1.500E+00	6.718E+00	1.500E-01
1.667E+00	7.265E+01	7.000E-02
1.833E+00	4.123E+02	0.000E+00
2.000E+00	8.199E+02	1.300E-01
2.167E+00	9.249E+02	3.100E-01
2.333E+00	6.445E+02	3.800E-01
2.500E+00	3.935E+02	3.600E-01
2.667E+00	2.181E+02	1.900E-01
2.833E+00	1.022E+02	3.730E+00
3.167E+00	1.673E+01	4.460E+00
3.500E+00	1.030E+01	5.270E+00
3.833E+00	5.887E+00	5.600E-01
4.167E+00	4.609E+00	1.100E-01
4.500E+00	3.810E+00	0.000E+00
4.833E+00	3.150E+00	1.100E-01
5.167E+00	2.707E+00	0.000E+00
5.500E+00	2.400E+00	9.000E-02
5.833E+00	2.212E+00	0.000E+00
6.167E+00	2.144E+00	1.100E-01
6.500E+00	1.953E+00	9.000E-02
6.833E+00	1.787E+00	9.000E-02
7.650E+00	1.498E+00	1.500E-01
8.950E+00	9.670E-01	1.300E-01
1.850E+01	0.000E+00	3.500E-01

TABLE C-3. TEMPORAL MOMENTS, COLUMN C, BROMIDE, p-XYLENE

Port	Zero Moment[1]	First Moment[2]	Second Moment[3]	Velocity[4]	Dispersion[5]	Predicted Mass[6]	Injected Mass[7]
Br							
1	0.25978E+03	0.10615E+05	0.61619E+06	5.1395	227.060	7949.9	11735.0
2	0.35180E+03	0.20082E+05	0.15908E+07	3.6789	149.7729	10765.1	11735.0
3	0.28329E+03	0.89642E+04	0.50813E+06	6.6365	551.4232	8668.7	11735.0
4	0.32169E+03	0.10828E+05	0.67622E+06	6.2390	560.3931	9844.0	11735.0
5	0.42160E+02	0.46242E+03	0.59312E+04	15.9550	236.4934	1290.1	11735.0
6	0.43230E+02	0.50850E+03	0.68792E+04	14.8776	195.4160	1322.8	11735.0
7	0.70535E+02	0.67561E+03	0.84580E+04	18.2704	490.8318	2158.5	11735.0
8	0.71865E+02	0.66023E+03	0.72395E+04	19.0486	322.6038	2200.1	11735.0
9	0.29976E+03	0.12210E+05	0.93808E+06	3.4371	213.2261	9173.9	11735.0
10	0.27775E+03	0.13566E+05	0.99687E+06	2.8664	101.2319	8500.7	11735.0
11	0.2589E+03	0.13047E+05	0.12564E+07	2.7784	177.1965	7923.6	11735.0
12	0.22370E+03	0.80489E+04	0.64869E+06	3.8910	337.7281	6845.2	11735.0
13	0.10335E+03	0.95454E+03	0.10693E+05	11.3686	127.0558	3164.0	11735.0
14	0.98965E+02	0.83007E+03	0.86408E+04	12.5186	158.4471	3029.4	11735.0
15	0.11933E+03	0.90126E+03	0.84114E+04	13.9029	172.0784	3650.6	11735.0
16	0.67530E+02	0.62286E+03	0.68644E+04	11.3840	116.4614	2066.4	11735.0
17	0.11621E+03	0.10812E+04	0.12713E+05	7.5237	69.4686	3556.0	11735.0
18	0.39805E+02	0.46115E+03	0.67771E+04	6.0422	56.7898	1217.9	11735.0
19	0.57330E+02	0.56743E+03	0.74910E+04	7.0725	82.6384	1754.3	11735.0
20	0.21489E+03	0.10164E=05	0.86807E+06	1.4799	41.7337	6575.9	11735.0
21	0.41577E+03	0.99814E+04	0.58498E+06	1.4579	36.7712	12723.5	11735.0
22	0.59559E+03	0.13962E+05	0.67095E+06	1.4930	27.4348	18225.6	11735.0
23	0.53301E+03	0.93700E+04	0.41540E+06	1.9910	53.0261	16309.8	11735.0
24	0.33263E+03	0.77134E+04	0.40292E+06	1.5093	33.0851	10177.6	11735.0
p-xylene							
25	0.13648E+03	0.17495E+04	0.11027E+06	23.4018	13747.820	4176.9	NA

[1]Zero Moment in mg-hr/L, [2]First Moment in hr, [3]Second Moment in hr^2, [4]Velocity in cm/hr, [5]Dispersion in cm2/hr, [6]Predicted Mass in mg, [7]injected Mass in mg.

TABLE C-4. TIME AND CONCENTRATION VALUES, PORT 1, COLUMN C.

Time (hr.)	Bromide (ppm)
1.000E+00	4.900E-01
2.000E+00	3.200E-01
3.000E+00	3.200E-01
4.000E+00	4.000E-01
5.000E+00	4.300E-01
6.000E+00	3.200E-01
7.000E+00	3.700E-01
8.000E+00	3.400E-01
9.000E+00	3.900E-01
1.000E+01	6.900E-01
1.100E+01	4.300E-01
1.200E+01	6.700E-01
1.300E+01	1.880E+00
1.400E+01	5.010E+00
1.500E+01	5.190E+00
1.600E+01	5.580E+00
1.700E+01	6.390E+00
1.800E+01	6.500E+00
1.900E+01	8.050E+00
2.000E+01	8.470E+00
2.100E+01	6.390E+00
2.300E+01	6.340E+00
2.400E+01	6.760E+00
2.800E+01	6.360E+00
3.200E+01	4.920E+00
3.600E+01	4.400E+00
3.900E+01	4.180E+00
4.800E+01	3.440E+00
5.200E+01	3.150E+00
5.600E+01	2.710E+00
6.000E+01	1.110E+00
8.400E+01	3.400E-01
1.080E+02	4.700E-01
1.420E+02	1.800E-01

Table C-5. TIME AND CONCENTRATION VALUES, PORT 2, COLUMN C.

Time (hr.)	Bromide (ppm)
1.000E+00	3.200E-01
2.000E+00	2.700E-01
3.000E+00	2.700E-01
4.000E+00	2.400E-01
5.000E+00	2.000E-01
6.000E+00	2.300E-01
7.000E+00	2.200E-01
8.000E+00	2.300E-01
9.000E+00	2.800E-01
1.000E+01	3.600E-01
1.100E+01	4.500E-01
1.200E+01	5.000E-01
1.300E+01	1.050E+00
1.400E+01	1.420E+00
1.500E+01	2.140E+00
1.600E+01	3.190E+00
1.700E+01	3.560E+00
1.800E+01	3.920E+00
1.900E+01	4.330E+00
2.000E+01	4.640E+00
2.100E+01	5.030E+00
2.300E+01	5.500E+00
2.400E+01	5.690E+00
2.800E+01	5.940E+00
3.200E+01	6.200E+00
3.600E+01	5.650E+00
3.900E+01	5.480E+00
4.800E+01	5.250E+00
5.200E+01	4.180E+00
5.600E+01	3.660E+00
6.000E+01	3.460E+00
8.400E+01	1.330E+00
1.080E+02	6.900E-01
1.420E+02	7.300E-01
1.660E+02	4.900E-01

TABLE C-6. TIME AND CONCENTRATION VALUES, PORT 3, COLUMN C.

Time (hr.)	Bromide (ppm)
1.000E+00	3.300E-01
2.000E+00	2.620E+00
3.000E+00	4.490E+00
4.000E+00	6.710E+00
5.000E+00	7.520E+00
6.000E+00	7.490E+00
7.000E+00	7.720E+00
8.000E+00	8.780E+00
9.000E+00	8.670E+00
1.000E+01	7.820E+00
1.100E+01	6.620E+00
1.200E+01	6.420E+00
1.300E+01	6.480E+00
1.400E+01	6.480E+00
1.500E+01	5.990E+00
1.600E+01	5.320E+00
1.700E+01	6.390E+00
1.800E+01	6.620E+00
1.900E+01	6.050E+00
2.000E+01	5.720E+00
2.100E+01	5.840E+00
2.300E+01	5.580E+00
2.400E+01	5.280E+00
2.800E+01	5.080E+00
3.200E+01	3.760E+00
3.600E+01	3.480E+00
3.900E+01	3.140E+00
4.800E+01	2.150E+00
5.200E+01	1.950E+00
5.600E+01	1.850E+00
6.000E+01	6.900E-01
8.400E+01	3.600E-01
1.080E+02	3.600E-01
1.420E+02	2.700E-01

59

TABLE C-7. TIME AND CONCENTRATION VALUES, PORT 4, COLUMN C.

Time (hr.)	Bromide (ppm)
1.000E+00	2.300E-01
2.000E+00	3.400E-01
3.000E+00	6.100E-01
4.000E+00	1.020E+00
5.000E+00	6.310E+00
6.000E+00	2.260E+00
7.000E+00	3.490E+00
8.000E+00	5.140E+00
9.000E+00	7.490E+00
1.000E+01	7.920E+00
1.100E+01	9.650E+00
1.200E+01	8.630E+00
1.300E+01	1.180E+01
1.400E+01	1.268E+01
1.500E+01	1.175E+01
1.600E+01	1.161E+01
1.700E+01	1.127E+01
1.800E+01	1.113E+01
1.900E+01	1.058E+01
2.000E+01	9.720E+00
2.100E+01	8.310E+00
2.300E+01	7.380E+00
2.400E+01	6.870E+00
2.800E+01	5.550E+00
3.200E+01	4.830E+00
3.600E+01	3.390E+00
3.900E+01	2.650E+00
4.800E+01	2.140E+00
5.200E+01	1.180E+00
5.600E+01	1.120E+00
6.000E+01	1.060E+00
8.400E+01	4.900E-01
1.080E+02	2.000E-01
1.420E+02	3.500E-01
1.660E+02	2.100E-01

TABLE C-8. TIME AND CONCENTRATION VALUES, PORT 5, COLUMN C.

Time (hr.)	Bromide (ppm)
1.000E+00	5.500E-01
2.000E+00	4.500E-01
3.000E+00	6.500E-01
4.000E+00	1.390E+00
5.000E+00	2.090E+00
6.000E+00	2.710E+00
7.000E+00	2.930E+00
8.000E+00	3.290E+00
9.000E+00	3.320E+00
1.000E+01	3.360E+00
1.100E+01	3.210E+00
1.200E+01	3.190E+00
1.300E+01	2.520E+00
1.400E+01	2.460E+00
1.500E+01	2.270E+00
1.600E+01	1.950E+00
1.700E+01	2.130E+00
1.800E+01	2.080E+00
1.900E+01	9.300E-01
2.000E+01	7.100E-01
2.100E+01	4.900E-01

TABLE C-9. TIME AND CONCENTRATION VALUES, PORT 6, COLUMN C.

Time (hr.)	Bromide (ppm)
1.000E+00	4.100E-01
2.000E+00	2.700E-01
3.000E+00	2.600E-01
4.000E+00	4.400E-01
5.000E+00	2.010E+00
6.000E+00	2.750E+00
7.000E+00	2.980E+00
8.000E+00	3.250E+00
9.000E+00	3.280E+00
1.000E+01	3.050E+00
1.100E+01	2.720E+00
1.200E+01	2.800E+00
1.300E+01	2.790E+00
1.400E+01	2.770E+00
1.500E+01	3.550E+00
1.600E+01	2.820E+00
1.700E+01	2.540E+00
1.800E+01	2.370E+00
1.900E+01	6.600E-01
2.000E+01	4.700E-01
2.100E+01	5.700E-01
2.300E+01	3.900E-01

TABLE C-10. TIME AND CONCENTRATION VALUES, PORT 7, COLUMN C.

Time (hr.)	Bromide (ppm)
1.000E+00	1.090E+00
2.000E+00	4.430E+00
3.000E+00	3.460E+00
4.000E+00	5.350E+00
5.000E+00	5.190E+00
6.000E+00	4.760E+00
7.000E+00	4.620E+00
9.000E+00	4.780E+00
1.000E+01	4.700E+00
1.100E+01	4.390E+00
1.200E+01	4.130E+00
1.300E+01	3.770E+00
1.400E+01	2.490E+00
1.500E+01	2.370E+00
1.600E+01	2.110E+00
1.700E+01	1.770E+00
1.800E+01	1.810E+00
1.900E+01	2.130E+00
2.000E+01	8.100E-01
2.100E+01	5.700E-01
2.300E+01	7.400E-01
2.400E+01	5.100E-01

TABLE C-11. TIME AND CONCENTRATION VALUES, PORT 8, COLUMN C.

Time (hr.)	Bromide (ppm)
1.000E+00	5.100E-01
2.000E+00	1.320E+00
3.000E+00	2.130E+00
4.000E+00	3.840E+00
5.000E+00	5.060E+00
6.000E+00	6.270E+00
7.000E+00	7.040E+00
9.000E+00	7.870E+00
1.000E+01	7.290E+00
1.100E+01	5.900E+00
1.200E+01	4.700E+00
1.300E+01	3.760E+00
1.400E+01	2.150E+00
1.500E+01	1.780E+00
1.600E+01	1.270E+00
1.700E+01	8.000E-01
1.800E+01	8.000E-01
1.900E+01	8.600E-01
2.000E+01	3.700E-01
2.100E+01	2.200E-01
2.300E+01	3.300E-01
2.400E+01	2.400E-01

TABLE C-12. TIME AND CONCENTRATION VALUES, PORT 9, COLUMN C.

Time (hr.)	Bromide (ppm)
1.000E+00	4.100E-01
2.000E+00	5.000E-01
3.000E+00	1.020E+00
4.000E+00	1.790E+00
5.000E+00	2.570E+00
6.000E+00	3.580E+00
7.000E+00	4.930E+00
8.000E+00	5.650E+00
9.000E+00	6.380E+00
1.000E+01	7.570E+00
1.100E+01	7.390E+00
1.200E+01	7.810E+00
1.300E+01	8.400E+00
1.400E+01	8.660E+00
1.500E+01	8.550E+00
1.600E+01	8.330E+00
1.700E+01	7.880E+00
1.800E+01	7.480E+00
1.900E+01	7.110E+00
2.000E+01	6.640E+00
2.100E+01	6.590E+00
2.300E+01	6.200E+00
2.400E+01	5.790E+00
2.800E+01	5.150E+00
3.200E+01	4.810E+00
3.600E+01	2.810E+00
3.900E+01	2.600E+00
4.800E+01	2.170E+00
5.200E+01	1.570E+00
5.600E+01	1.460E+00
6.000E+01	1.450E+00
8.400E+01	5.400E-01
1.080E+02	3.400E-01
1.420E+02	4.100E-01
1.660E+02	2.600E-01
1.970E+02	0.000E+00

TABLE C-13. TIME AND CONCENTRATION VALUES, PORT 10, COLUMN C.

Time (hr.)	Bromide (ppm)
1.000E+00	3.600E-01
2.000E+00	3.900E-01
3.000E+00	3.700E-01
4.000E+00	2.500E-01
5.000E+00	1.700E-01
6.000E+00	1.700E-01
7.000E+00	1.600E-01
8.000E+00	2.000E-01
9.000E+00	2.600E-01
1.000E+01	3.500E-01
1.100E+01	5.400E-01
1.200E+01	1.060E+00
1.300E+01	1.340E+00
1.400E+01	2.400E+00
1.500E+01	2.660E+00
1.600E+01	2.980E+00
1.700E+01	3.420E+00
1.800E+01	3.930E+00
1.900E+01	4.350E+00
2.000E+01	4.940E+00
2.100E+01	5.180E+00
2.300E+01	5.710E+00
2.400E+01	5.940E+00
2.800E+01	6.950E+00
3.200E+01	6.860E+00
3.600E+01	5.640E+00
3.900E+01	5.180E+00
4.800E+01	4.630E+00
5.200E+01	2.090E+00
5.600E+01	1.840E+00
6.000E+01	1.630E+00
8.400E+01	6.800E-01
1.080E+02	3.000E-01
1.420E+02	3.400E-01
1.660E+02	2.500E-01
1.970E+02	0.000E+00

TABLE C-14. TIME AND CONCENTRATION VALUES, PORT 11, COLUMN \ C.

Time (hr.)	Bromide (ppm)
1.000E+00	4.600E-01
2.000E+00	1.620E+00
3.000E+00	3.060E+00
4.000E+00	5.270E+00
5.000E+00	6.270E+00
6.000E+00	7.060E+00
7.000E+00	8.110E+00
8.000E+00	7.490E+00
9.000E+00	5.850E+00
1.000E+01	6.730E+00
1.100E+01	5.290E+00
1.200E+01	5.640E+00
1.300E+01	4.740E+00
1.400E+01	3.510E+00
1.500E+01	3.510E+00
1.600E+01	3.590E+00
1.700E+01	3.820E+00
1.800E+01	3.680E+00
1.900E+01	3.650E+00
2.000E+01	4.110E+00
2.100E+01	3.590E+00
2.300E+01	3.510E+00
2.400E+01	3.940E+00
2.800E+01	3.210E+00
3.200E+01	2.570E+00
3.600E+01	2.390E+00
3.900E+01	1.570E+00
4.800E+01	1.560E+00
5.200E+01	1.530E+00
5.600E+01	1.370E+00
6.000E+01	1.450E+00
8.400E+01	7.400E-01
1.080E+02	4.700E-01
1.420E+02	6.000E-01
1.660E+02	4.900E-01
1.970E+02	0.000E+00

TABLE C-15. TIME AND CONCENTRATION VALUES, PORT 12, COLUMN C.

Time (hr.)	Bromide (ppm)
1.000E+00	4.100E-01
2.000E+00	1.590E+00
3.000E+00	3.710E+00
4.000E+00	6.400E+00
5.000E+00	5.210E+00
6.000E+00	6.170E+00
7.000E+00	7.530E+00
8.000E+00	8.610E+00
9.000E+00	9.070E+00
1.000E+01	8.840E+00
1.100E+01	8.280E+00
1.200E+01	4.910E+00
1.300E+01	7.150E+00
1.400E+01	7.660E+00
1.500E+01	6.880E+00
1.600E+01	6.230E+00
1.700E+01	6.330E+00
1.800E+01	5.810E+00
1.900E+01	4.760E+00
2.000E+01	3.100E+00
2.100E+01	2.650E+00
2.300E+01	2.630E+00
2.400E+01	2.780E+00
2.800E+01	2.430E+00
3.200E+01	2.250E+00
3.600E+01	1.640E+00
3.900E+01	1.480E+00
4.800E+01	1.310E+00
5.200E+01	7.600E-01
5.600E+01	8.700E-01
6.000E+01	9.000E-01
8.400E+01	3.700E-01
1.080E+02	2.000E-01
1.420E+02	2.900E-01
1.660E+02	2.300E-01
1.970E+02	0.000E+00

TABLE C-16. TIME AND CONCENTRATION VALUES, PORT 13, COLUMN C.

Time (hr.)	Bromide (ppm)
2.000E+00	1.740E+00
3.000E+00	4.130E+00
4.000E+00	6.380E+00
5.000E+00	8.490E+00
6.000E+00	9.020E+00
7.000E+00	9.130E+00
9.000E+00	9.490E+00
1.000E+01	9.090E+00
1.100E+01	8.450E+00
1.200E+01	6.890E+00
1.300E+01	6.430E+00
1.400E+01	3.160E+00
1.500E+01	2.790E+00
1.600E+01	2.490E+00
1.700E+01	1.140E+00
1.800E+01	1.420E+00
1.900E+01	9.400E-01
2.000E+01	1.140E+00
2.100E+01	3.600E-01
2.300E+01	4.300E-01
2.400E+01	3.900E-01

TABLE C-17. TIME AND CONCENTRATION VALUES, PORT 14, COLUMN C.

Time (hr.)	Bromide (ppm)
1.000E+00	1.470E+00
2.000E+00	3.730E+00
3.000E+00	5.660E+00
4.000E+00	7.010E+00
5.000E+00	8.830E+00
6.000E+00	9.950E+00
7.000E+00	9.950E+00
9.000E+00	8.790E+00
1.000E+01	7.010E+00
1.100E+01	7.560E+00
1.200E+01	5.660E+00
1.300E+01	4.580E+00
1.400E+01	2.180E+00
1.500E+01	1.930E+00
1.600E+01	1.970E+00
1.700E+01	9.900E-01
1.800E+01	9.800E-01
1.900E+01	8.300E-01
2.000E+01	5.000E-01
2.100E+01	1.900E-01
2.300E+01	2.500E-01
2.400E+01	1.800E-01

TABLE C-18. TIME AND CONCENTRATION VALUES, PORT 15, COLUMN C.

Time (hr.)	Bromide (ppm)
1.000E+00	2.320E+00
2.000E+00	8.830E+00
3.000E+00	8.100E+00
4.000E+00	8.390E+00
5.000E+00	1.031E+01
6.000E+00	1.125E+01
7.000E+00	1.265E+01
9.000E+00	1.150E+01
1.000E+01	1.091E+01
1.100E+01	9.480E+00
1.200E+01	5.820E+00
1.300E+01	4.080E+00
1.400E+01	1.310E+00
1.500E+01	1.110E+00
1.600E+01	5.400E-01
1.700E+01	2.800E-01
1.800E+01	3.200E-01
1.900E+01	2.900E-01
2.000E+01	2.500E-01
2.100E+01	1.800E-01
2.300E+01	2.300E-01
2.400E+01	1.300E-01

TABLE C-19. TIME AND CONCENTRATION VALUES, PORT 16, COLUMN C.

Time (hr.)	Bromide (ppm)
1.000E+00	4.900E-01
2.000E+00	2.040E+00
3.000E+00	2.490E+00
4.000E+00	3.720E+00
5.000E+00	4.190E+00
6.000E+00	5.040E+00
7.000E+00	5.790E+00
9.000E+00	6.620E+00
1.000E+01	6.650E+00
1.100E+01	6.280E+00
1.200E+01	5.390E+00
1.300E+01	5.130E+00
1.400E+01	2.150E+00
1.500E+01	1.440E+00
1.600E+01	1.050E+00
1.700E+01	6.400E-01
1.800E+01	7.500E-01
1.900E+01	5.700E-01
2.000E+01	2.500E-01
2.100E+01	3.000E-01
2.300E+01	2.300E-01
2.400E+01	1.900E-01

Table C-20. TIME AND CONCENTRATION VALUES, PORT 17, COLUMN C.

Time (hr.)	Bromide (ppm)
1.000E+00	1.630E+00
2.000E+00	2.850E+00
3.000E+00	5.320E+00
4.000E+00	7.710E+00
5.000E+00	9.350E+00
6.000E+00	1.170E+01
7.000E+00	1.033E+01
9.000E+00	9.360E+00
1.000E+01	8.260E+00
1.100E+01	8.340E+00
1.200E+01	6.710E+00
1.300E+01	6.030E+00
1.400E+01	3.440E+00
1.500E+01	3.140E+00
1.600E+01	2.770E+00
1.700E+01	1.220E+00
1.800E+01	1.920E+00
1.900E+01	1.640E+00
2.000E+01	2.390E+00
2.100E+01	9.800E-01
2.300E+01	8.700E-01
2.400E+01	5.900E-01

TABLE C-21. TIME AND CONCENTRATION VALUES, PORT 18, COLUMN C.

Time (hr.)	Bromide (ppm)
1.000E+00	8.000E-01
2.000E+00	1.180E+00
3.000E+00	1.810E+00
4.000E+00	2.280E+00
5.000E+00	2.280E+00
6.000E+00	2.170E+00
7.000E+00	2.310E+00
9.000E+00	1.940E+00
1.000E+01	1.700E+00
1.100E+01	2.270E+00
1.200E+01	2.320E+00
1.300E+01	1.930E+00
1.400E+01	1.310E+00
1.500E+01	1.430E+00
1.600E+01	1.490E+00
1.700E+01	1.760E+00
1.800E+01	2.420E+00
1.900E+01	2.970E+00
2.000E+01	9.700E-01
2.100E+01	8.600E-01
2.300E+01	7.700E-01
2.400E+01	5.900E-01

TABLE C-22. TIME AND CONCENTRATION VALUES, PORT 19, COLUMN C.

Time (hr.)	Bromide (ppm)
1.000E+00	9.200E-01
2.000E+00	3.100E+00
3.000E+00	2.920E+00
4.000E+00	4.070E+00
5.000E+00	4.840E+00
6.000E+00	5.060E+00
7.000E+00	4.900E+00
8.000E+00	0.000E+00
9.000E+00	4.290E+00
1.000E+01	4.030E+00
1.100E+01	3.640E+00
1.200E+01	3.130E+00
1.300E+01	2.650E+00
1.400E+01	1.670E+00
1.500E+01	2.170E+00
1.600E+01	1.980E+00
1.700E+01	1.300E+00
1.800E+01	1.600E+00
1.900E+01	1.780E+00
2.000E+01	1.030E+00
2.100E+01	6.700E-01
2.300E+01	5.200E-01
2.400E+01	3.700E-01
2.800E+01	0.000E+00

TABLE C-23. TIME AND CONCENTRATION VALUES, PORT 20, COLUMN C.

Time (hr.)	Bromide (ppm)
2.000E+00	6.500E-01
4.000E+00	2.740E+00
6.000E+00	2.810E+00
8.000E+00	4.510E+00
1.000E+01	5.490E+00
1.200E+01	5.050E+00
1.400E+01	6.290E+00
1.800E+01	5.920E+00
2.000E+01	4.770E+00
2.300E+01	3.560E+00
2.800E+01	2.200E+00
3.200E+01	1.870E+00
3.600E+01	9.000E-01
3.900E+01	9.500E-01
4.800E+01	8.600E-01
5.200E+01	1.000E+00
5.600E+01	9.600E-01
8.000E+01	1.170E+00
8.400E+01	8.400E-01
1.080E+02	5.700E-01
1.420E+02	4.300E-01
1.660E+02	3.200E-01

TABLE C-24. TIME AND CONCENTRATION VALUES, PORT 21, COLUMN C.

Time (hr.)	Bromide (ppm)
1.000E+00	1.330E+01
2.000E+00	2.164E+01
3.000E+00	2.206E+01
4.000E+00	1.958E+01
5.000E+00	1.958E+01
6.000E+00	1.885E+01
7.000E+00	1.630E+01
8.000E+00	2.202E+01
9.000E+00	1.548E+01
1.000E+01	1.460E+01
1.100E+01	1.259E+01
1.200E+01	1.157E+01
1.300E+01	1.046E+01
1.400E+01	1.016E+01
1.500E+01	9.340E+00
1.600E+01	9.030E+00
1.700E+01	8.260E+00
1.800E+01	7.790E+00
1.900E+01	7.310E+00
2.000E+01	6.500E+00
2.100E+01	5.570E+00
2.300E+01	5.380E+00
2.400E+01	5.160E+00
2.800E+01	4.390E+00
3.200E+01	4.000E+00
3.600E+01	2.250E+00
3.900E+01	2.130E+00
4.800E+01	1.540E+00
5.200E+01	5.900E-01
5.600E+01	8.500E-01
6.000E+01	1.080E+00
8.400E+01	7.400E-01
1.080E+02	2.100E-01
1.420E+02	2.000E-01
1.660E+02	1.600E-01

TABLE C-25. TIME AND CONCENTRATION VALUES, PORT 22, COLUMN C.

Time (hr.)	Bromide (ppm)
2.000E+00	5.280E+00
3.000E+00	1.199E+01
4.000E+00	1.184E+01
5.000E+00	1.784E+01
6.000E+00	1.463E+01
7.000E+00	1.959E+01
8.000E+00	1.887E+01
9.000E+00	1.770E+01
1.000E+01	7.971E+01
1.100E+01	1.690E+01
1.200E+01	1.621E+01
1.300E+01	1.621E+01
1.400E+01	1.607E+01
1.500E+01	1.719E+01
1.600E+01	1.655E+01
1.700E+01	1.561E+01
1.800E+01	1.515E+01
1.900E+01	1.417E+01
2.000E+01	1.335E+01
2.100E+01	1.249E+01
2.300E+01	1.133E+01
2.400E+01	1.157E+01
2.800E+01	1.010E+01
3.200E+01	8.340E+00
3.600E+01	4.740E+00
3.900E+01	3.860E+00
4.800E+01	3.360E+00
5.200E+01	9.600E-01
5.600E+01	0.000E+00
6.000E+01	8.500E-01
8.400E+01	3.900E-01
1.080E+02	1.900E-01
1.420E+02	1.700E-01
1.660E+02	1.600E-01
1.900E+02	0.000E+00

72

TABLE C-26. TIME AND CONCENTRATION VALUES, PORT 23, COLUMN C.

Time (hr.)	Bromide (ppm)
1.000E+00	3.200E-01
2.000E+00	7.300E-01
3.000E+00	2.070E+01
4.000E+00	3.141E+01
5.000E+00	3.496E+01
6.000E+00	3.248E+01
7.000E+00	1.942E+01
8.000E+00	3.276E+01
9.000E+00	3.096E+01
1.000E+01	3.129E+01
1.100E+01	2.577E+01
1.200E+01	2.408E+01
1.300E+01	2.300E+01
1.400E+01	1.947E+01
1.500E+01	1.591E+01
1.600E+01	1.490E+01
1.700E+01	1.280E+01
1.800E+01	1.230E+01
1.900E+01	1.559E+01
2.000E+01	1.370E+01
2.100E+01	8.540E+00
2.300E+01	8.100E+00
2.400E+01	7.160E+00
2.800E+01	4.090E+00
3.200E+01	3.680E+00
3.600E+01	1.230E+00
3.900E+01	2.450E+00
4.800E+01	1.360E+00
5.200E+01	5.100E-01
5.600E+01	3.700E-01
6.000E+01	0.000E+00
8.400E+01	1.600E-01
1.080E+02	1.400E-01
1.420E+02	1.400E-01
1.660E+02	1.400E-01
1.900E+02	0.000E+00

TABLE C-27. TIME AND CONCENTRATION VALUES, PORT 24, COLUMN C.

Time (hr.)	Bromide (ppm)
1.000E+00	5.100E-01
2.000E+00	1.900E+00
3.000E+00	6.440E+00
4.000E+00	8.230E+00
5.000E+00	1.074E+01
6.000E+00	1.240E+01
7.000E+00	1.444E+01
8.000E+00	1.537E+01
9.000E+00	1.516E+01
1.000E+01	1.628E+01
1.100E+01	1.353E+01
1.200E+01	1.312E+01
1.300E+01	1.289E+01
1.400E+01	1.140E+01
1.500E+01	1.067E+01
1.600E+01	1.030E+01
1.700E+01	9.430E+00
1.800E+01	9.640E+00
1.900E+01	8.300E+00
2.000E+01	7.910E+00
2.100E+01	7.190E+00
2.300E+01	6.360E+00
2.400E+01	6.000E+00
2.800E+01	5.300E+00
3.200E+01	4.800E+00
3.600E+01	2.360E+00
3.900E+01	1.900E+00
4.800E+01	8.000E-01
5.200E+01	1.030E+00
5.600E+01	8.100E-01
6.000E+01	0.000E+00
8.400E+01	2.100E-01
1.080E+02	1.400E-01
1.420E+02	1.400E-01
1.660E+02	1.300E-01
1.900E+02	0.000E+00

TABLE C-28. TIME AND CONCENTRATION VALUES, PORT 25, COLUMN C.

Time (hr.)	Bromide (ppm)	p-Xylene (ppm)
0.000E+00	4.400E-01	0.000E+00
3.000E-01	4.600E-01	0.000E+00
8.000E-01	5.630E+00	0.000E+00
1.000E+00	9.120E+00	0.000E+00
1.500E+00	1.710E+01	1.156E+01
2.500E+00	2.087E+01	1.229E+01
3.000E+00	2.369E+01	1.271E+01
3.500E+00	2.644E+01	1.633E+01
4.500E+00	2.927E+01	1.972E+01
4.000E+00	2.782E+01	1.749E+01
5.000E+00	2.701E+01	1.975E+01
5.500E+00	2.578E+01	4.830E+00
6.000E+00	2.622E+01	1.045E+01
6.500E+00	2.409E+01	5.890E+00
7.000E+00	2.252E+01	6.190E+00
7.500E+00	1.161E+01	1.641E+01
8.000E+00	1.097E+01	1.764E+01
8.500E+00	1.097E+01	1.546E+01
9.000E+00	1.066E+01	7.490E+00
9.500E+00	9.510E+00	1.709E+01
1.000E+01	9.470E+00	5.180E+00
1.050E+01	9.430E+00	1.560E+00
1.100E+01	8.340E+00	2.400E-01
1.200E+01	7.950E+00	7.900E-01
1.200E+01	1.200E+01	3.150E+00
1.250E+01	1.185E+01	1.100E+00
1.300E+01	1.101E+01	1.290E+00
1.350E+01	1.023E+01	1.600E+00
1.400E+01	9.700E+00	8.700E-01
1.450E+01	8.660E+00	0.000E+00
1.500E+01	9.240E+00	5.100E-01
1.550E+01	1.007E+01	9.660E+00
1.600E+01	7.910E+00	6.400E-01
1.650E+01	5.400E-01	1.300E-01
1.700E+01	4.800E-01	2.500E-01
1.750E+01	6.080E+00	4.000E-01
1.800E+01	5.780E+00	1.400E-01
1.850E+01	5.430E+00	6.500E-01
1.900E+01	5.040E+00	1.000E-01
1.950E+01	4.790E+00	3.100E-01
2.000E+01	4.460E+00	6.400E-01
2.100E+01	4.070E+00	4.100E-01
2.200E+01	3.730E+00	8.900E-01
2.300E+01	3.460E+00	2.400E-01
3.200E+01	1.790E+00	0.000E+00
4.800E+01	9.300E-01	0.000E+00
5.200E+01	6.400E-01	0.000E+00
5.600E+01	6.100E-01	0.000E+00
7.200E+01	4.200E-01	0.000E+00
1.295E+02	2.300E-01	2.000E-01
1.508E+02	1.300E-01	0.000E+00
1.745E+02	9.000E-02	0.000E+00

TABLE C-29. TEMPORAL MOMENTS, COLUMN D, BROMIDE

Port	Zero Moment[1]	First Moment[2]	Second Moment[3]	Corrected Velocity[4]	Corrected Dispersion[5]	Predicted Mass[6]	Injected Mass[7]
1	0.58007E+03	0.34040E+05	0.23441E+07	3.5979	66.2407	10122.7	11000.0
2	0.28663E+03	0.21271E+05	0.16712E+07	2.8419	17.6810	5001.7	11000.0
3	0.87531E+03	0.35358E+05	0.19837E+07	5.2398	217.3405	15224.2	11000.0
4	0.13131E+04	0.61154E+05	0.35364E+07	4.5398	116.7598	22913.6	11000.0
5	0.56151E+03	0.25845E+05	0.17540E+07	3.4640	64.0485	9798.4	11000.0
6	0.40646E+03	0.24743E+05	0.18318E+07	2.8899	55.2340	7092.7	11000.0
7	0.13303E+04	0.58037E+05	0.32371E+07	4.0405	99.8831	23213.7	11000.0
8	0.11127E+04	0.50994E+05	0.28836E+07	3.8450	79.7643	19416.6	11000.0
9	0.11065E+04	0.45385E+05	0.2464E+07	3.4399	79.1533	19308.4	11000.0
10	0.13358E+04	0.64666E+05	0.38801E+07	2.9111	49.4478	23309.7	11000.0
11	0.13066E+04	0.48323E+05	0.25118E+07	3.8181	110.2439	22800.1	11000.0
12	0.13637E+04	0.46725E+05	0.21531E+07	4.1240	101.3993	23796.5	11000.0
13	0.11242E+04	0.31480E+05	0.10763E+07	3.7927	45.0123	19617.3	11000.0
14	0.17271E+04	0.55617E+05	0.24762E+07	3.2930	67.4572	30137.9	11000.0
15	0.15288E+04	0.25761E+05	0.53733E+06	6.3508	82.3421	26677.6	11000.0
16	0.12957E+04	0.49950E+05	0.24896E+07	2.7462	42.9223	22610.0	11000.0
17	0.14040E+04	0.42462E+05	0.18907E+07	2.3390	39.4844	24499.8	11000.0
18	0.10074E+04	0.47677E+05	0.31003E+07	1.4890	19.7552	17579.1	11000.0
19	0.13556E+04	0.37657E+05	0.16230E+07	2.5489	50.3399	23655.2	11000.0
20	0.14633E+04	0.49426E+05	0.23858E+07	2.0920	32.0108	25534.6	11000.0
21	0.14523E+04	0.26053E+05	0.81027E+06	1.9861	26.4227	25342.6	11000.0
22	0.15675E+04	0.43777E+05	0.19925E+07	1.2676	14.2897	27352.9	11000.0
23	0.24083E+04	0.10480E+06	0.58829E+07	0.8102	4.1711	42024.8	11000.0
24	0.12808E+04	0.32500E+05	0.11457E+07	1.3968	9.7561	22350.0	11000.0
25	0.70945E03	0.14384E+05	0.39327E+05	15.0319	810.9565	726.85	11000.0

[1]Zero Moment in mg-hr/L, [2]First Moment in hr, [3]Second Moment in hr^2, [4]Corrected Velocity in cm/hr, [5]Corrected Dispersion in cm^2/hr, [6]Predicted Mass in mg, [7]Injected Mass in mg.

TABLE C-30. TEMPORAL MOMENTS, COLUMN D, NAPHTHALENE

Port	Zero Moment[1]	First Moment[2]	Second Moment[3]	Corrected Velocity[4]	Corrected Dispersion[5]	Predicted Mass[6]	Injected Mass[7]
2	0.34530E+01	0.13605E+03	0.73626E+04	5.3730	214.1061	60.2	450.0
3	0.54722E+01	0.25301E+03	0.14859E+05	4.5733	131.5376	95.4	450.0
4	0.12645E+01	0.26973E+02	0.65361E+03	9.9931	140.5658	147	450.0
6	0.98500E+00	0.22542E+02	0.79270E+03	7.7543	374.3768	17.2	450.0
7	0.46500E+01	0.18592E+03	0.10789E+05	4.4119	177.0330	81.1	450.0
9	0.30557E+01	0.13959E+03	0.95553E+04	3.0862	109.2077	53.3	450.0
10	0.35117E+01	0.17326E+03	0.11041E+05	2.8559	59.0375	61.2	450.0
16	0.22327E+01	0.37778E+02	0.71559E+03	6.3241	41.1740	38.9	450.0
17	0.50625E+01	0.17919E+03	0.85694E+04	1.9955	24.9695	88.3	450.0
18	0.41465E+01	0.16868E+0.	0.84395E+04	1.7343	14.1781	72.4	450.0
19	0.43618E+01	0.23910E+03	0.16649E+05	1.2844	12.2903	76.1	450.0
20	0.11319E+02	0.64825E+03	0.46684E+05	1.2291	11.1987	197.5	450.0
23	0.10797E+02	0.52972E+03	0.35001E+05	0.7180	4.4145	188.5	450.0
24	0.11499E+02	0.34699E+03	0.16414E+05	1.1722	11.8926	200.7	450.0
25	0.75772E+01	0.20176E+03	0.89552E+04	11.4020	1168.0244	1168.0	450.0

[1]Zero Moment in mg-hr/L, [2]First Moment in hr, [3]Second Moment in hr^2, [4]Corrected Velocity in cm/hr, [5]Corrected Dispersion in cm^2/hr, [6]Predicted Mass in mg, [7]Injected Mass in mg.

TABLE C-31. TIME AND CONCENTRATION VALUES, PORT 1, COLUMN D.

Time (hr.)	Bromide (ppm)
0.000E+00	0.000E+00
1.000E+00	0.000E+00
2.000E+00	0.000E+00
3.000E+00	0.000E+00
4.000E+00	0.000E+00
5.000E+00	0.000E+00
6.000E+00	0.000E+00
7.000E+00	0.000E+00
8.000E+00	0.000E+00
9.000E+00	0.000E+00
1.000E+01	1.069E+00
1.100E+01	1.451E+00
1.200E+01	1.559E+00
1.300E+01	2.158E+00
1.400E+01	2.631E+00
1.500E+01	2.301E+00
1.600E+01	2.158E+00
1.700E+01	3.024E+00
1.800E+01	3.694E+00
1.900E+01	3.930E+00
2.000E+01	4.006E+00
2.100E+01	4.649E+00
2.200E+01	5.737E+00
3.000E+01	7.142E+00
4.700E+01	6.967E+00
5.400E+01	7.597E+00
7.800E+01	6.753E+00
1.025E+02	5.488E+00

TABLE C-32. TIME AND CONCENTRATION VALUES, PORT 2, COLUMN D.

Time (hr.)	Bromide (ppm)	Naphthalene (ppm)
0.000E+00	0.000E+00	1.030E-01
1.000E+00	0.000E+00	2.800E-02
2.000E+00	0.000E+00	9.200E-02
3.000E+00	0.000E+00	0.000E+00
4.000E+00	0.000E+00	0.000E+00
5.000E+00	0.000E+00	0.000E+00
6.000E+00	0.000E+00	0.000E+00
7.000E+00	0.000E+00	0.000E+00
8.000E+00	0.000E+00	0.000E+00
9.000E+00	0.000E+00	3.700E-02
1.000E+01	0.000E+00	1.580E-01
1.100E+01	0.000E+00	4.300E-02
1.200E+01	0.000E+00	5.900E-02
1.300E+01	0.000E+00	7.500E-02
1.400E+01	0.000E+00	7.500E-02
1.500E+01	0.000E+00	8.000E-02
1.600E+01	0.000E+00	0.000E+00
1.700E+01	0.000E+00	0.000E+00
1.800E+01	0.000E+00	1.430E-01
1.900E+01	0.000E+00	0.000E+00
2.000E+01	0.000E+00	0.000E+00
2.100E+01	0.000E+00	1.000E-02
2.200E+01	0.000E+00	1.020E-01
2.600E+01	NA	4.000E-02
3.000E+01	0.000E+00	9.600E-02
4.700E+01	2.423E+00	0.000E+00
5.400E+01	3.644E+00	5.100E-02
7.800E+01	5.592E+00	1.600E-02
1.025E+02	5.344E+00	0.000E+00

TABLE C-33. TIME AND CONCENTRATION VALUES, PORT 3, COLUMN D.

Time (hr.)	Bromide (ppm)	Naphthalene (ppm)
0.000E+00	0.000E+00	0.000E+00
1.000E+00	0.000E+00	0.000E+00
2.000E+00	0.000E+00	4.600E-02
3.000E+00	0.000E+00	7.100E-02
4.000E+00	0.000E+00	3.700E-02
5.000E+00	1.767E+00	0.000E+00
6.000E+00	0.000E+00	0.000E+00
7.500E+00	2.584E+00	0.000E+00
8.000E+00	3.839E+00	0.000E+00
9.000E+00	7.337E+00	0.000E+00
1.000E+01	1.298E+01	3.630E-01
1.100E+01	9.228E+00	7.500E-02
1.200E+01	1.156E+01	3.100E-02
1.350E+01	1.525E+01	0.000E+00
1.400E+01	1.800E+01	0.000E+00
1.500E+01	2.169E+01	1.010E-01
1.600E+01	2.105E+01	0.000E+00
1.800E+01	2.316E+01	9.500E-02
2.000E+01	2.453E+01	6.700E-02
2.100E+01	2.557E+01	1.510E-01
2.200E+01	2.402E+01	0.000E+00
2.600E+01	2.060E+01	0.000E+00
3.000E+01	1.622E+01	1.480E-01
4.700E+01	6.300E+00	0.000E+00
5.400E+01	5.020E+00	1.250E-01
7.800E+01	5.052E+00	3.100E-02
1.025E+02	3.740E+00	0.000E+00

TABLE C-34. TIME AND CONCENTRATION VALUES, PORT 4, COLUMN D.

Time (hr.)	Bromide (ppm)	Naphthalene (ppm)
0.000E+00	0.000E+00	0.000E+00
1.000E+00	0.000E+00	0.000E+00
2.000E+00	0.000E+00	0.000E+00
3.000E+00	0.000E+00	0.000E+00
4.000E+00	0.000E+00	0.000E+00
5.000E+00	0.000E+00	0.000E+00
6.000E+00	0.000E+00	7.300E-02
7.500E+00	2.571E+00	0.000E+00
8.000E+00	2.880E+00	6.000E-02
9.000E+00	4.281E+00	3.500E-02
1.000E+01	4.853E+00	1.150E-01
1.100E+01	6.377E+00	3.600E-02
1.200E+01	7.443E+00	0.000E+00
1.350E+01	7.785E+00	0.000E+00
1.400E+01	9.136E+00	0.000E+00
1.500E+01	9.702E+00	0.000E+00
1.600E+01	1.025E+01	0.000E+00
1.700E+01	1.133E+01	3.600E-02
1.800E+01	1.174E+01	0.000E+00
1.900E+01	1.291E+01	0.000E+00
2.000E+01	1.723E+01	4.200E-02
2.100E+01	2.835E+01	0.000E+00
2.200E+01	3.044E+01	4.300E-02
2.600E+01	2.777E+01	1.330E-01
3.000E+01	2.570E+01	1.140E-01
4.700E+01	1.880E+01	NA
5.400E+01	1.631E+01	NA
7.800E+01	6.816E+00	NA
1.025E+02	5.440E+00	NA

TABLE C-35. TIME AND CONCENTRATION VALUES, PORT 5, COLUMN D.

Time (hr.)	Bromide (ppm)
1.000E+00	0.000E+00
4.000E+00	0.000E+00
5.000E+00	0.000E+00
7.000E+00	0.000E+00
1.000E+01	0.000E+00
1.100E+01	9.011E-01
1.300E+01	1.786E+00
1.500E+01	3.290E+00
1.700E+01	6.925E+00
1.900E+01	1.003E+01
2.100E+01	6.260E+00
2.600E+01	7.829E+00
3.000E+01	7.974E+00
4.700E+01	1.086E+01
5.400E+01	7.136E+00
7.800E+01	4.004E+00
1.020E+02	3.184E+00

TABLE C-36. TIME AND CONCENTRATION VALUES, PORT 6, COLUMN D.

Time (hr.)	Bromide (ppm)	Naphthalene (ppm)
1.000E+00	0.000E+00	3.200E-02
4.000E+00	0.000E+00	1.630E-01
5.000E+00	0.000E+00	0.000E+00
7.000E+00	0.000E+00	0.000E+00
9.000E+00	0.000E+00	0.000E+00
1.100E+01	3.418E+01	0.000E+00
1.300E+01	0.000E+00	0.000E+00
1.500E+01	0.000E+00	0.000E+00
1.700E+01	0.000E+00	2.200E-02
2.100E+01	0.000E+00	0.000E+00
2.600E+01	0.000E+00	0.000E+00
3.000E+01	0.000E+00	0.000E+00
4.700E+01	4.498E+00	5.400E-02
5.400E+01	5.415E+00	0.000E+00
7.800E+01	5.346E+00	0.000E+00
1.020E+02	5.991E+00	0.000E+00

TABLE C-37. TIME AND CONCENTRATION VALUES, PORT 7, COLUMN D.

Time (hr.)	Bromide (ppm)	Naphthalene (ppm)
1.000E+00	0.000E+00	6.800E-02
4.000E+00	0.000E+00	0.000E+00
5.000E+00	2.631E+00	9.900E-02
7.500E+00	7.012E+00	1.940E-01
9.500E+00	1.313E+01	5.200E-02
1.100E+01	1.241E+01	0.000E+00
1.300E+01	1.241E+01	2.800E-02
1.500E+01	1.224E+01	7.200E-02
1.700E+01	1.385E+01	0.000E+00
1.900E+01	1.496E+01	1.040E-01
2.100E+01	2.920E+01	8.400E-02
2.600E+01	2.846E+01	4.400E-02
3.000E+01	2.406E+01	4.000E-02
4.700E+01	2.082E+01	1.240E-01
5.400E+01	1.349E+01	2.200E-02
7.800E+01	7.459E+00	0.000E+00
1.025E+02	2.902E+00	5.700E-02

TABLE C-38. TIME AND CONCENTRATION VALUES, PORT 8 , COLUMN D.

Time (hr.)	Bromide (ppm)
1.000E+00	0.000E+00
4.000E+00	0.000E+00
5.000E+00	0.000E+00
7.500E+00	1.808E+00
9.500E+00	3.243E+00
1.100E+01	3.676E+00
1.300E+01	6.242E+00
1.500E+01	8.130E+00
1.700E+01	1.163E+01
1.900E+01	1.385E+01
2.100E+01	2.431E+01
2.600E+01	2.269E+01
3.000E+01	2.060E+01
4.700E+01	1.818E+01
5.400E+01	1.346E+01
7.800E+01	6.650E+00
1.025E+02	2.060E+00

TABLE C-39. TIME AND CONCENTRATION VALUES, PORT 9, COLUMN D.

Time (hr.)	Bromide (ppm)	Naphthalene (ppm)
0.000E+00	0.000E+00	0.000E+00
1.000E+00	0.000E+00	7.800E-02
2.000E+00	0.000E+00	7.800E-02
3.000E+00	0.000E+00	0.000E+00
4.000E+00	0.000E+00	6.400E-02
5.000E+00	0.000E+00	5.900E-02
6.000E+00	0.000E+00	8.800E-02
7.000E+00	9.606E-01	0.000E+00
8.000E+00	1.527E+00	0.000E+00
9.000E+00	2.885E+00	0.000E+00
1.000E+01	6.383E+00	0.000E+00
1.100E+01	1.361E+01	0.000E+00
1.200E+01	1.538E+01	0.000E+00
1.300E+01	1.857E+01	6.300E-02
1.400E+01	2.148E+01	1.670E-01
1.500E+01	1.936E+01	7.800E-02
1.600E+01	2.598E+01	1.800E-02
1.700E+01	2.728E+01	0.000E+00
1.800E+01	2.822E+01	8.600E-02
1.900E+01	3.190E+01	0.000E+00
2.000E+01	2.407E+01	6.200E-02
2.100E+01	2.763E+01	4.300E-02
2.200E+01	2.680E+01	0.000E+00
3.000E+01	1.490E+01	1.170E-01
4.700E+01	1.473E+01	0.000E+00
5.400E+01	1.054E+01	0.000E+00
7.800E+01	5.449E+00	0.000E+00
1.020E+02	2.752E+00	7.700E-02

TABLE C-40. TIME AND CONCENTRATION VALUES, PORT 10, COLUMN D.

Time (hr.)	Bromide (ppm)	Naphthalene (ppm)
0.000E+00	0.000E+00	3.200E-02
1.000E+00	0.000E+00	4.600E-02
2.000E+00	0.000E+00	6.800E-02
3.000E+00	0.000E+00	0.000E+00
4.000E+00	0.000E+00	2.700E-02
5.000E+00	0.000E+00	0.000E+00
6.000E+00	0.000E+00	0.000E+00
7.000E+00	0.000E+00	0.000E+00
8.000E+00	0.000E+00	0.000E+00
9.000E+00	0.000E+00	3.600E-02
1.000E+01	0.000E+00	9.400E-02
1.100E+01	7.395E-01	0.000E+00
1.200E+01	1.799E+00	4.500E-02
1.300E+01	4.241E+00	0.000E+00
1.400E+01	1.429E+01	1.610E-01
1.500E+01	2.423E+01	0.000E+00
1.600E+01	2.736E+01	8.900E-02
1.700E+01	2.960E+01	0.000E+00
1.800E+01	2.300E+01	4.300E-02
1.900E+01	2.115E+01	0.000E+00
2.000E+01	1.696E+01	0.000E+00
2.100E+01	1.686E+01	0.000E+00
2.200E+01	2.405E+01	0.000E+00
2.600E+01	2.282E+01	0.000E+00
3.000E+01	1.972E+01	8.100E-02
4.700E+01	1.978E+01	0.000E+00
5.400E+01	1.778E+01	9.500E-02
7.800E+01	8.847E+01	0.000E+00
1.020E+02	5.989E+00	3.900E-02

TABLE C-41. TIME AND CONCENTRATION VALUES, PORT 11, COLUMN D.

Time (hr.)	Bromide (ppm)
0.000E+00	0.000E+00
1.000E+00	0.000E+00
2.000E+00	0.000E+00
3.000E+00	1.421E+00
4.000E+00	2.773E+00
5.000E+00	7.334E+00
6.000E+00	1.683E+01
7.500E+00	2.844E+01
8.000E+00	2.801E+01
9.000E+00	3.251E+01
1.000E+01	1.658E+01
1.100E+01	1.965E+01
1.200E+01	2.323E+01
1.350E+01	2.494E+01
1.400E+01	2.519E+01
1.500E+01	2.494E+01
1.600E+01	2.456E+01
1.700E+01	2.532E+01
1.800E+01	2.395E+01
1.900E+01	2.407E+01
2.000E+01	2.831E+01
2.100E+01	2.935E+01
2.200E+01	2.890E+01
2.600E+01	2.659E+01
3.000E+01	2.444E+01
4.700E+01	1.188E+01
5.400E+01	1.103E+01
7.800E+01	5.156E+00
1.025E+02	2.341E+00

TABLE C-42. TIME AND CONCENTRATION VALUES, PORT 12, COLUMN D.

Time (hr.)	Concentration (ppm)
0.000E+00	0.000E+00
1.000E+00	0.000E+00
2.000E+00	0.000E+00
3.000E+00	0.000E+00
4.000E+00	0.000E+00
5.000E+00	7.422E+00
6.000E+00	1.245E+01
7.500E+00	9.914E+00
8.000E+00	1.096E+01
9.000E+00	1.659E+01
1.000E+01	3.418E+01
1.100E+01	3.190E+01
1.200E+01	2.586E+01
1.350E+01	3.088E+01
1.400E+01	3.002E+01
1.500E+01	3.723E+01
1.600E+01	3.907E+01
1.700E+01	3.706E+01
1.800E+01	3.250E+01
1.900E+01	3.016E+01
2.000E+01	2.773E+01
2.100E+01	3.091E+01
2.200E+01	2.730E+01
2.600E+01	2.951E+01
3.000E+01	2.510E+01
4.700E+01	1.878E+01
5.400E+01	1.047E+01
7.800E+01	3.382E+00
1.025E+02	0.000E+00

TABLE C-43. TIME AND CONCENTRATION VALUES, PORT 13, COLUMN D.

Time (hr.)	Bromide (ppm)
1.000E+00	0.000E+00
4.000E+00	0.000E+00
5.000E+00	0.000E+00
7.000E+00	2.143E+00
9.000E+00	6.369E+00
1.100E+01	1.877E+01
1.350E+01	3.519E+01
1.500E+01	4.118E+01
1.700E+01	4.555E+01
1.900E+01	4.843E+01
2.100E+01	3.146E+01
2.600E+01	3.114E+01
3.000E+01	3.570E+01
4.700E+01	4.546E+00
5.400E+01	3.544E+00
7.800E+01	0.000E+00
1.025E+02	0.000E+00

TABLE C-44. TIME AND CONCENTRATION VALUES, PORT 14, COLUMN D.

Time (hr.)	Bromide (ppm)
1.000E+00	0.000E+00
4.000E+00	0.000E+00
5.000E+00	3.051E+00
7.000E+00	7.945E+00
9.000E+00	1.696E+01
1.100E+01	5.187E+01
1.350E+01	6.288E+01
1.500E+01	6.698E+01
1.700E+01	5.938E+01
1.900E+01	5.599E+01
2.100E+01	2.902E+01
2.600E+01	3.675E+01
3.000E+01	3.124E+01
4.700E+01	1.668E+01
5.400E+01	1.254E+01
7.800E+01	3.828E+00
1.025E+02	0.000E+00

TABLE C-45. TIME AND CONCENTRATION VALUES, PORT 15, COLUMN D.

Time (hr.)	Bromide (ppm)
1.000E+00	0.000E+00
4.000E+00	7.564E+00
5.000E+00	2.726E+01
7.500E+00	7.051E+01
9.500E+00	6.959E+01
1.100E+01	7.764E+01
1.350E+01	8.049E+01
1.500E+01	7.997E+01
1.700E+01	7.408E+01
1.900E+01	5.630E+01
2.100E+01	5.190E+01
2.600E+01	4.177E+01
3.000E+01	9.429E+00
4.700E+01	0.000E+00
5.400E+01	0.000E+00
7.800E+01	0.000E+00
1.025E+02	0.000E+00

TABLE C-46. TIME AND CONCENTRATION VALUES, PORT 16, COLUMN D.

Time (hr.)	Bromide (ppm)	Naphthalene (ppm)
1.000E+00	0.000E+00	0.000E+00
4.000E+00	0.000E+00	2.200E-02
5.000E+00	8.051E-01	7.400E-02
7.500E+00	5.281E+00	0.000E+00
9.500E+00	7.857E+00	6.300E-02
1.100E+01	1.286E+01	1.980E-01
1.350E+01	2.650E+01	4.300E-02
1.500E+01	2.728E+01	2.720E-01
1.700E+01	3.161E+01	1.470E-01
2.100E+01	2.673E+01	6.100E-02
2.600E+01	2.831E+01	7.800E-02
3.000E+01	2.631E+01	0.000E+00
4.700E+01	1.665E+01	0.000E+00
5.400E+01	1.361E+01	0.000E+00
7.800E+01	4.645E+00	0.000E+00
1.025E+02	0.000E+00	0.000E+00

TABLE C-47. TIME AND CONCENTRATION VALUES, PORT 17, COLUMN D.

Time (hr)	Bromide (ppm)	Naphthalene (ppm)
1.000E+00	0.000E+00	0.000E+00
4.000E+00	5.357E+00	3.500E-02
5.000E+00	1.024E+01	0.000E+00
7.000E+00	1.975E+01	0.000E+00
9.500E+00	3.079E+01	0.000E+00
1.100E+01	4.325E+01	1.840E-01
1.300E+01	4.834E+01	7.100E-02
1.500E+01	6.996E+01	1.760E-01
1.700E+01	4.998E+01	2.320E-01
1.900E+01	4.654E+01	9.200E-02
2.100E+01	2.571E+01	1.580E-01
2.600E+01	2.254E+01	1.480E-01
3.000E+01	1.690E+01	6.200E-02
4.700E+01	1.351E+01	0.000E+00
5.400E+01	1.039E+01	1.070E-01
7.800E+01	3.073E+00	0.000E+00
1.025E+02	0.000E+00	0.000E+00

TABLE C-48. TIME AND CONCENTRATION VALUES, PORT 18, COLUMN D

Time (hr.)	Bromide (ppm)	Naphthalene (ppm)
1.000E+00	0.000E+00	1.110E-01
4.000E+00	0.000E+00	0.000E+00
5.000E+00	3.387E+00	0.000E+00
7.000E+00	6.330E+00	0.000E+00
9.500E+00	7.481E+00	0.000E+00
1.100E+01	2.253E+01	5.200E-02
1.300E+01	2.373E+01	7.200E-02
1.500E+01	2.460E+01	1.040E-01
1.700E+01	2.253E+01	3.100E-02
1.900E+01	1.995E+01	0.000E+00
2.600E+01	1.323E+01	8.000E-02
3.000E+01	1.690E+01	0.000E+00
4.700E+01	NA	1.360E-01
5.400E+01	NA	8.200E-02
7.800E+01	NA	0.000E+00
1.025E+02	0.000E+00	0.000E+00

TABLE C-49. TIME AND CONCENTRATION VALUES, PORT 19, COLUMN D.

Time (hr.)	Bromide (ppm)	Naphthalene (ppm)
1.000E+00	0.000E+00	0.000E+00
4.000E+00	3.318E+00	5.000E-02
5.000E+00	2.202E+01	0.000E+00
7.500E+00	4.854E+01	7.800E-02
9.500E+00	5.279E+01	0.000E+00
1.100E+01	5.266E+01	2.470E-01
1.350E+01	4.753E+01	0.000E+00
1.500E+01	4.512E+01	0.000E+00
1.700E+01	4.098E+01	1.370E-01
1.900E+01	2.918E+01	0.000E+00
2.100E+01	2.604E+01	0.000E+00
2.600E+01	2.162E+01	0.000E+00
3.000E+01	1.749E+01	0.000E+00
4.700E+01	9.764E+00	5.300E-02
5.400E+01	8.945E+00	5.500E-02
7.800E+01	2.527E+00	7.800E-02
1.025E+02	0.000E+00	0.000E+00

TABLE C-50. TIME AND CONCENTRATION VALUES, PORT 20, COLUMN D.

Time (hr.)	Bromide (ppm)	Naphthalene (ppm)
1.000E+00	0.000E+00	0.000E+00
4.000E+00	7.472E+00	2.500E-02
5.000E+00	9.675E+00	0.000E+00
7.500E+00	2.168E+01	4.600E-02
9.500E+00	2.586E+01	2.670E-01
1.100E+01	2.742E+01	1.120E-01
1.300E+01	3.537E+01	6.600E-02
1.500E+01	3.904E+01	3.120E-01
1.700E+01	3.961E+01	6.400E-02
1.900E+01	4.469E+01	9.200E-02
2.100E+01	3.728E+01	6.300E-02
2.600E+01	2.945E+01	7.900E-02
3.000E+01	2.496E+01	1.410E-01
4.700E+01	1.314E+01	4.900E-02
5.400E+01	1.033E+01	0.000E+00
7.800E+01	4.545E+00	2.800E-01
1.025E+02	1.538E+00	0.000E+00

TABLE C-51. TIME AND CONCENTRATION VALUES, PORT 21, COLUMN D.

Time (hr.)	Bromide (ppm)
1.000E+00	0.000E+00
2.000E+00	2.223E+00
3.000E+00	6.790E+01
4.000E+00	9.218E+01
5.000E+00	9.569E+01
6.000E+00	8.909E+01
7.000E+00	8.315E+01
8.000E+00	8.092E+01
9.000E+00	8.219E+01
1.000E+01	6.048E+01
1.100E+01	5.252E+01
1.200E+01	4.331E+01
1.300E+01	4.481E+01
1.400E+01	4.569E+01
1.500E+01	3.100E+01
1.600E+01	2.885E+01
1.700E+01	2.841E+01
1.800E+01	2.522E+01
1.900E+01	2.383E+01
2.000E+01	2.335E+01
2.100E+01	2.143E+01
2.200E+01	1.785E+01
2.600E+01	1.457E+01
3.800E+01	1.640E+01
4.700E+01	4.081E+00
5.400E+01	4.133E+00
7.800E+01	0.000E+00
1.025E+02	0.000E+00

TABLE C-52. TIME AND CONCENTRATION VALUES, PORT 22, COLUMN D.

Time (hr.)	Bromide (ppm)	Naphthalene (ppm)
0.000E+00	0.000E+00	0.000E+00
1.000E+00	0.000E+00	5.300E-02
2.000E+00	0.000E+00	0.000E+00
3.000E+00	6.570E+00	0.000E+00
4.000E+00	1.744E+01	9.000E-02
5.000E+00	4.643E+01	0.000E+00
6.000E+00	6.562E+01	4.630E-01
7.000E+00	6.562E+01	4.210E-01
8.000E+00	6.620E+01	7.900E-02
9.000E+00	7.561E+01	8.200E-02
1.000E+01	4.268E+01	1.870E-01
1.100E+01	6.424E+01	2.320E-01
1.200E+01	5.930E+01	2.110E-01
1.300E+01	5.413E+01	3.360E-01
1.400E+01	5.440E+01	1.620E-01
1.500E+01	1.422E+01	0.000E+00
1.600E+01	4.202E+01	1.050E-01
1.700E+01	3.379E+01	0.000E+00
1.800E+01	3.291E+01	1.120E-01
1.900E+01	2.690E+01	4.400E-02
2.000E+01	2.650E+01	0.000E+00
2.100E+01	2.323E+01	9.800E-02
2.200E+01	2.037E+01	1.020E-01
2.600E+01	1.869E+01	0.000E+00
3.800E+01	2.082E+01	1.610E-01
4.700E+01	1.236E+01	0.000E+00
5.400E+01	8.327E+00	0.000E+00
7.800E+01	3.590E+00	0.000E+00
1.025E+02	1.277E+00	0.000E+00

TABLE C-53. TIME AND CONCENTRATION VALUES, PORT 23, COLUMN D.

Time (hr.)	Bromide (ppm)	Naphthalene (ppm)
0.000E+00	0.000E+00	0.000E+00
1.000E+00	0.000E+00	0.000E+00
2.000E+00	0.000E+00	4.900E-02
3.000E+00	0.000E+00	4.500E-02
4.000E+00	0.000E+00	4.600E-02
5.000E+00	8.274E+00	0.000E+00
6.000E+00	1.054E+01	0.000E+00
7.500E+00	1.443E+01	2.280E-01
8.000E+00	7.859E+00	2.040E-01
9.500E+00	2.748E+00	1.880E-01
1.000E+01	2.453E+01	3.400E-02
1.100E+01	1.404E+01	1.010E-01
1.200E+01	3.120E+01	2.780E-01
1.350E+01	2.813E+01	1.160E-01
1.400E+01	5.325E+01	1.260E-01
1.500E+01	3.300E+01	5.100E-02
1.600E+01	3.871E+01	1.260E-01
1.700E+01	3.851E+01	9.700E-02
1.800E+01	3.992E+01	7.700E-02
1.900E+01	2.925E+01	7.470E-01
2.100E+01	4.054E+01	1.200E-01
2.200E+01	4.273E+01	3.800E-02
3.800E+01	4.610E+01	1.220E-01
4.700E+01	2.637E+01	1.280E-01
5.400E+01	2.245E+01	6.100E-02
7.800E+01	1.882E+01	1.170E-01
1.025E+02	0.000E+00	7.800E-02

TABLE C-54. TIME AND CONCENTRATION VALUES, PORT 24, COLUMN D.

Time (hr.)	Bromdie (ppm)	Naphthalene (ppm)
0.000E+00	7.716E+00	0.000E+00
1.000E+00	0.000E+00	7.600E-02
2.000E+00	0.000E+00	0.000E+00
3.000E+00	0.000E+00	0.000E+00
4.000E+00	1.795E+00	2.100E-01
5.000E+00	5.568E+00	3.100E-01
6.000E+00	1.356E+01	3.410E-01
7.000E+00	2.922E+01	4.350E-01
8.000E+00	5.027E+01	9.240E-01
9.000E+00	5.147E+01	4.200E-02
1.000E+01	5.976E+01	8.340E-01
1.100E+01	5.656E+01	3.820E-01
1.200E+01	5.375E+01	1.300E-01
1.300E+01	5.154E+01	1.670E-01
1.400E+01	4.339E+01	3.700E-01
1.500E+01	3.688E+01	1.550E-01
1.600E+01	3.451E+01	1.700E-01
1.800E+01	2.925E+01	2.560E-01
2.000E+01	2.749E+01	9.500E-02
2.100E+01	2.938E+01	2.400E-01
2.200E+01	2.938E+01	5.160E-01
2.600E+01	2.777E+01	9.600E-02
3.000E+01	2.453E+01	4.100E-02
4.700E+01	9.347E+00	9.900E-02
5.400E+01	5.768E+00	1.150E-01
7.800E+01	0.000E+00	9.200E-02
1.025E+02	0.000E+00	

TABLE C-55. TIME AND CONCENTRATION VALUES, PORT 25, COLUMN D.

Time (hr.)	Bromide (ppm)	Naphthalene (ppm)
0.000E+00	0.000E+00	0.000E+00
5.000E-01	2.090E+01	9.394E-02
1.000E+00	0.000E+00	0.000E+00
1.500E+00	0.000E+00	1.879E-02
2.000E+00	0.000E+00	0.000E+00
2.500E+00	1.341E+00	0.000E+00
3.000E+00	1.940E+00	8.172E-02
3.500E+00	2.155E+00	4.227E-02
4.000E+00	4.134E+00	6.059E-02
4.500E+00	7.164E+00	1.357E-01
5.000E+00	1.082E+01	1.456E-01
5.500E+00	1.552E+01	2.870E-01
6.000E+00	2.359E+01	1.606E-01
6.500E+00	2.558E+01	2.607E-01
7.000E+00	2.874E+01	3.245E-01
7.500E+00	2.845E+01	1.559E-01
8.000E+00	2.817E+01	2.236E-01
9.500E+00	2.993E+01	5.138E-01
1.050E+01	3.039E+01	3.241E-01
1.100E+01	2.746E+01	2.574E-01
1.150E+01	3.037E+01	2.856E-01
1.200E+01	3.112E+01	3.114E-01
1.250E+01	2.971E+01	3.058E-01
1.300E+01	2.880E+01	6.482E-02
1.350E+01	2.880E+01	0.000E+00
1.400E+01	2.850E+01	5.758E-01
1.450E+01	2.778E+01	2.560E-01
1.500E+01	2.584E+01	2.851E-01
1.550E+01	2.479E+01	1.879E-01
1.600E+01	2.479E+01	1.733E-01
1.650E+01	2.458E+01	1.123E-01
1.700E+01	2.236E+01	3.635E-01
1.750E+01	2.236E+01	2.503E-01
1.800E+01	2.224E+01	4.969E-01
1.850E+01	2.213E+01	3.607E-01
1.900E+01	2.146E+01	4.359E-01
1.950E+01	1.905E+01	3.457E-01
2.000E+01	1.955E+01	2.837E-01
2.100E+01	1.915E+01	2.734E-01
2.200E+01	1.828E+01	3.184E-01
2.600E+01	1.511E+01	3.645E-01
3.000E+01	1.077E+01	1.451E-01
4.700E+01	4.317E+00	1.738E-01
5.400E+01	0.000E+00	6.810E-02
7.800E+01	NA	1.691E-02
1.025E+02	0.000E+00	2.724E-02
1.203E+02	0.000E+00	1.710E-02

TABLE C-56. TEMPORAL MOMENTS, COLUMN E, BROMIDE

Port	Zero Moment[1]	First Moment[2]	Second Moment[3]	Corrected Velocity[4]	Corrected Dispersion[5]	Predicted Mass[6]	Injected Mass[7]
1	0.17967E+03	0.59391E+04	0.21930E+06	5.9898	70.4404	6288.4	14077.0
2	0.12800E+03	0.46632E+04	0.18198E+06	5.4271	38.6957	4480.0	14077.0
3	0.31142E+03	0.79163E+04	0.26297E+06	7.8251	243.4480	10899.7	14077.0
4	0.24644E+03	0.54383E+04	0.16236E+06	9.0413	325.4631	8625.4	14077.0
5	0.16911E+03	0.48786E+04	0.16651E+06	5.6441	85.5545	5918.8	14077.0
6	0.14633E+03	0.56747E+04	0.23087E+06	4.1798	16.8360	5121.6	14077.0
7	0.24187E+03	0.44920E+04	0.12885E+06	8.8537	407.1283	8465.45	14077.0
8	0.10108E+03	0.15654E+04	0.28468E+05	10.6757	158.5835	3537.8	14077.0
9	0.17326E+03	0.3527E+04	0.98177E+05	6.2948	151.7763	6064.1	14077.0
10	0.21904E+03	0.60964E+04	0.19596E+06	4.5732	45.8649	7666.4	14077.0
11	0.22352E+03	0.50803E+04	0.16127E+06	5.6234	145.6962	7823.2	14077.0
12	0.39090E+03	0.80546E+04	0.24772E+06	6.2173	200.9588	201.0	14077.0
13	0.43576E+03	0.82397E+04	0.21551E+06	4.8889	88.8959	15251.6	14077.0
14	0.40005E+03	0.73500E+04	0.19929E+06	5.0355	113.8676	14001.8	14077.0
15	0.35751E+03	0.72544E+04	0.20377E+06	4.5474	82.6188	12512.8	14077.0
16	0.33525E+03	0.86844E+04	0.28491E+06	3.5427	44.1504	11733.75	14077.0
17	0.40890E+03	0.91208E+04	0.28173E+06	2.5223	27.9144	14311.5	14077.0
18	0.30696E+03	0.80424E+04	0.27352E+06	2.1401	18.2239	10743.6	14077.0
19	0.40468E+03	0.89957E+04	0.27997E+06	2.5312	29.1340	14163.8	14077.0
20	0.32902E+03	0.81572E+04	0.27054E+06	2.2641	21.8964	11515.7	14077.0
21	0.48246E+03	0.72141E+04	0.18686E+06	1.3838	10.8410	16886.1	14077.0
22	0.15590E+04	0.35723E+05	0.11324E+07	0.8923	3.5741	54565.0	14077.0
23	0.86134E+03	0.19459E+05	0.58570E+06	0.9053	3.1443	30146.9	14077.0
24	0.14211E+04	0.37721E+05	0.12609E+07	0.7679	2.0676	49738.5	14077.0
25	0.22594E+03	0.20629E+04	0.27790E+05	33.0233	2498.6521	7906.5	14077.0

[1] Zero Moment in mg-hr/L, [2] First Moment in hr, [3] Second Moment in hr[2], [4] Corrected Velocity in cm/hr, [5] Corrected Dispersion [6] Pedicted Mass in mg, Injected Mass in mg.

TABLE C-57. TEMPORAL MOMENTS, COLUMN E, NAPHTHALENE

Port	Zero Moment[1]	First Moment[2]	Second Moment[3]	Corrected. Velocity[4]	Corrected Dispersion[5]	Predicted Mass[6]	Injected Mass[7]
2	0.75180E+01	0.25901E+03	0.10084E+05	5.7434	74.9602	263.2	450.0
12	0.24275E+01	0.28200E+02	0.40854E+03	11.244	189.1237	85.1	450.0
22	0.26968E+02	0.71459E+03	0.24512E+05	7.5008	223.7098	944	450.0
25	0.90419E+01	0.11189E+03	0.24867E+04	24.0018	2955.1179	316.4	450.0

[1] Zero Moment in mg-hr/L, [2] First Moment in hr, [3] Second Moment in hr^2, [4] Corrected Velocity in cm/hr, [5] Corrected Dispersion
[6] Pedicted Mass in mg, [7] Injected Mass in mg.

TABLE C-58. TIME AND CONCENTRATION VALUES, PORT 1, COLUMN E.

Time (hr.)	Bromide (ppm)
0.000E+00	0.000E+00
1.000E+00	0.000E+00
2.000E+00	0.000E+00
3.000E+00	0.000E+00
4.000E+00	0.000E+00
5.000E+00	0.000E+00
6.000E+00	0.000E+00
8.000E+00	0.000E+00
9.000E+00	0.000E+00
1.000E+01	0.000E+00
1.100E+01	0.000E+00
1.200E+01	0.000E+00
1.300E+01	2.045E+00
1.400E+01	2.339E+00
1.500E+01	3.519E+00
1.600E+01	4.173E+00
1.700E+01	4.669E+00
1.800E+01	4.883E+00
1.900E+01	4.384E+00
2.000E+01	3.902E+00
2.100E+01	5.176E+00
2.500E+01	5.246E+00
3.000E+01	4.565E+00
5.300E+01	4.287E+00

TABLE C-59. TIME AND CONCENTRATION VALUES, PORT 2, COLUMN E.

Time (hr.)	Bromide (ppm)	Naphthalene (ppm)
0.000E+00	0.000E+00	0.000E+00
1.000E+00	0.000E+00	0.000E+00
2.000E+00	0.000E+00	8.700E-02
3.000E+00	0.000E+00	0.000E+00
4.000E+00	0.000E+00	0.000E+00
5.000E+00	0.000E+00	0.000E+00
6.000E+00	0.000E+00	1.020E-01
8.000E+00	0.000E+00	0.000E+00
9.000E+00	0.000E+00	0.000E+00
1.000E+01	0.000E+00	0.000E+00
1.100E+01	0.000E+00	0.000E+00
1.200E+01	0.000E+00	1.270E-01
1.300E+01	0.000E+00	1.060E-01
1.400E+01	0.000E+00	3.320E-01
1.500E+01	0.000E+00	0.000E+00
1.600E+01	0.000E+00	1.420E-01
1.700E+01	0.000E+00	1.020E-01
1.800E+01	0.000E+00	2.600E-02
1.900E+01	2.620E+00	2.600E-02
2.000E+01	2.826E+00	1.280E-01
2.100E+01	3.288E+00	0.000E+00
2.500E+01	3.244E+00	1.550E-01
3.000E+01	3.982E+00	1.570E-01
5.300E+01	3.825E+00	2.890E-01

TABLE C-60. TIME AND CONCENTRATION VALUES, PORT 3, COLUMN E.

Time (hr.)	Bromide (ppm)
0.000E+00	0.000E+00
1.000E+00	0.000E+00
2.000E+00	0.000E+00
3.000E+00	0.000E+00
4.000E+00	5.077E+00
5.000E+00	6.566E+00
6.000E+00	7.771E+00
8.000E+00	7.634E+00
9.000E+00	5.851E+00
1.000E+01	9.076E+00
1.100E+01	1.001E+01
1.300E+01	9.830E+00
1.400E+01	1.005E+01
1.500E+01	9.917E+00
1.600E+01	8.877E+00
1.700E+01	8.342E+00
1.800E+01	8.159E+00
1.900E+01	7.434E+00
2.000E+01	7.271E+00
2.100E+01	5.499E+00
2.500E+01	6.624E+00
3.000E+01	5.799E+00
5.300E+01	4.104E+00

TABLE C-61. TIME AND CONCENTRATION VALUES, PORT 4, COLUMN E.

Time (hr.)	Bromide (ppm)
0.000E+00	0.000E+00
1.000E+00	0.000E+00
2.000E+00	0.000E+00
3.000E+00	2.401E+00
4.000E+00	3.014E+00
5.000E+00	5.332E+00
6.000E+00	8.704E+00
8.000E+00	8.474E+00
9.000E+00	9.306E+00
1.000E+01	1.045E+01
1.100E+01	8.512E+00
1.200E+01	8.251E+00
1.400E+01	7.615E+00
1.500E+01	6.149E+00
1.600E+01	7.316E+00
1.700E+01	6.873E+00
1.800E+01	7.059E+00
1.900E+01	7.186E+00
2.000E+01	6.149E+00
2.100E+01	6.722E+00
2.500E+01	6.287E+00
3.000E+01	5.145E+00
5.300E+01	0.000E+00

TABLE C-62. TIME AND CONCENTRATION VALUES, PORT 5, COLUMN E.

Time (hr.)	Bromide (ppm)
1.000E+00	0.000E+00
3.000E+00	0.000E+00
5.000E+00	0.000E+00
9.000E+00	0.000E+00
1.100E+01	3.780E+00
1.300E+01	6.029E+00
1.500E+01	6.002E+00
1.700E+01	4.552E+00
1.900E+01	5.457E+00
2.100E+01	5.608E+00
3.000E+01	3.532E+00
5.300E+01	2.619E+00

TABLE C-63. TIME AND CONCENTRATION VALUES, PORT 6, COLUMN E.

Time (hr.)	Bromide (ppm)
1.000E+00	0.000E+00
3.000E+00	0.000E+00
5.000E+00	0.000E+00
9.000E+00	0.000E+00
1.100E+01	0.000E+00
1.300E+01	0.000E+00
1.500E+01	0.000E+00
1.700E+01	0.000E+00
1.900E+01	0.000E+00
2.100E+01	0.000E+00
3.000E+01	5.529E+00
5.300E+01	5.032E+00

TABLE C-64. TIME AND CONCENTRATION VALUES, PORT 7, COLUMN E.

Time (hr.)	Bromide (ppm)
1.000E+00	0.000E+00
3.000E+00	5.097E+00
5.000E+00	1.564E+01
9.000E+00	1.290E+01
1.100E+01	6.618E+00
1.300E+01	6.127E+00
1.500E+01	4.369E+00
1.700E+01	5.771E+00
1.900E+01	5.435E+00
2.100E+01	4.028E+00
3.000E+01	4.204E+00
5.300E+01	0.000E+00

TABLE C-65. TIME AND CONCENTRATION VALUES, PORT 8, COLUMN E.

Time (hr.)	Bromide (ppm)
1.000E+00	0.000E+00
3.000E+00	0.000E+00
5.000E+00	3.619E+00
9.000E+00	4.115E+00
1.100E+01	4.259E+00
1.300E+01	4.369E+00
1.500E+01	6.590E+00
1.700E+01	6.154E+00
1.900E+01	6.675E+00
2.100E+01	3.960E+00
3.000E+01	0.000E+00
5.300E+01	0.000E+00

TABLE C-66. TIME AND CONCENTRATION VALUES, PORT 9, COLUMN E.

Time (hr.)	Bromide (ppm)
0.000E+00	0.000E+00
1.000E+00	0.000E+00
2.000E+00	0.000E+00
3.000E+00	0.000E+00
4.000E+00	0.000E+00
5.000E+00	3.879E+00
6.000E+00	5.771E+00
8.000E+00	8.660E+00
9.000E+00	9.172E+00
1.000E+01	8.509E+00
1.100E+01	8.070E+00
1.200E+01	7.227E+00
1.300E+01	7.825E+00
1.400E+01	7.790E+00
1.500E+01	4.837E+00
1.600E+01	6.005E+00
1.700E+01	4.837E+00
1.800E+01	4.332E+00
1.900E+01	4.527E+00
2.000E+01	5.670E+00
2.100E+01	3.252E+00
2.500E+01	4.649E+00
3.000E+01	2.849E+00
5.300E+01	0.000E+00

TABLE C-67. TIME AND CONCENTRATION VALUES, PORT 10, COLUMN E

Time (hr.)	Bromide (ppm)
0.000E+00	0.000E+00
1.000E+00	0.000E+00
2.000E+00	0.000E+00
3.000E+00	0.000E+00
4.000E+00	0.000E+00
5.000E+00	0.000E+00
6.000E+00	0.000E+00
8.000E+00	0.000E+00
9.000E+00	0.000E+00
1.000E+01	0.000E+00
1.100E+01	0.000E+00
1.200E+01	3.534E+00
1.300E+01	5.369E+00
1.400E+01	5.443E+00
1.500E+01	5.201E+00
1.600E+01	8.047E+00
1.700E+01	9.874E+00
1.800E+01	9.565E+00
1.900E+01	1.010E+01
2.000E+01	9.308E+00
2.100E+01	1.019E+01
2.500E+01	9.016E+00
3.000E+01	6.182E+00
5.300E+01	0.000E+00

TABLE C-68. TIME AND CONCENTRATION VALUES, PORT 11, COLUMN E

Time (hr.)	Bromide (ppm)
0.000E+00	0.000E+00
1.000E+00	0.000E+00
2.000E+00	0.000E+00
3.000E+00	3.011E+00
5.000E+00	7.445E+00
6.000E+00	6.402E+00
8.000E+00	8.852E+00
9.000E+00	8.356E+00
1.000E+01	9.091E+00
1.100E+01	8.852E+00
1.200E+01	8.505E+00
1.300E+01	7.185E+00
1.400E+01	5.859E+00
1.500E+01	5.409E+00
1.600E+01	6.234E+00
1.700E+01	5.128E+00
1.800E+01	5.385E+00
1.900E+01	4.449E+00
2.000E+01	4.949E+00
2.100E+01	4.371E+00
2.500E+01	3.860E+00
3.000E+01	3.776E+00
5.300E+01	2.121E+00

TABLE C-69. TIME AND CONCENTRATION VALUES, PORT 12, COLUMN E

Time (hr.)	Bromide (ppm)	Naphthalene (ppm)
0.000E+00	1.764E+00	0.000E+00
1.000E+00	1.446E+00	0.000E+00
2.000E+00	1.610E+00	1.640E-01
3.000E+00	5.693E+00	0.000E+00
4.000E+00	1.580E+01	1.510E-01
5.000E+00	1.523E+01	2.070E-01
6.000E+00	2.262E+01	9.600E-02
8.000E+00	1.838E+01	2.020E-01
9.000E+00	1.370E+01	6.500E-02
1.000E+01	1.425E+01	0.000E+00
1.100E+01	1.442E+01	0.000E+00
1.200E+01	1.465E+01	1.580E-01
1.300E+01	1.181E+01	3.000E-01
1.400E+01	9.942E+00	0.000E+00
1.500E+01	9.903E+00	0.000E+00
1.600E+01	8.875E+00	2.170E-01
1.700E+01	8.601E+00	1.200E-01
1.800E+01	7.860E+00	2.750E-01
1.900E+01	7.769E+00	2.530E-01
2.000E+01	7.072E+00	1.410E-01
2.100E+01	6.881E+00	
2.500E+01	5.614E+00	
3.000E+01	5.680E+00	
5.300E+01	3.296E+00	

TABLE C-70. TIME AND CONCENTRATION VALUES, PORT 13, COLUMN E

Time (hr.)	Bromide (ppm)
1.000E+00	0.000E+00
3.000E+00	0.000E+00
5.000E+00	8.867E+00
9.000E+00	2.293E+01
1.100E+01	2.349E+01
1.300E+01	2.483E+01
1.500E+01	2.013E+01
1.700E+01	1.632E+01
1.900E+01	1.426E+01
2.100E+01	1.023E+01
3.000E+01	3.922E+00
5.300E+01	2.025E+00

TABLE C-71. TIME AND CONCENTRATION VALUES, PORT 14, COLUMN E.

Time (hr.)	Bromide (ppm)
1.000E+00	0.000E+00
3.000E+00	2.326E+00
5.000E+00	1.333E+01
9.000E+00	2.593E+01
1.100E+01	2.386E+01
1.300E+01	1.677E+01
1.500E+01	1.415E+01
1.700E+01	1.107E+01
1.900E+01	8.456E+00
2.100E+01	6.910E+00
3.000E+01	4.400E+00
5.300E+01	1.791E+00

TABLE C-72. TIME AND CONCENTRATION VALUES, PORT 15, COLUMN E.

Time (hr.)	Bromide (ppm)
1.000E+00	0.000E+00
3.000E+00	0.000E+00
5.000E+00	1.276E+01
9.000E+00	1.472E+01
1.100E+01	1.472E+01
1.300E+01	1.420E+01
1.500E+01	1.266E+01
1.700E+01	1.246E+01
1.900E+01	1.094E+01
2.100E+01	9.868E+00
3.000E+01	4.725E+00
5.300E+01	1.325E+00

TABLE C-73. TIME AND CONCENTRATION VALUES, PORT 16, COLUMN E.

Time (hr.)	Bromide (ppm)
1.000E+00	9.072E-01
3.000E+00	3.666E+00
5.000E+00	1.698E+00
9.000E+00	6.492E+00
1.100E+01	9.277E+00
1.300E+01	1.004E+01
1.500E+01	1.062E+01
1.700E+01	1.074E+01
1.900E+01	9.964E+00
2.100E+01	9.807E+00
3.000E+01	6.728E+00
5.300E+01	3.441E+00

TABLE C-74. TIME AND CONCENTRATION VALUES, PORT 17, COLUMN E.

Time (hr.)	Bromide (ppm)
1.000E+00	1.639E+00
3.000E+00	4.116E+00
5.000E+00	9.622E+00
9.000E+00	1.736E+01
1.100E+01	1.504E+01
1.300E+01	1.277E+01
1.500E+01	1.232E+01
1.700E+01	1.161E+01
1.900E+01	1.059E+01
2.100E+01	9.661E+00
3.000E+01	6.256E+00
5.300E+01	3.495E+00

TABLE C-75. TIME AND CONCENTRATION VALUES, PORT 18, COLUMN E.

Time (hr.)	Bromide (ppm)
1.000E+00	1.321E+00
3.000E+00	3.623E+00
5.000E+00	7.367E+00
9.000E+00	5.964E+00
1.100E+01	6.059E+00
1.300E+01	7.164E+00
1.500E+01	6.911E+00
1.700E+01	7.051E+00
1.900E+01	7.545E+00
2.100E+01	7.308E+00
3.000E+01	6.510E+00
5.300E+01	3.877E+00

TABLE C-76. TIME AND CONCENTRATION VALUES, PORT 19, COLUMN E.

Time (hr.)	Bromide (ppm)
1.000E+00	9.505E-01
3.000E+00	3.768E+00
5.000E+00	1.310E+01
9.000E+00	1.637E+01
1.100E+01	1.401E+01
1.300E+01	1.224E+01
1.500E+01	1.167E+01
1.700E+01	1.113E+01
1.900E+01	1.007E+01
2.100E+01	8.623E+00
3.000E+01	6.321E+00
5.300E+01	3.564E+00

TABLE C-77. TIME AND CONCENTRATION VALUES, PORT 20, COLUMN E.

Time (hr.)	Bromide (ppm)
1.000E+00	1.653E+00
3.000E+00	4.597E+00
5.000E+00	7.837E+00
9.000E+00	8.902E+00
1.100E+01	9.009E+00
1.300E+01	8.386E+00
1.500E+01	7.869E+00
1.700E+01	7.806E+00
1.900E+01	8.521E+00
2.100E+01	7.532E+00
3.000E+01	6.027E+00
5.300E+01	4.080E+00

TABLE C-78. TIME AND CONCENTRATION VALUES, PORT 21, COLUMN E.

Time (hr.)	Bromide (ppm)
0.000E+00	0.000E+00
1.000E+00	1.281E+00
2.000E+00	3.209E+01
3.000E+00	4.948E+01
4.000E+00	4.001E+01
5.000E+00	2.606E+01
6.000E+00	2.099E+01
8.000E+00	1.857E+01
9.000E+00	1.733E+01
1.000E+01	1.424E+01
1.100E+01	1.291E+01
1.200E+01	1.075E+01
1.300E+01	1.002E+01
1.400E+01	9.015E+00
1.500E+01	8.376E+00
1.600E+01	6.802E+00
1.700E+01	6.970E+00
1.800E+01	6.117E+00
1.900E+01	6.637E+00
2.000E+01	5.731E+01
2.100E+01	5.824E+00
3.000E+01	3.539E+00
5.300E+01	1.911E+00

TABLE C-79. TIME AND CONCENTRATION VALUES, PORT 22, COLUMN E.

Time (hr.)	Bromide (ppm)	Naphthalene (ppm)
0.000E+00	0.000E+00	1.210E-01
1.000E+00	0.000E+00	0.000E+00
2.000E+00	3.468E+00	0.000E+00
3.000E+00	1.302E+01	0.000E+00
4.000E+00	2.512E+01	1.770E-01
5.000E+00	3.343E+01	4.240E-01
6.000E+00	4.907E+01	5.110E-01
8.000E+00	6.168E+01	8.910E-01
9.000E+00	6.887E+01	1.070E+00
1.000E+01	5.970E+01	4.750E-01
1.100E+01	5.524E+01	1.055E+00
1.200E+01	6.347E+01	8.480E-01
1.300E+01	4.413E+01	7.070E-01
1.400E+01	5.196E+01	1.020E+00
1.500E+01	5.897E+01	8.530E-01
1.600E+01	4.467E+01	6.850E-01
1.700E+01	4.560E+01	0.000E+00
1.800E+01	3.540E+01	5.480E-01
1.900E+01	3.733E+01	4.930E-01
2.000E+01	5.238E+00	1.303E-01
2.100E+01	3.952E+01	6.050E-01
2.500E+01	2.471E+01	4.760E-01
3.000E+01	2.373E+01	6.500E-01
5.300E+01	1.783E+01	3.100E-01

TABLE C-80. TIME AND CONCENTRATION VALUES, PORT 23, COLUMN E.

Time (hr.)	Bromide (ppm)
0.000E+00	1.175E+01
1.000E+00	0.000E+00
2.000E+00	0.000E+00
3.000E+00	1.006E+00
4.000E+00	3.677E+00
5.000E+00	5.331E+00
6.000E+00	1.194E+01
8.000E+00	2.440E+01
9.000E+00	4.031E+01
1.000E+01	3.069E+01
1.100E+01	3.609E+01
1.200E+01	3.875E+01
1.300E+01	4.031E+01
1.400E+01	3.968E+01
1.500E+01	3.725E+01
1.600E+01	3.361E+01
1.700E+01	3.081E+01
1.800E+01	3.193E+01
1.900E+01	2.748E+01
2.000E+01	2.346E+01
2.100E+01	2.134E+01
2.500E+01	1.593E+01
3.000E+01	1.170E+01
5.300E+01	7.977E+00

TABLE C-81. TIME AND CONCENTRATION DATA, PORT 24, COLUMN E.

Time (hr.)	Bromide (ppm)
0.000E+00	0.000E+00
1.000E+00	0.000E+00
2.000E+00	1.829E+00
3.000E+00	1.001E+01
5.000E+00	2.010E+01
6.000E+00	2.410E+01
8.000E+00	3.908E+01
9.000E+00	2.644E+01
1.000E+01	2.797E+01
1.100E+01	2.924E+01
1.200E+01	2.429E+01
1.300E+01	2.622E+01
1.400E+01	2.763E+01
1.500E+01	3.169E+01
1.600E+01	3.505E+01
1.700E+01	3.491E+01
1.800E+01	3.845E+01
1.900E+01	3.876E+01
2.000E+01	4.003E+01
2.100E+01	4.896E+01
2.500E+01	3.678E+01
3.000E+01	3.380E+01
5.300E+01	1.196E+01

TABLE C-82. TIME AND CONCENTRATION VALUES, PORT 25, COLUMN E.

Time (hr.)	Bromide (ppm)	Naphthalene (ppm)
0.000E+00	0.000E+00	0.000E+00
5.000E-01	0.000E+00	0.000E+00
1.000E+00	0.000E+00	1.180E-01
1.500E+00	0.000E+00	2.330E-01
2.000E+00	1.191E+01	4.760E-01
3.000E+00	2.679E+01	5.930E-01
4.000E+00	2.643E+01	6.699E-01
5.000E+00	2.270E+01	8.900E-01
6.000E+00	2.048E+01	8.570E-01
8.000E+00	1.291E+01	5.810E-01
9.000E+00	1.046E+01	3.560E-01
1.000E+01	9.395E+00	2.600E-01
1.100E+01	7.997E+00	3.600E-01
1.200E+01	7.214E+00	3.110E-01
1.300E+01	6.140E+00	2.120E-01
1.400E+01	5.742E+00	2.830E-01
1.500E+01	5.614E+00	0.000E+00
1.600E+01	5.111E+00	3.450E-01
1.700E+01	4.673E+00	2.310E-01
1.800E+01	4.197E+00	0.000E+00
1.900E+01	3.920E+00	0.000E+00
2.000E+01	3.715E+00	7.600E-02
2.100E+01	3.121E+00	9.100E-02
2.500E+01	2.006E+00	1.520E-01
3.000E+01	0.000E+00	6.100E-02
5.300E+01	0.000E+00	0.000E+00

APPENDIX D

PLOTS OF DATA FROM STEEL COLUMN TESTS

The following figures are for Br⁻ data from steel column experiments C, D, and E.
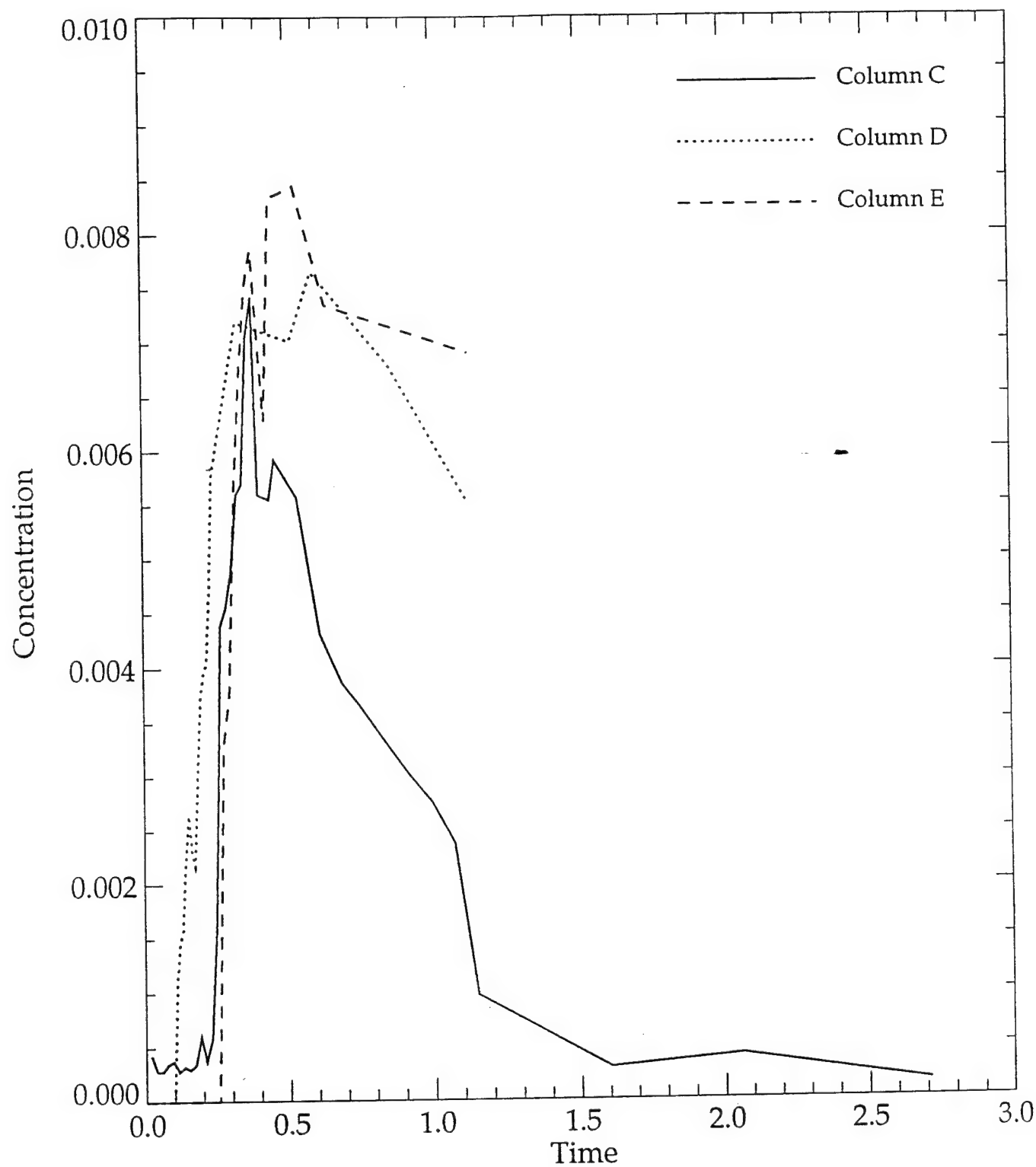
Figure D-1. Bromide concentrations vs. time from Port 1, column tests C, D, and E.
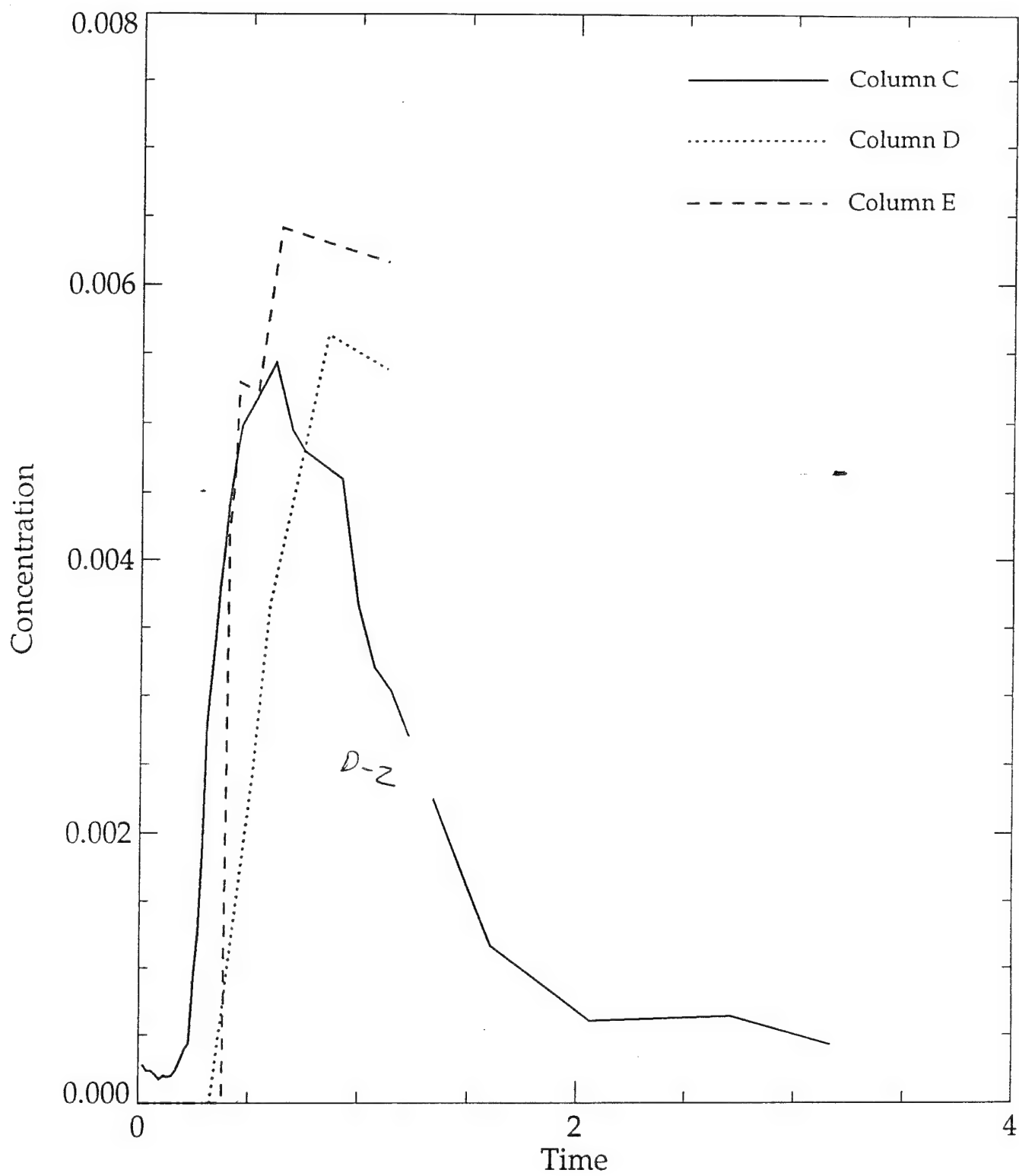
Figure D-2. Bromide concentrations vs. time from Port 2, column tests C, D, and E.

115
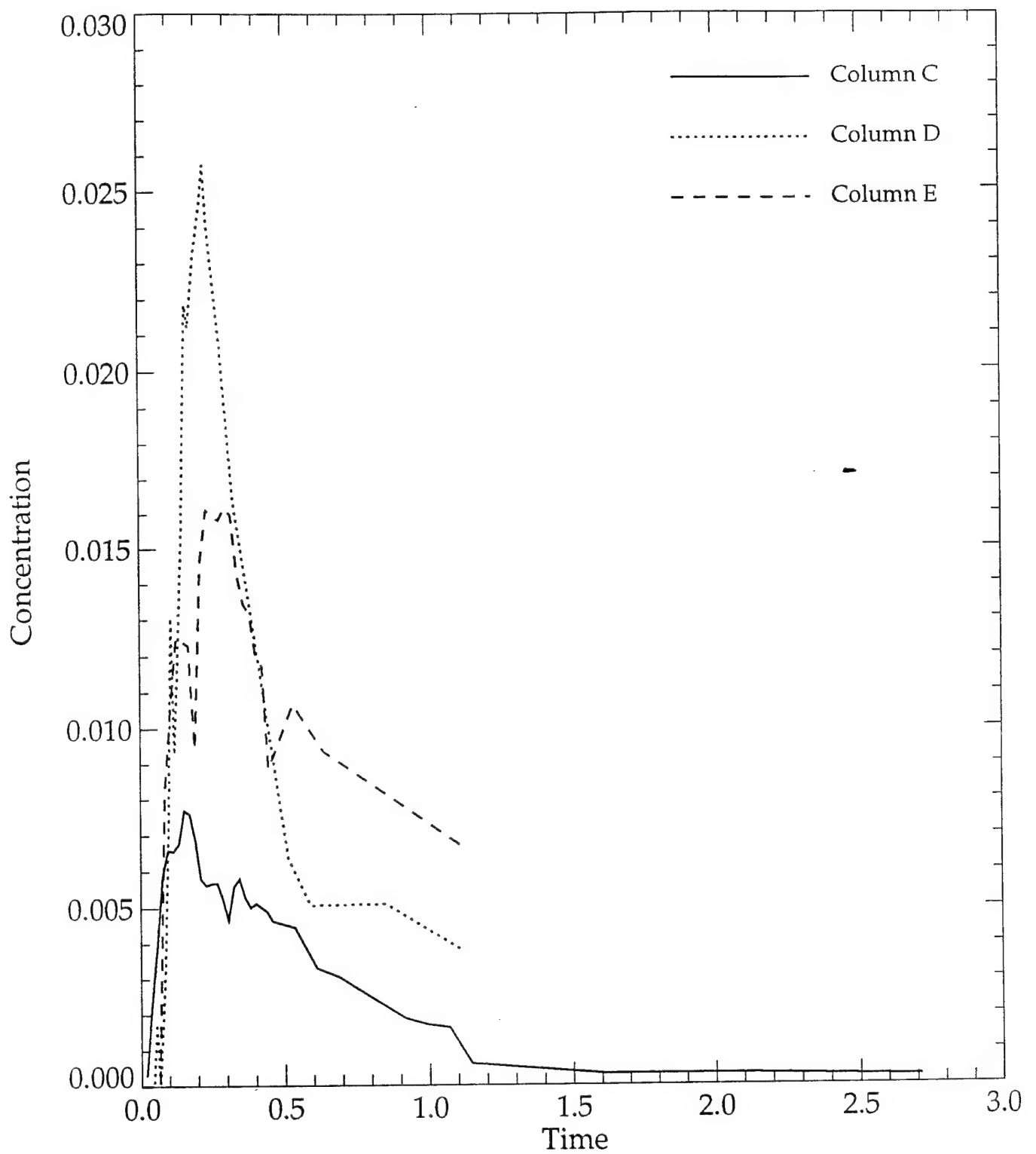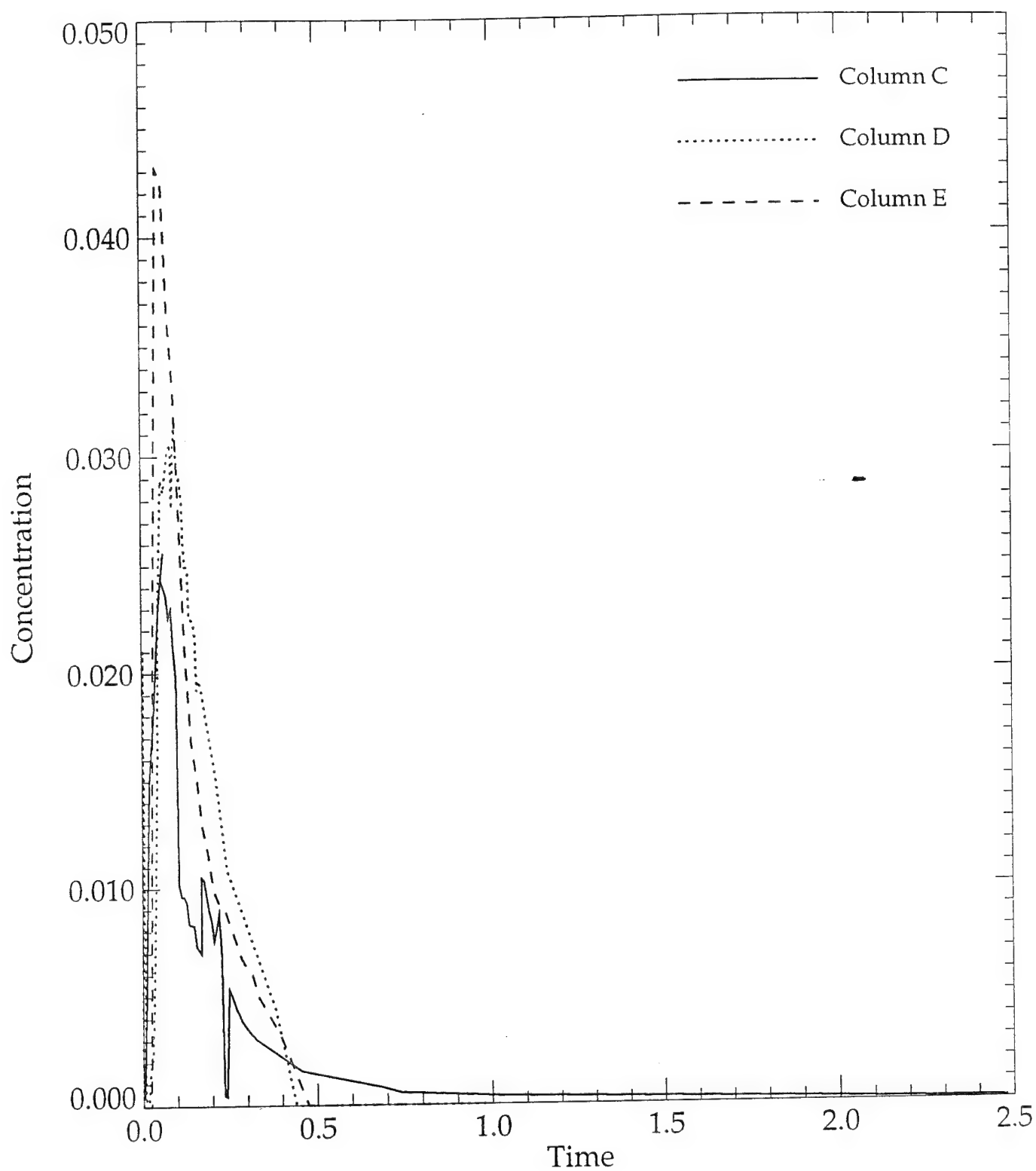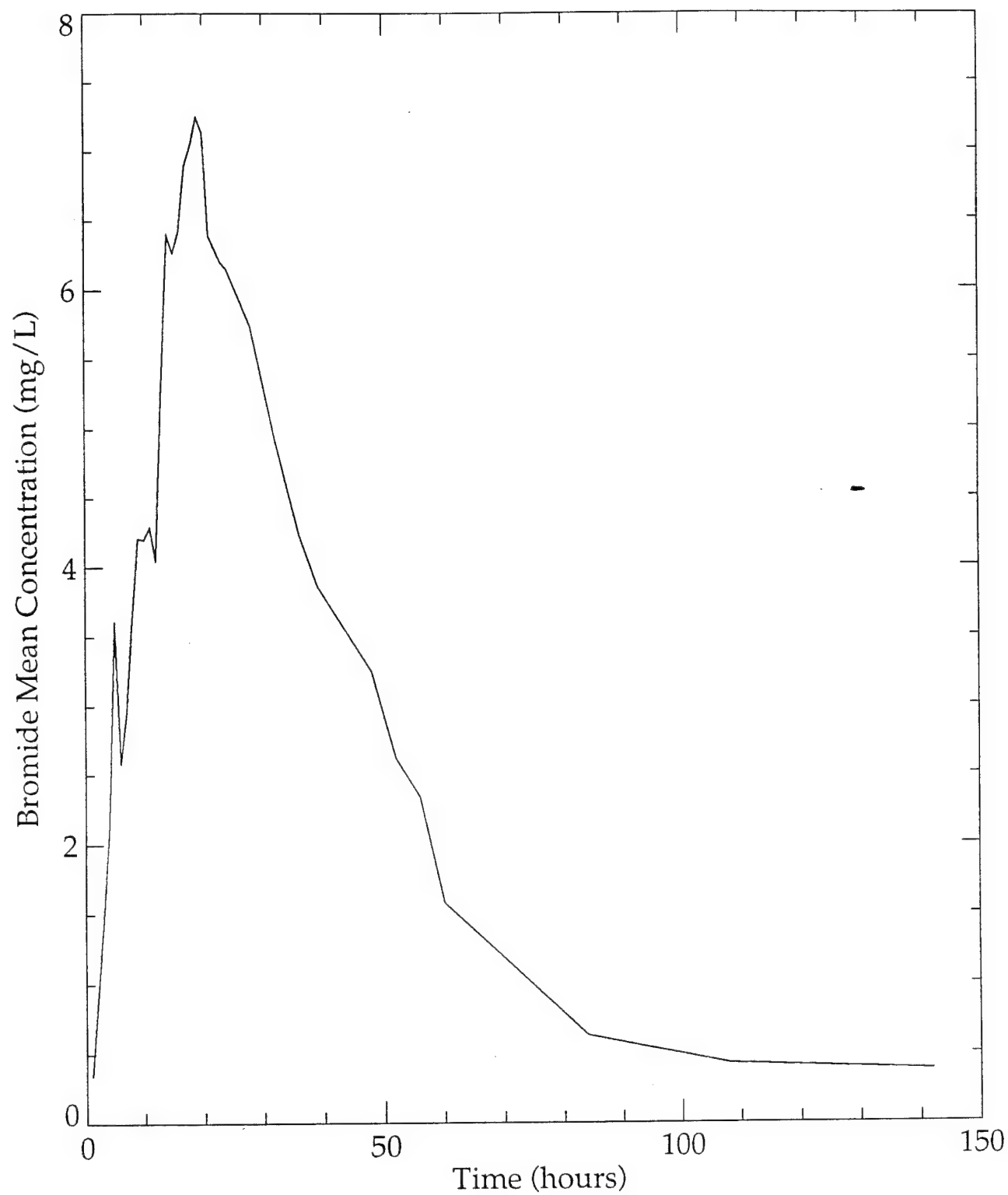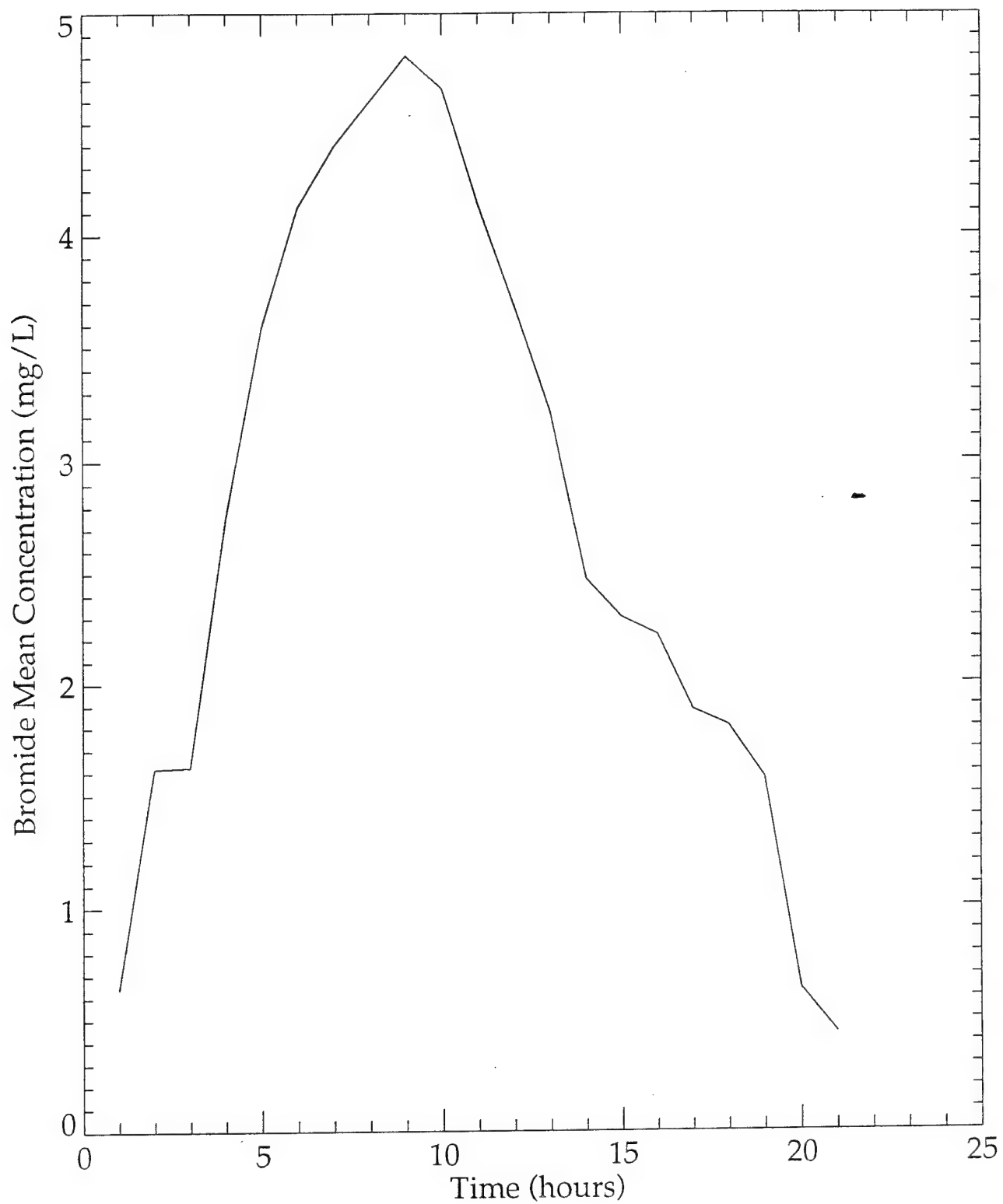
Figure D-3. Bromide concentrations vs. time from Port 3, column tests C, D, and E.
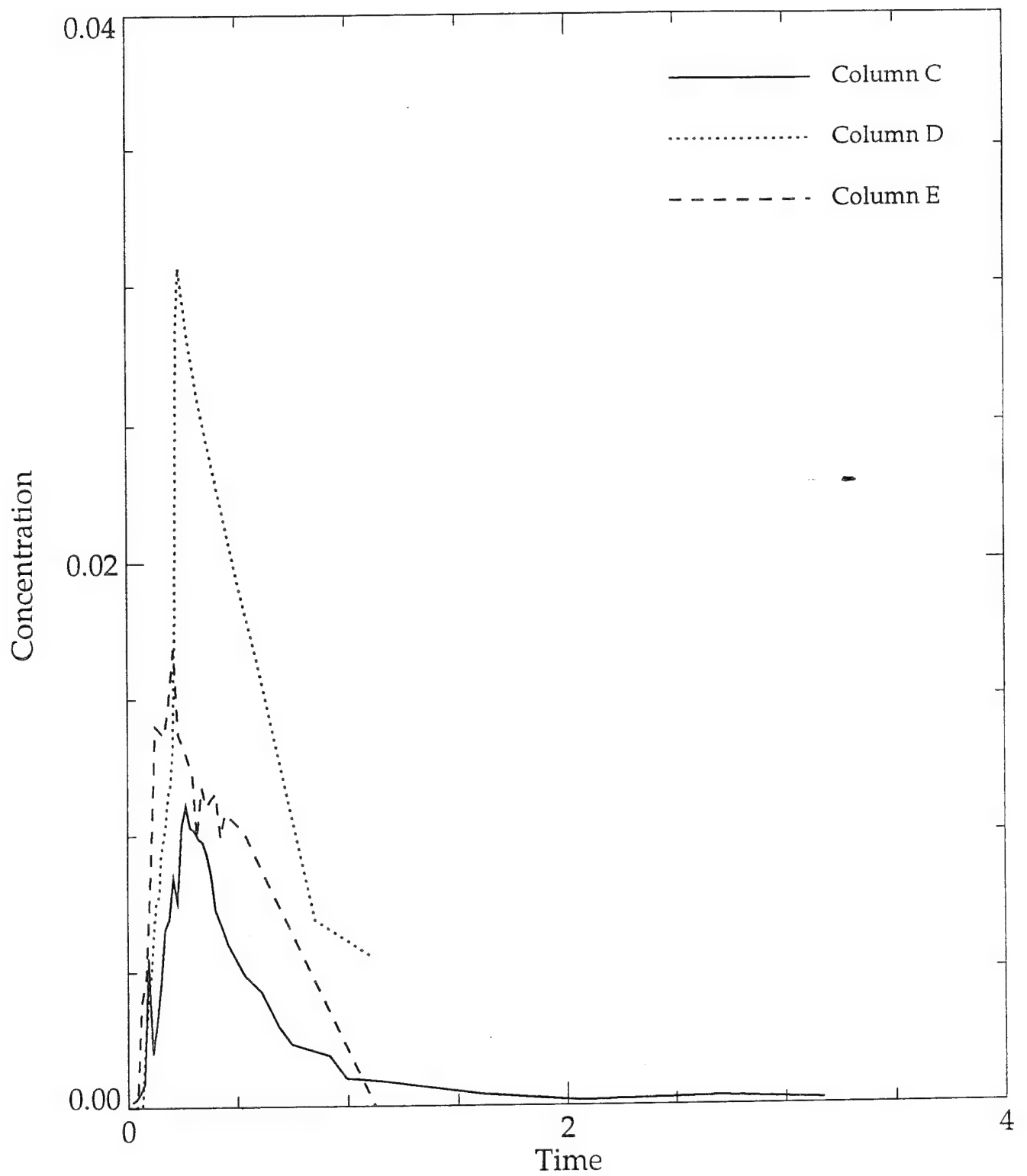
Figure D-4. Bromide concentrations vs. time from Port 4, column tests C, D, and E.
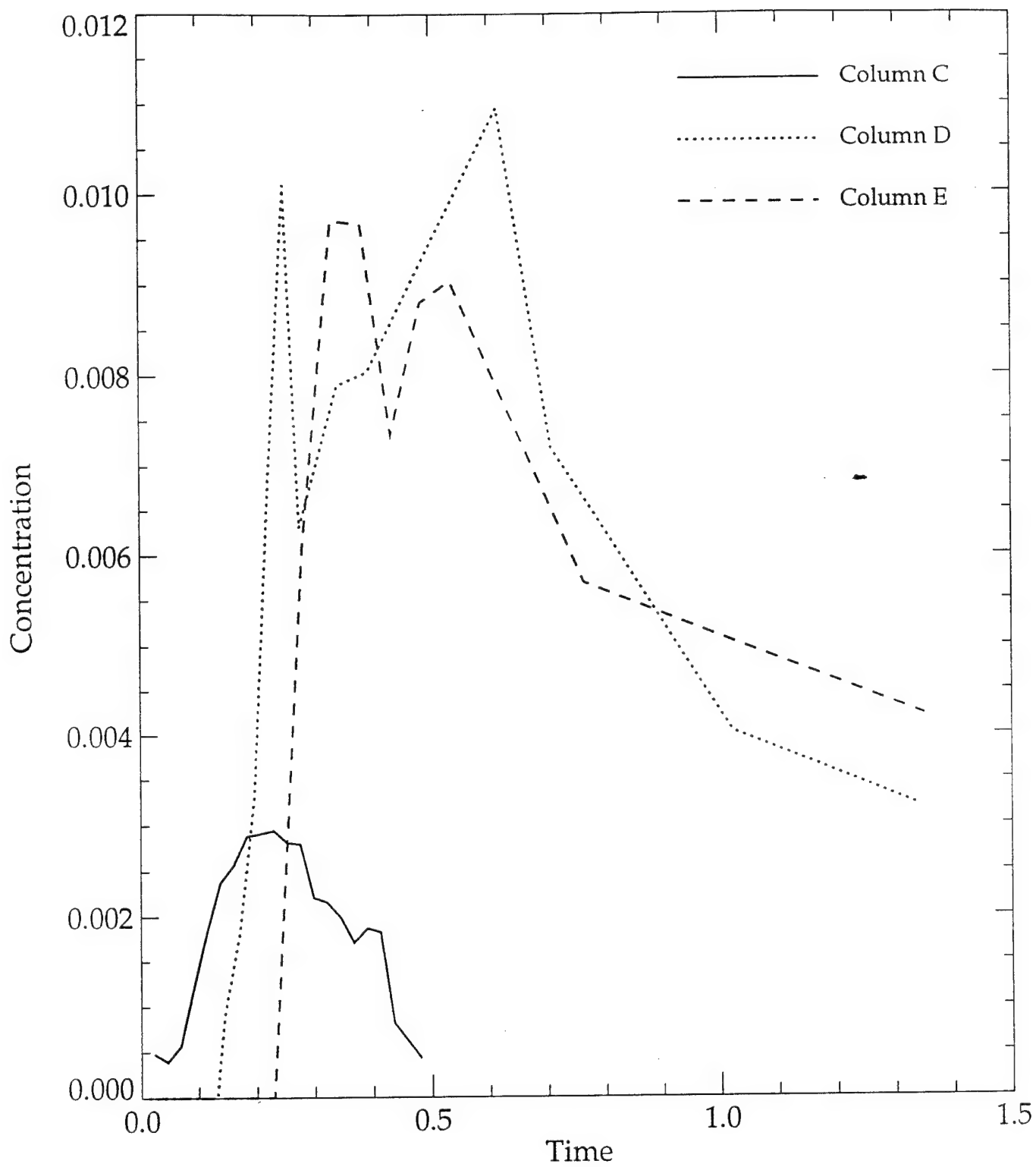
Figure D-5. Bromide concentrations vs. time from Port 5, column tests C, D, and E.

118
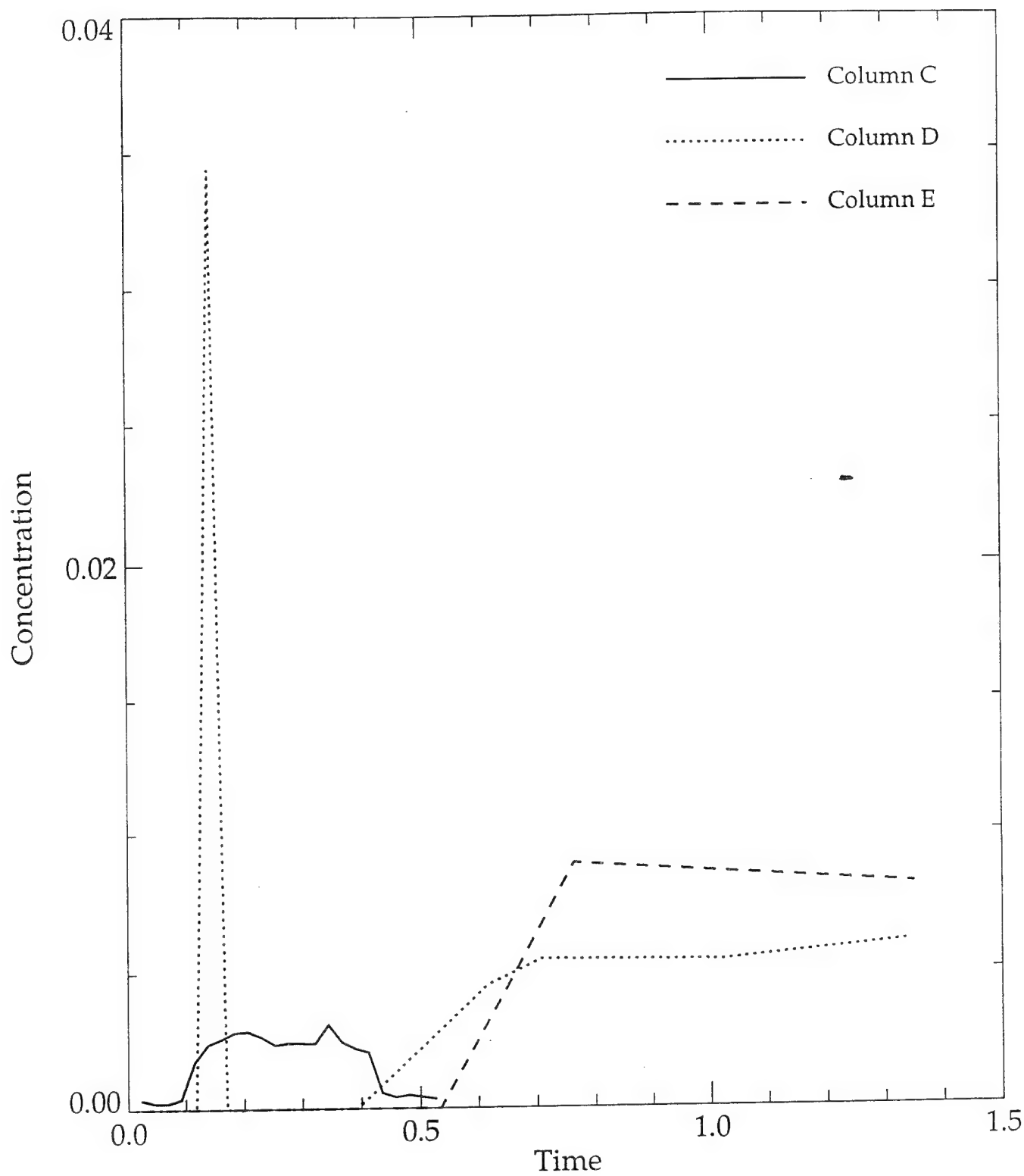
Figure D-6. Bromide concentrations vs. time from Port 6, column tests C, D, and E.
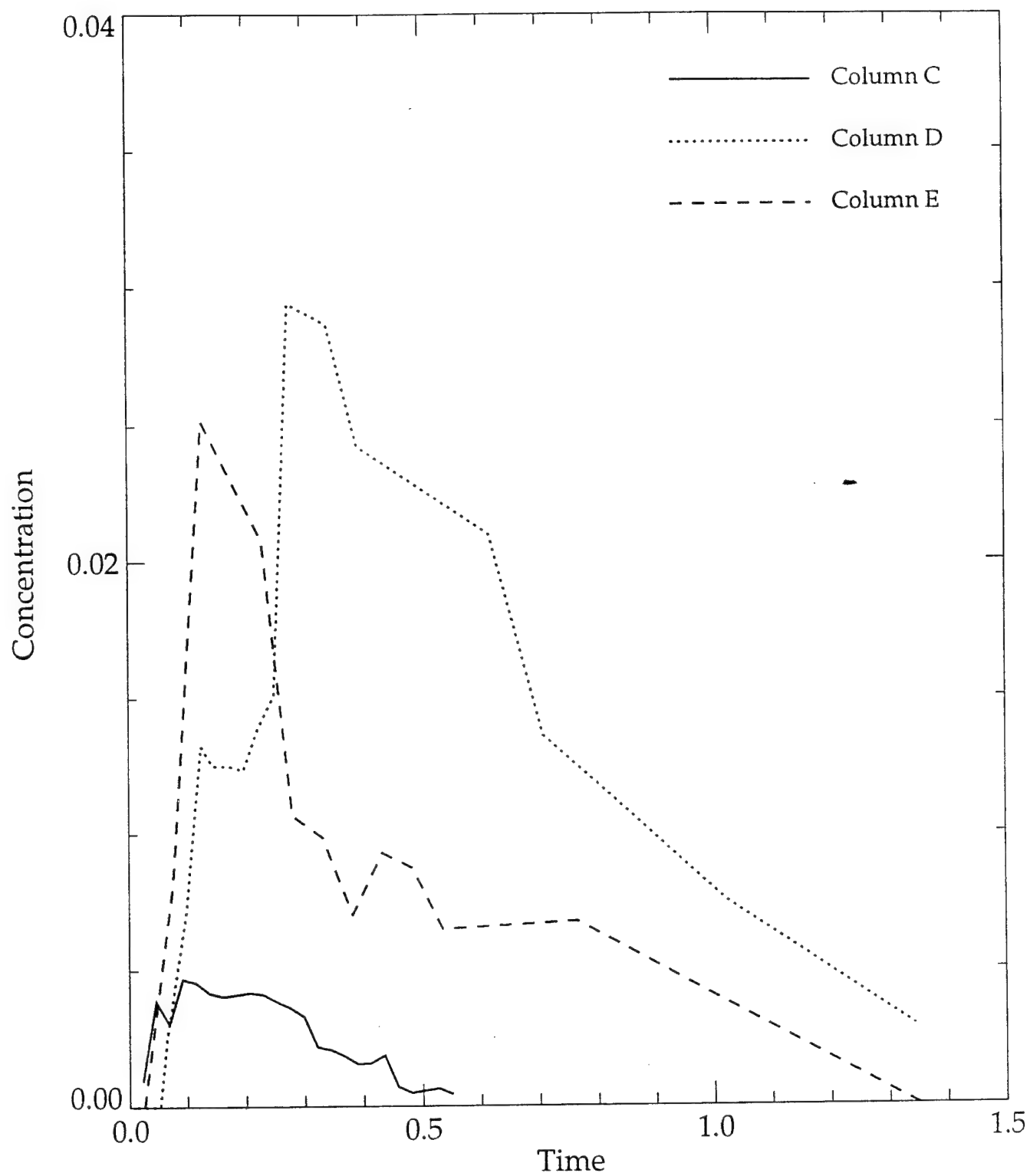
Figure D-7. Bromide concentrations vs. time from Port 7, column tests C, D, and E.
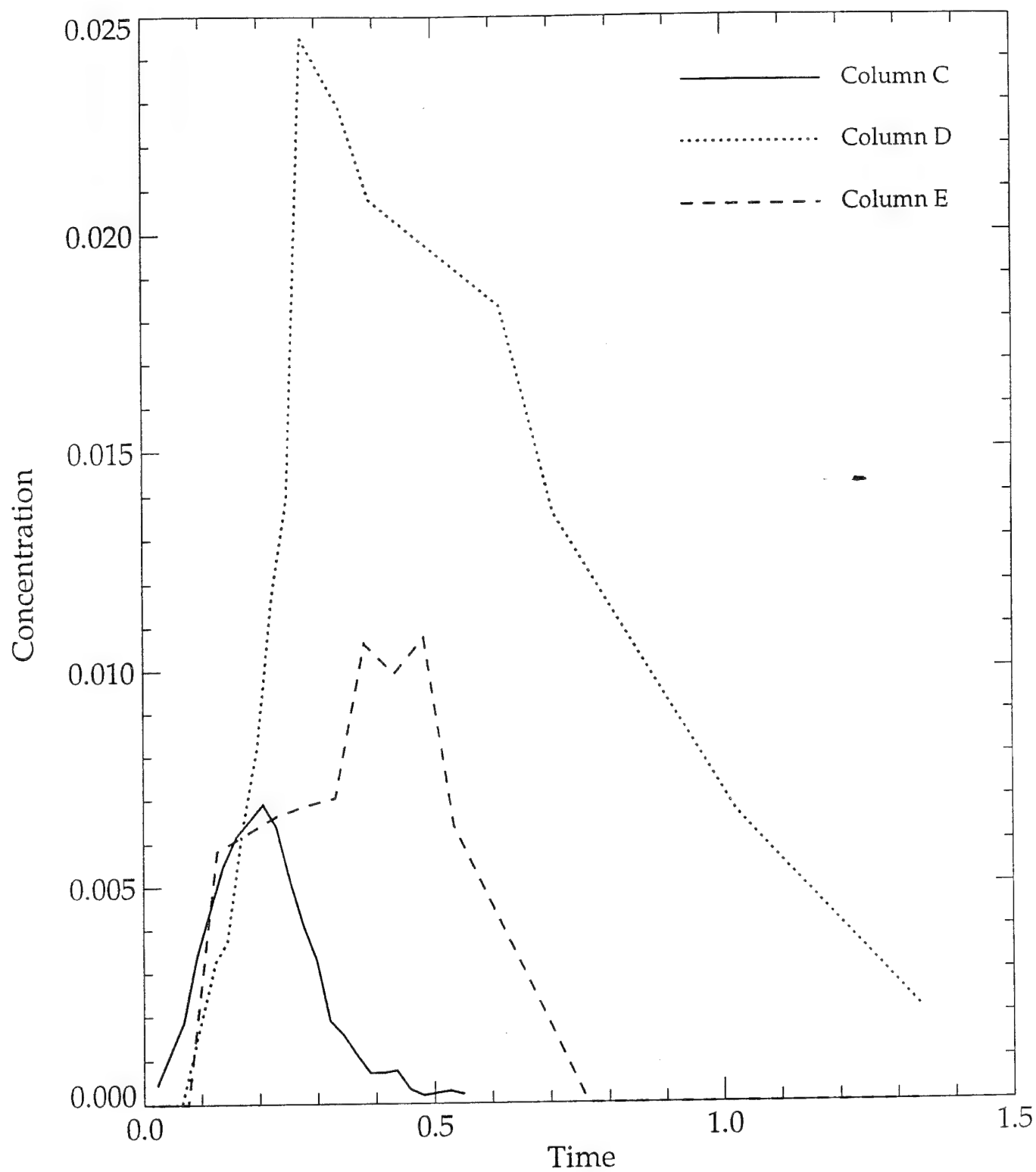
Figure D-8. Bromide concentrations vs. time from Port 8, column tests, C, D, and E.
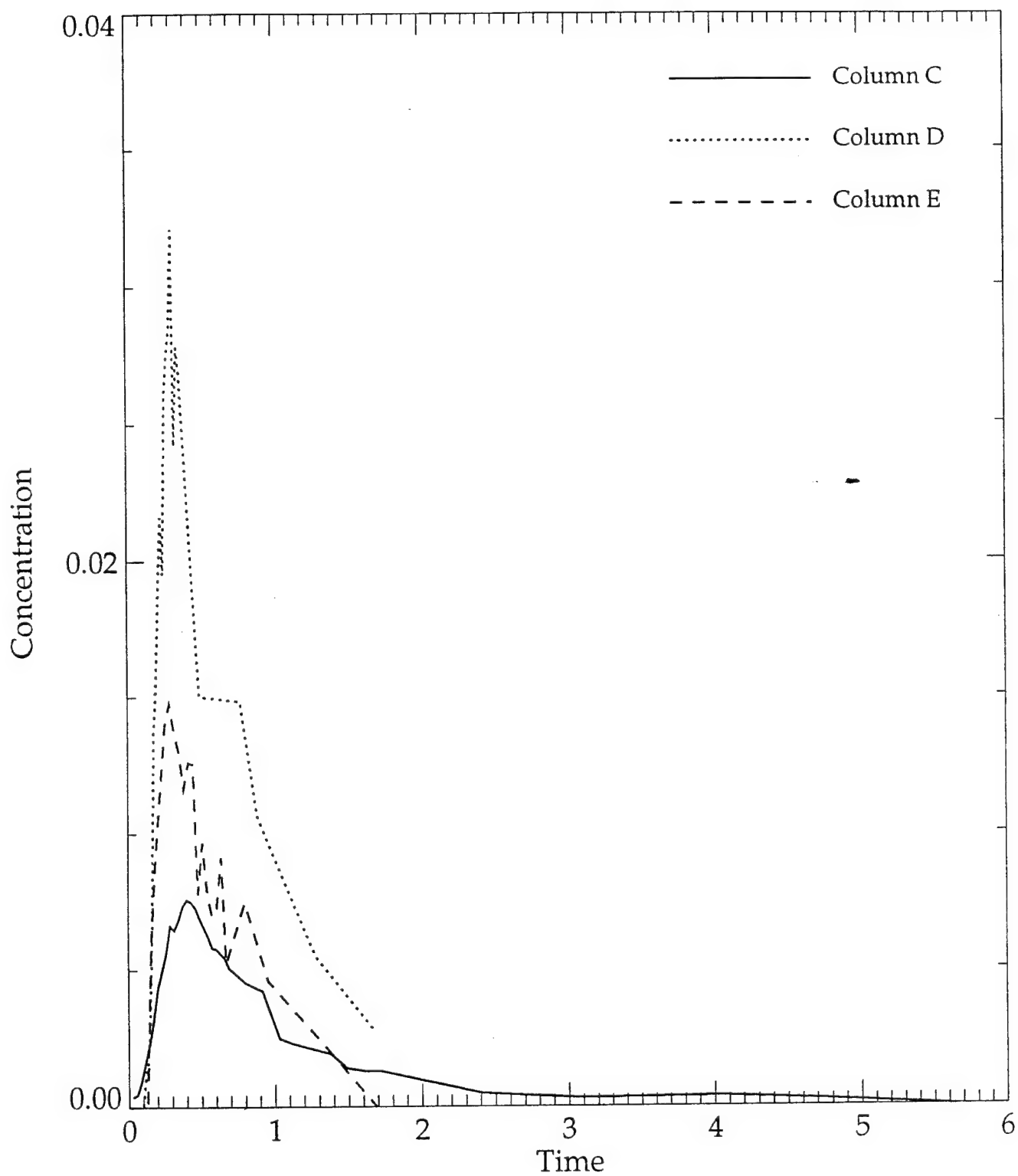
Figure D-9. Bromide concentrations vs. time from Port 9, column tests, C, D, and E.
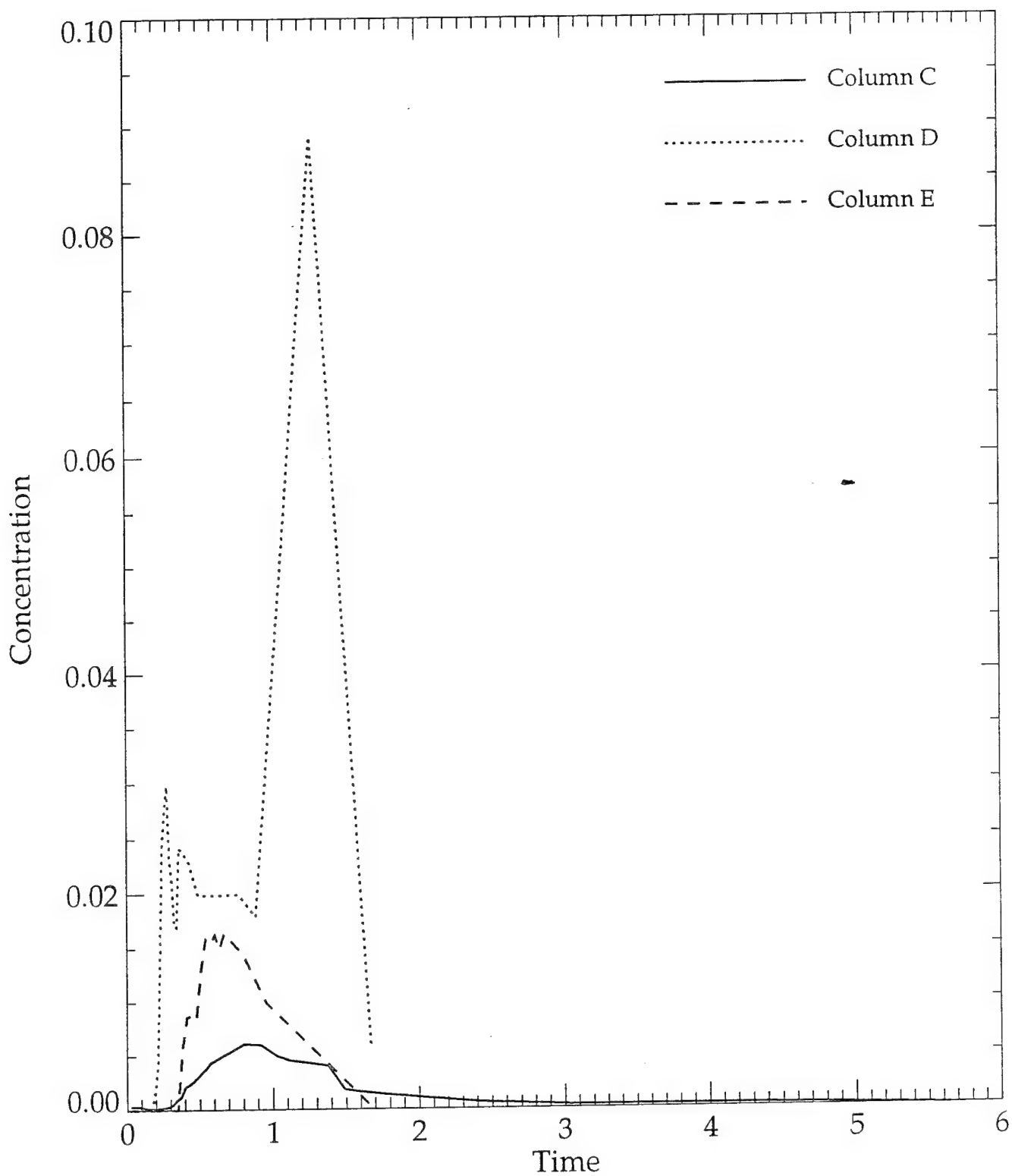
Figure D-10. Bromide concentrations vs. time from Port 10, column tests, C, D, and E.
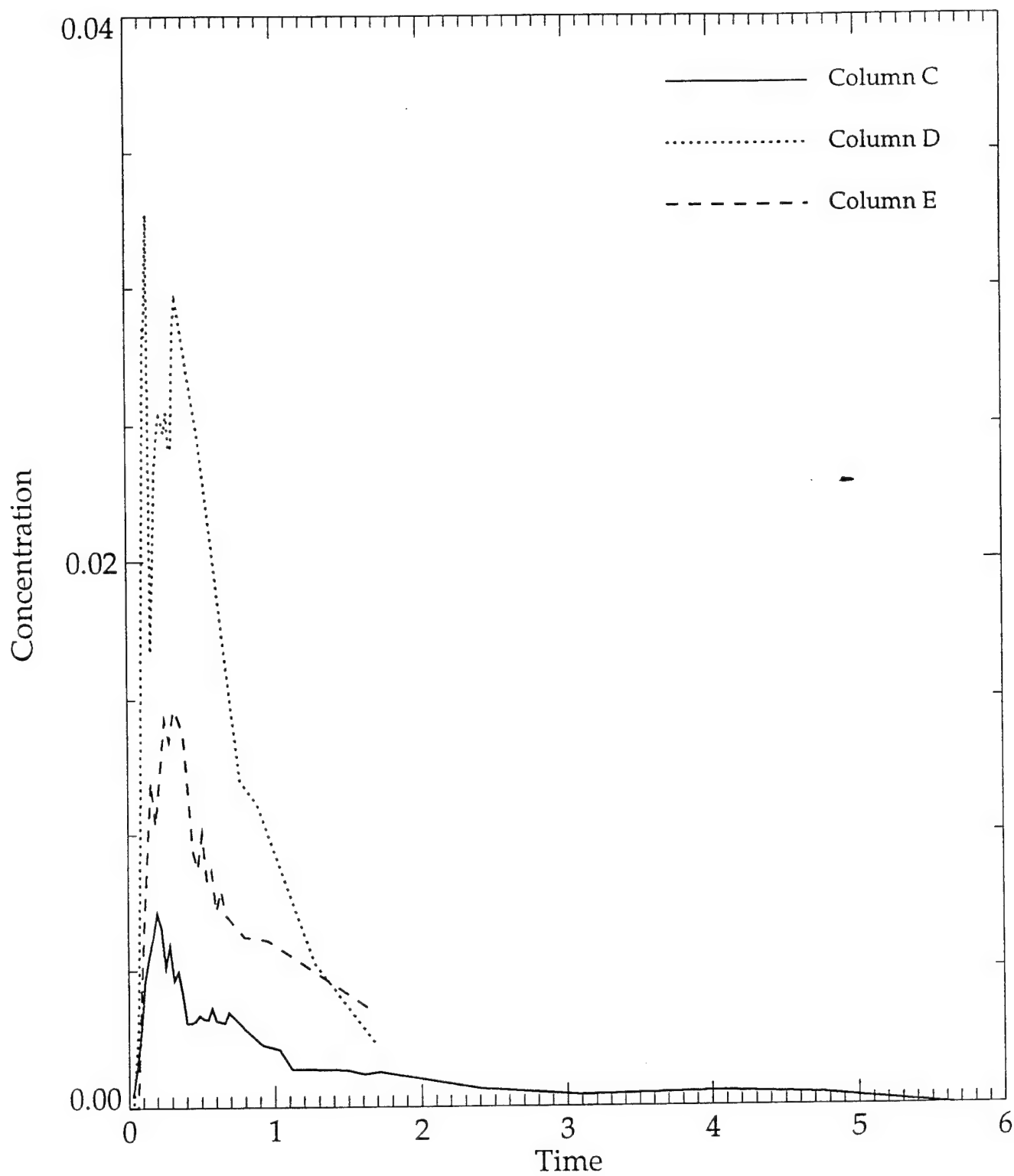
Figure D-11. Bromide concentrations vs. time from Port 11, column tests, C, D, and E.
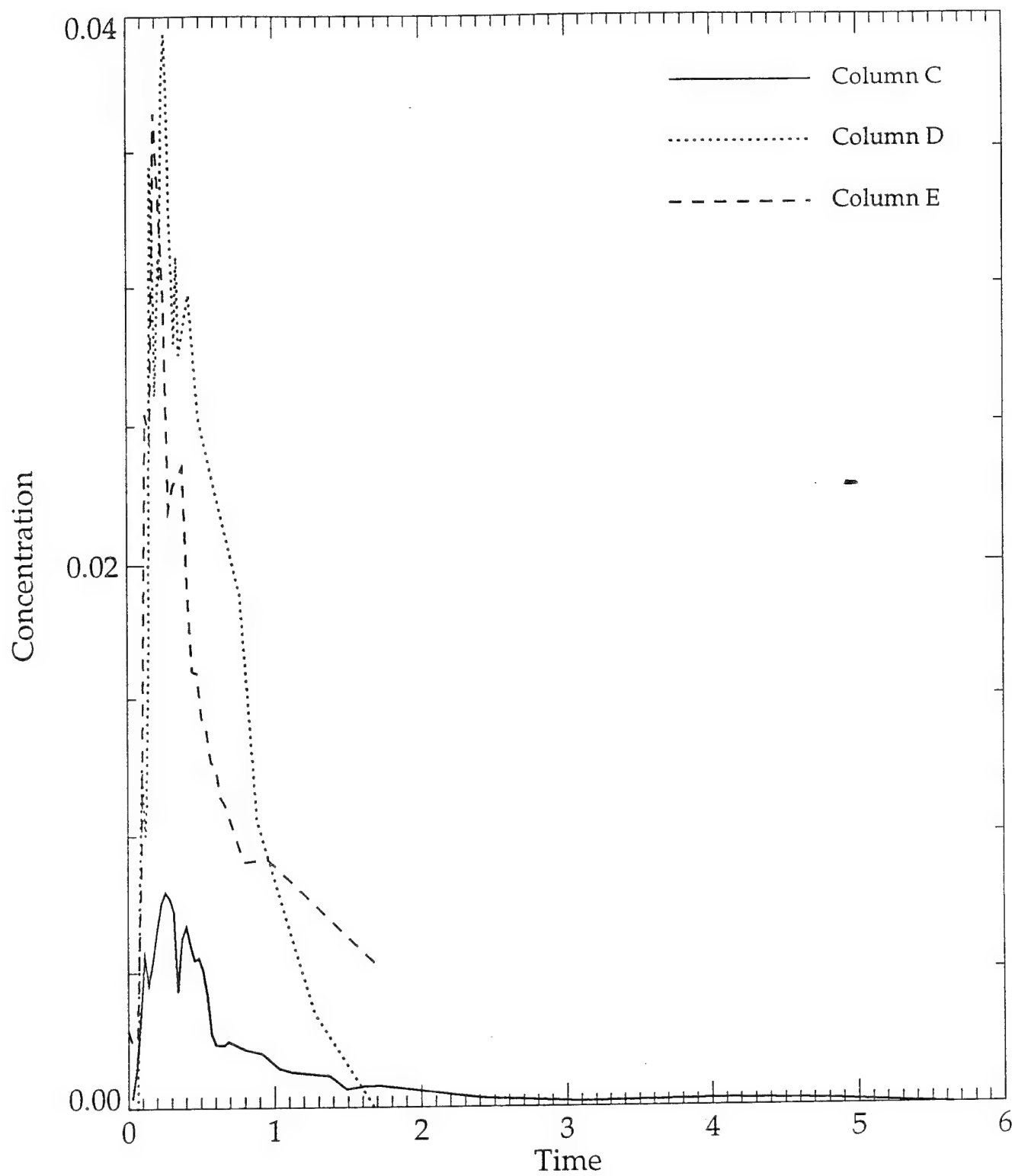
Figure D-12. Bromide concentrations vs. time from Port 12, column tests, C, D, and E.
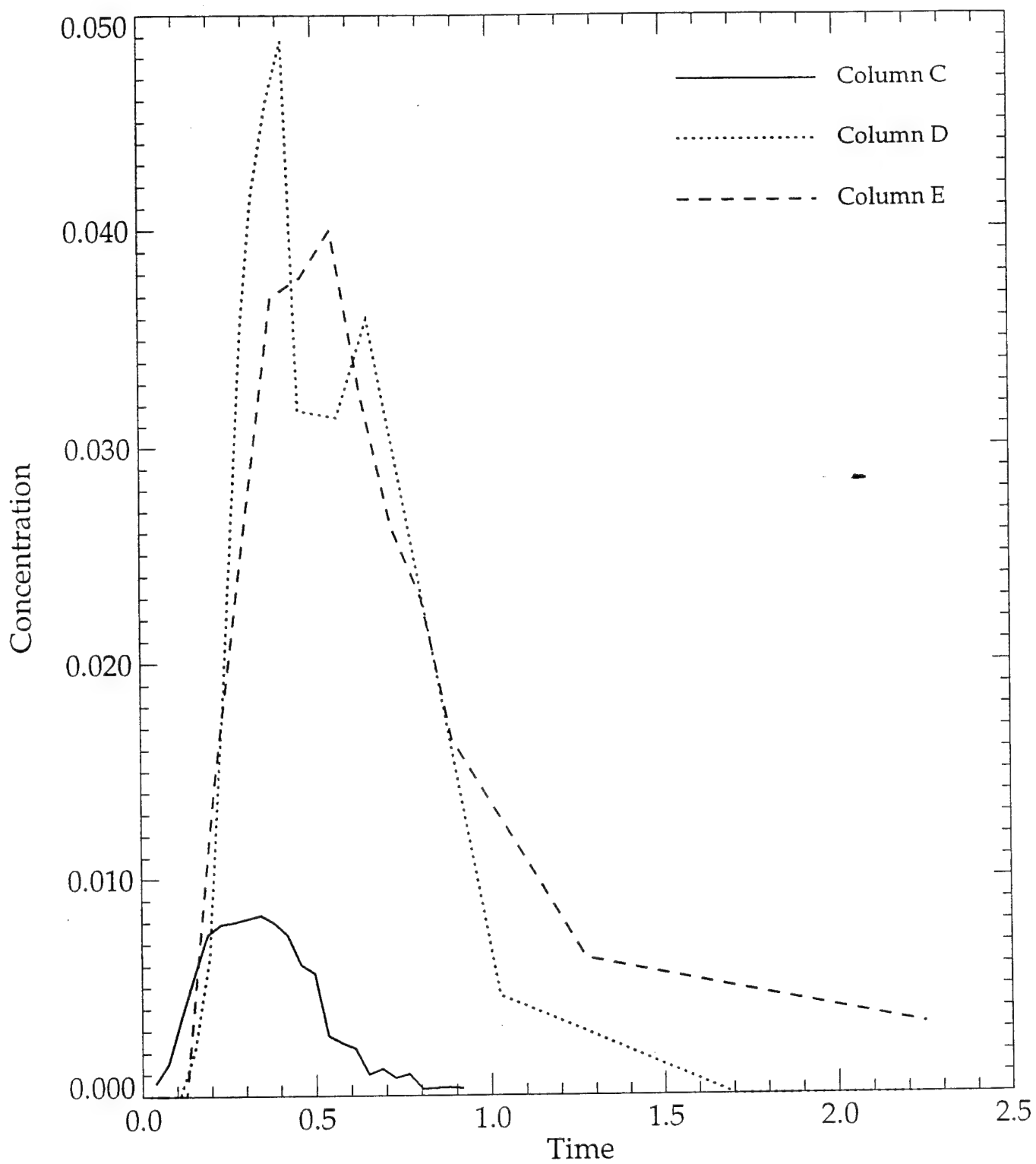
Figure D-13. Bromide concentrations vs. time from Port 13, column tests, C, D, and E.
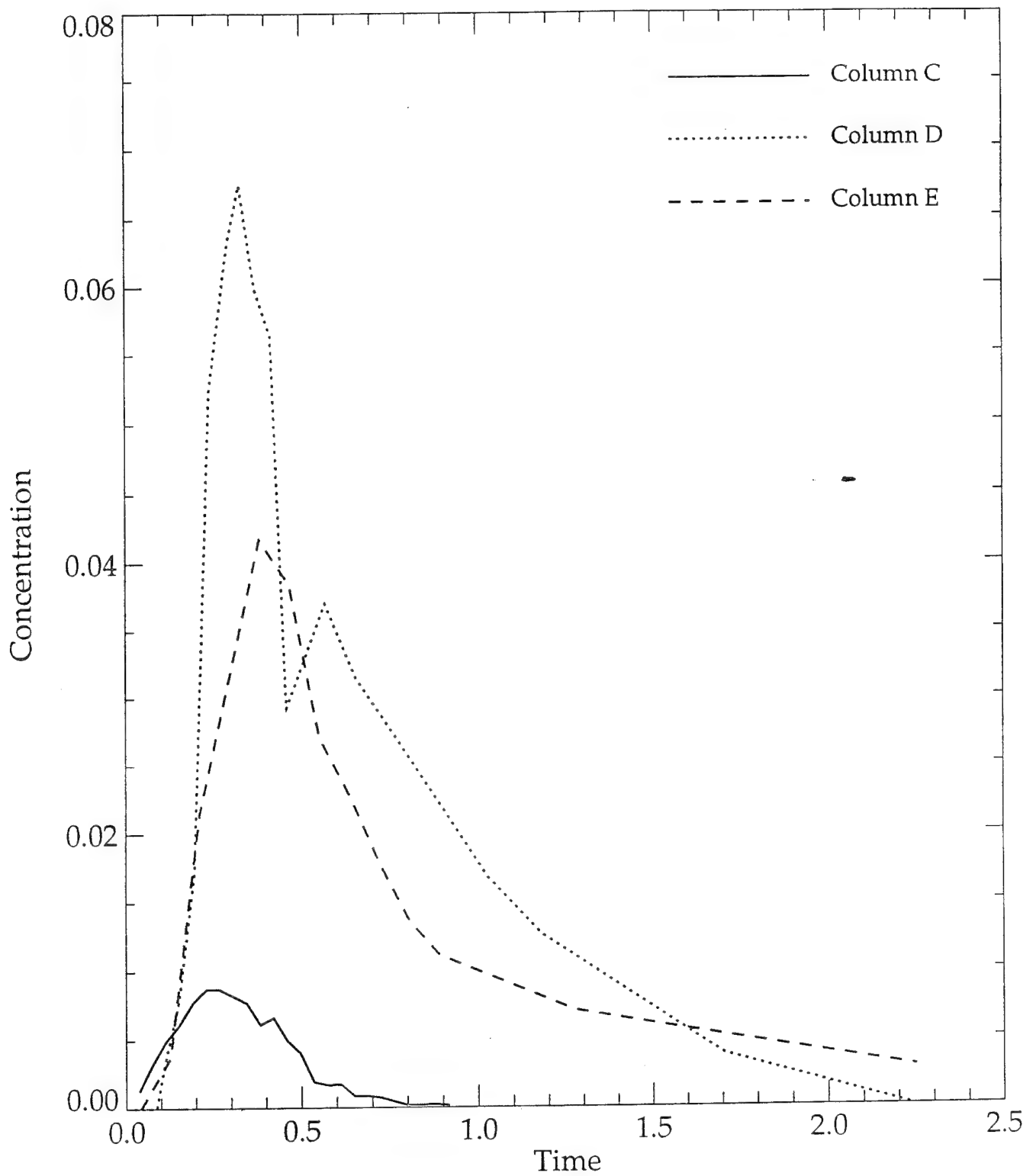
Figure D-14. Bromide concentrations vs. time from Port 14, column tests, C, D, and E.
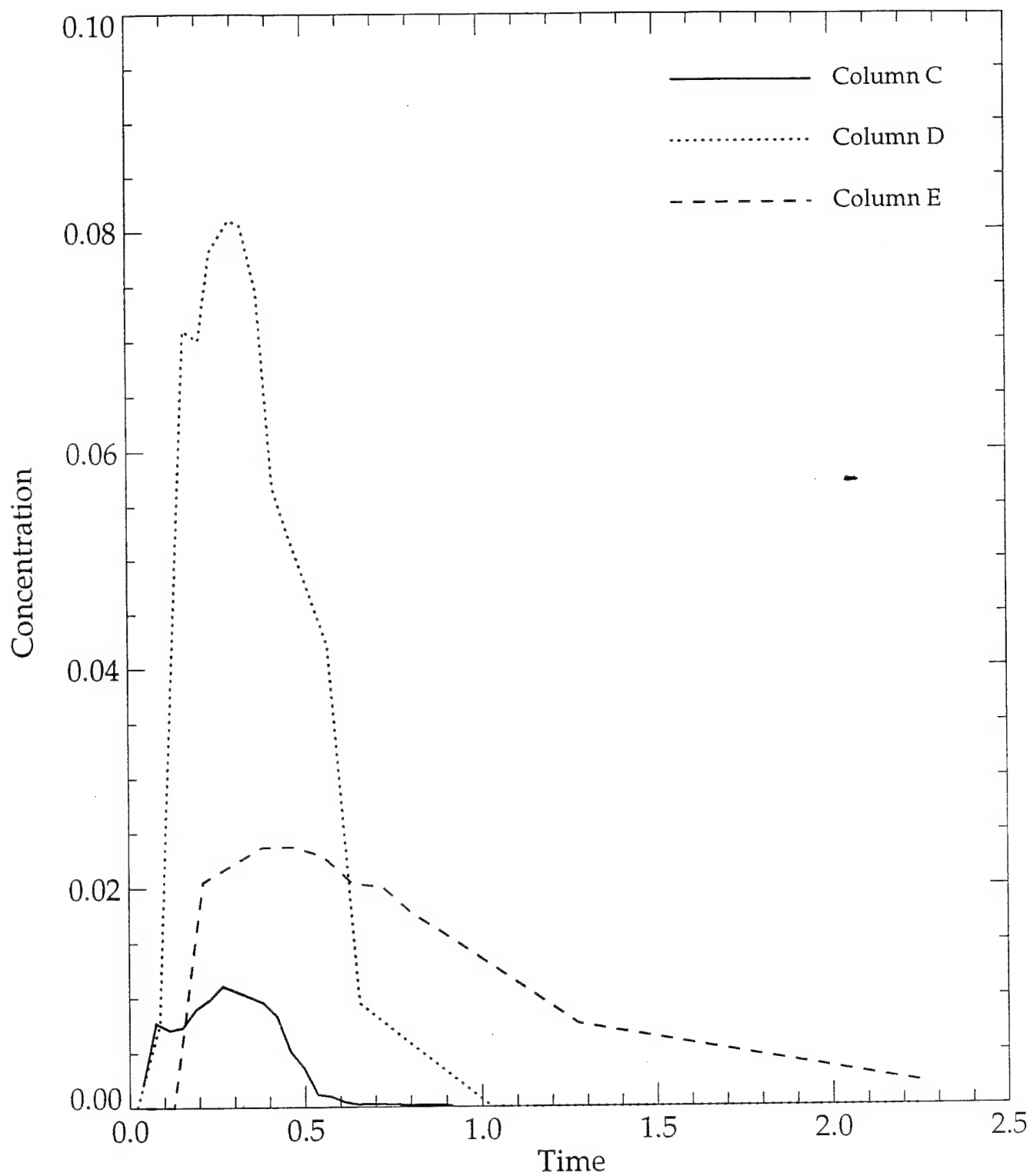
Figure D-15. Bromide concentrations vs. time from Port 15, column tests, C, D, and E.
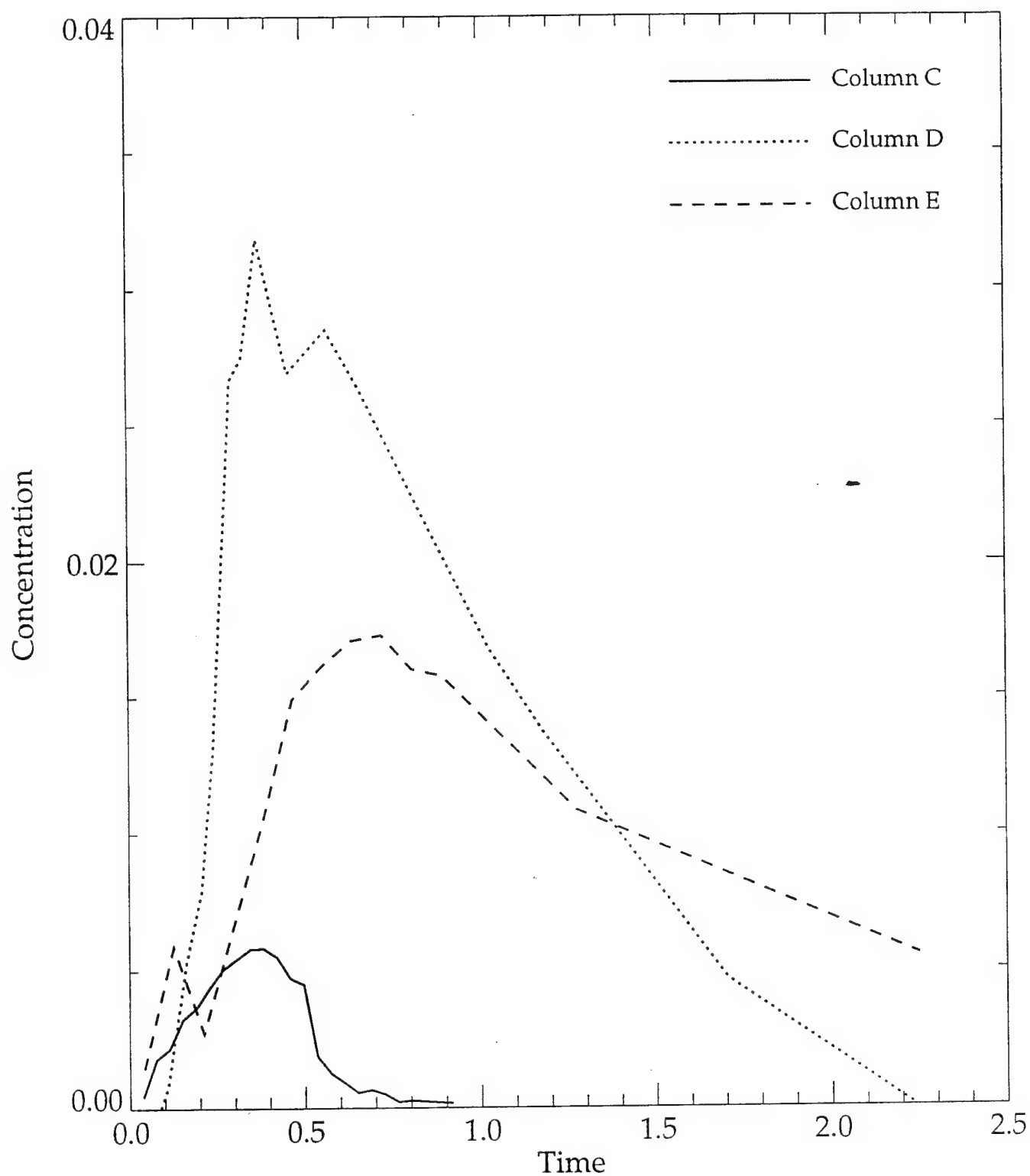
Figure D-16. Bromide concentrations vs. time from Port 16, column tests, C, D, and E.
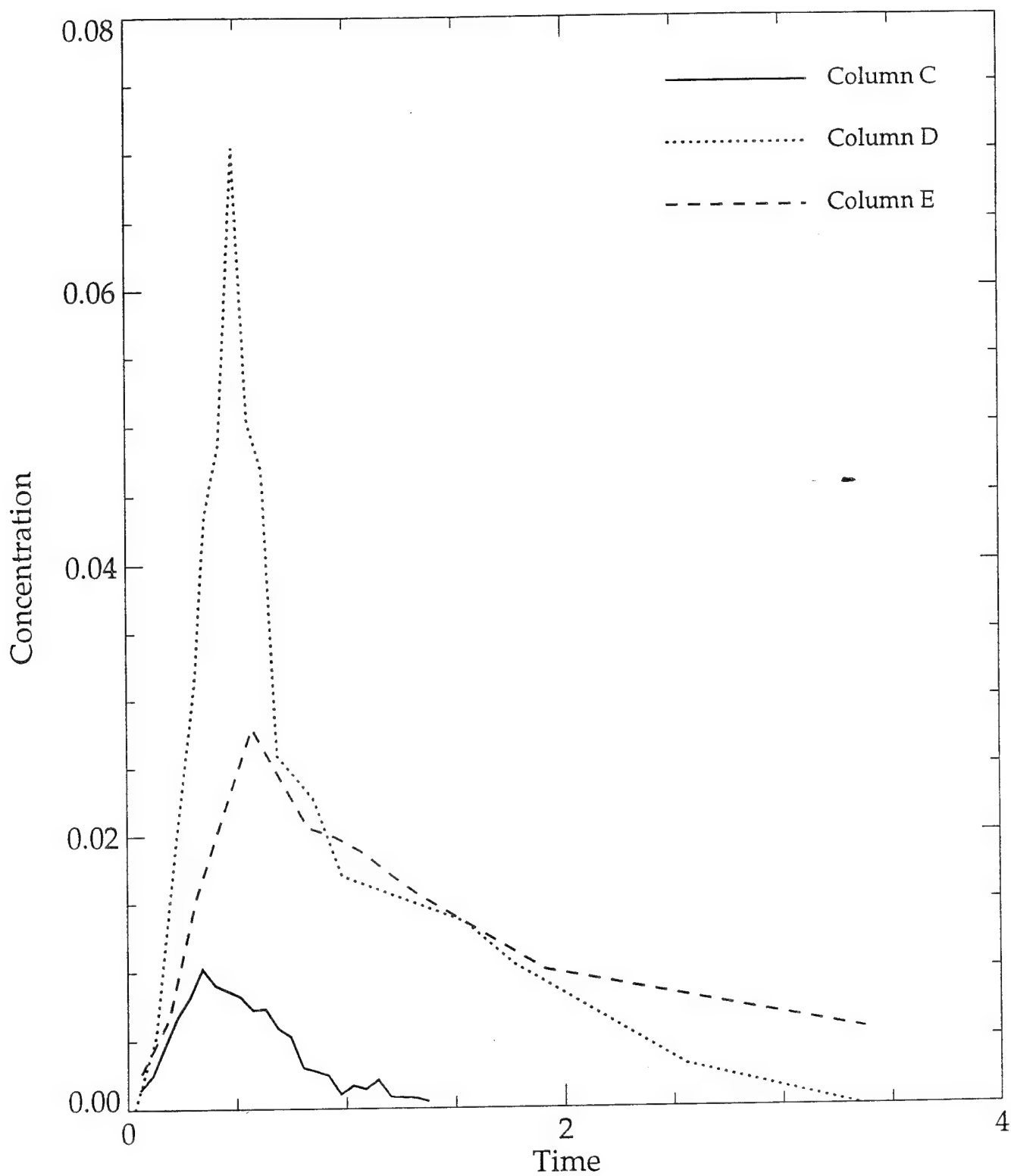
Figure D-17. Bromide concentrations vs. time from Port 17, column tests, C, D, and E.
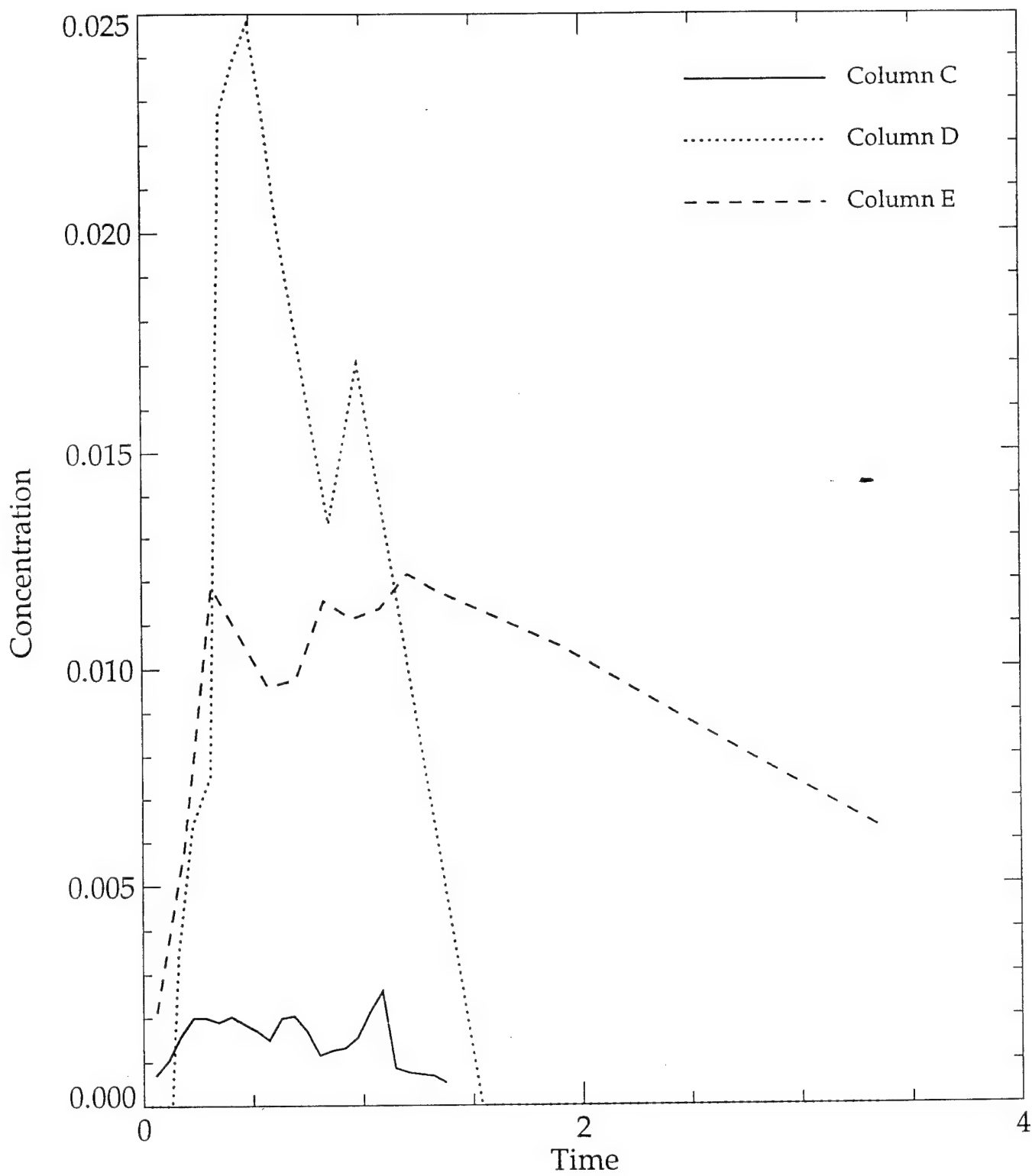
Figure D-18. Bromide concentrations vs. time from Port 18, column tests, C, D, and E.
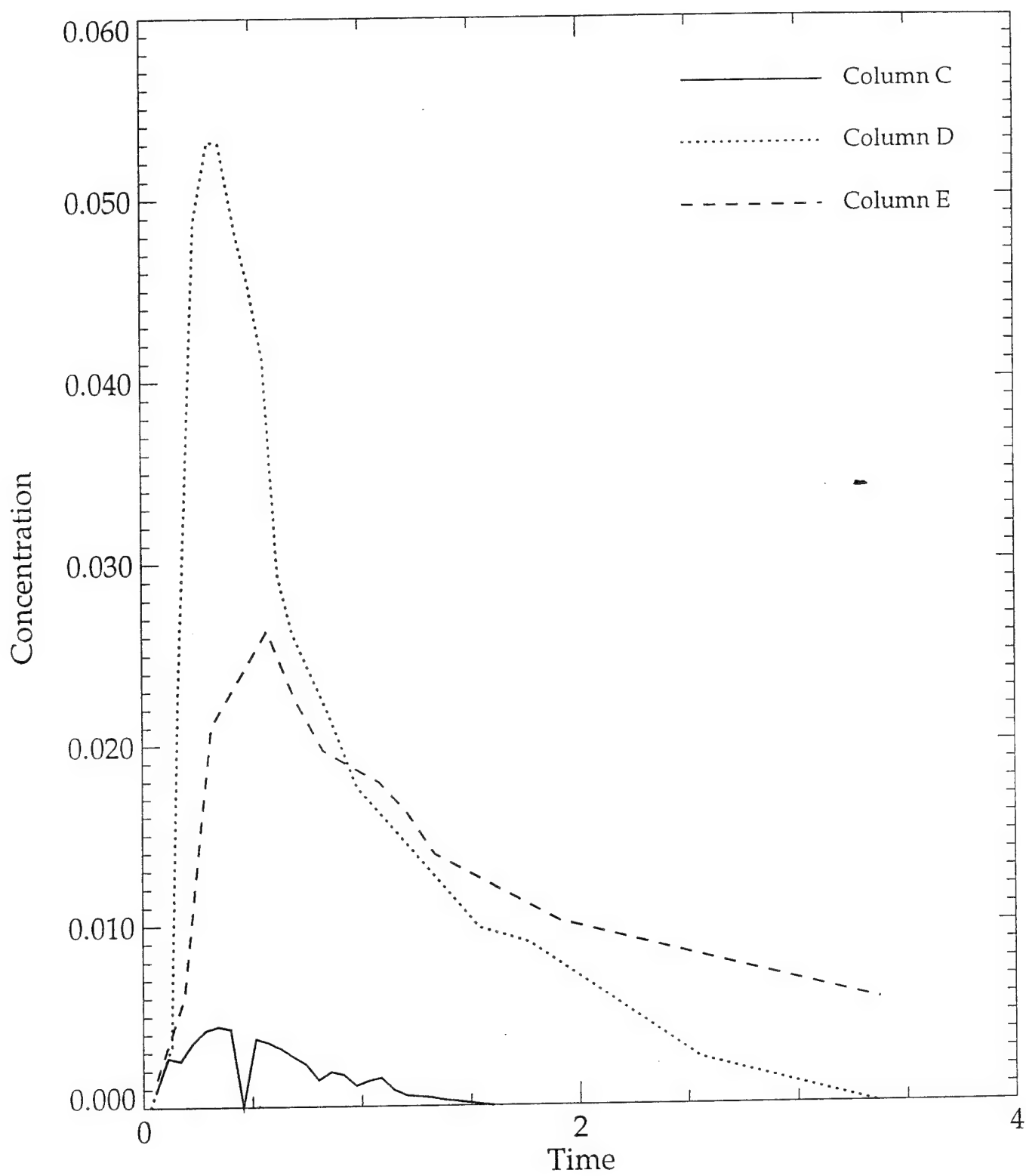
Figure D-19. Bromide concentrations vs. time from Port 19, column tests, C, D, and E.
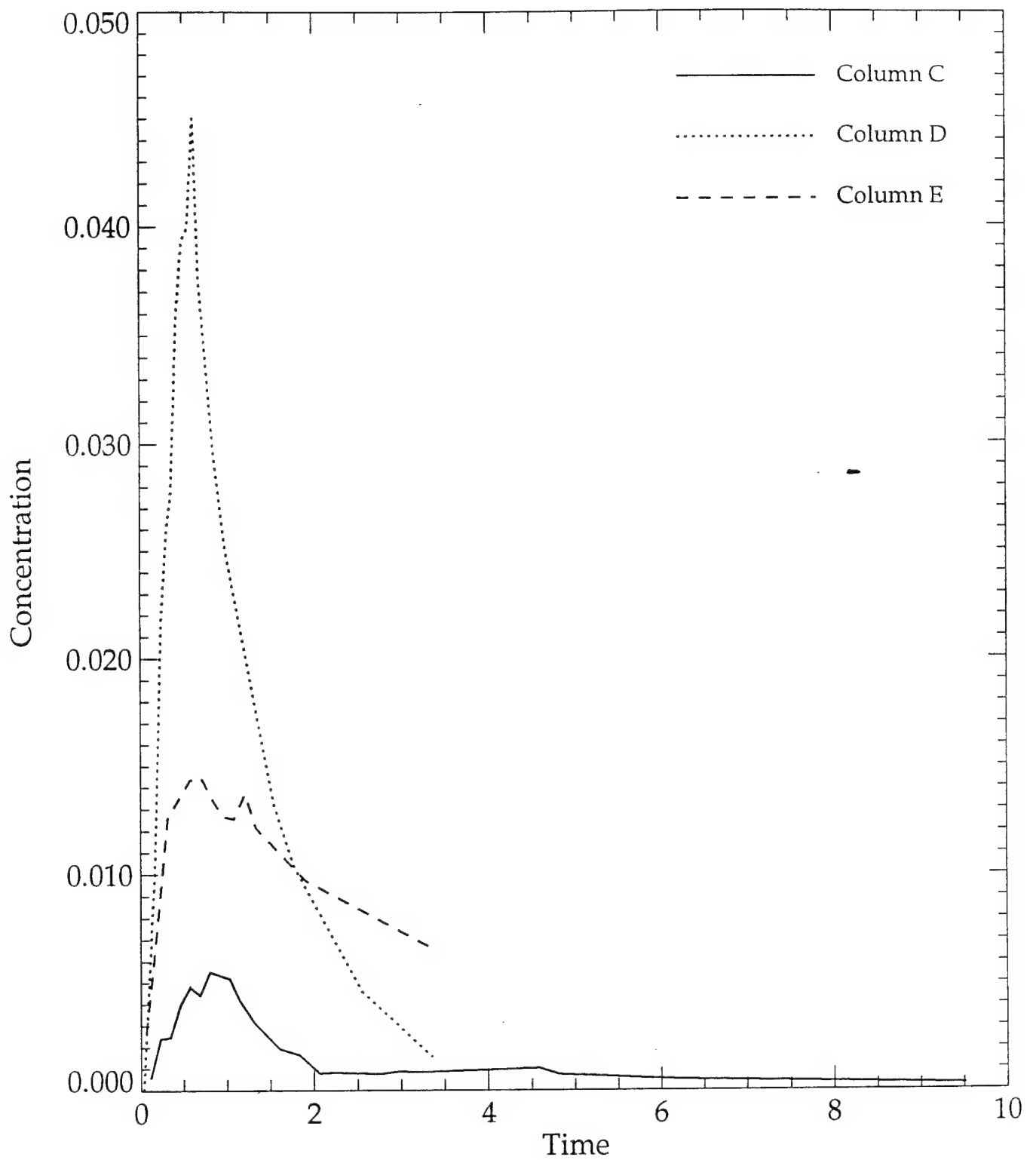
Figure D-20. Bromide concentrations vs. time from Port 20, column tests, C, D, and E.

133
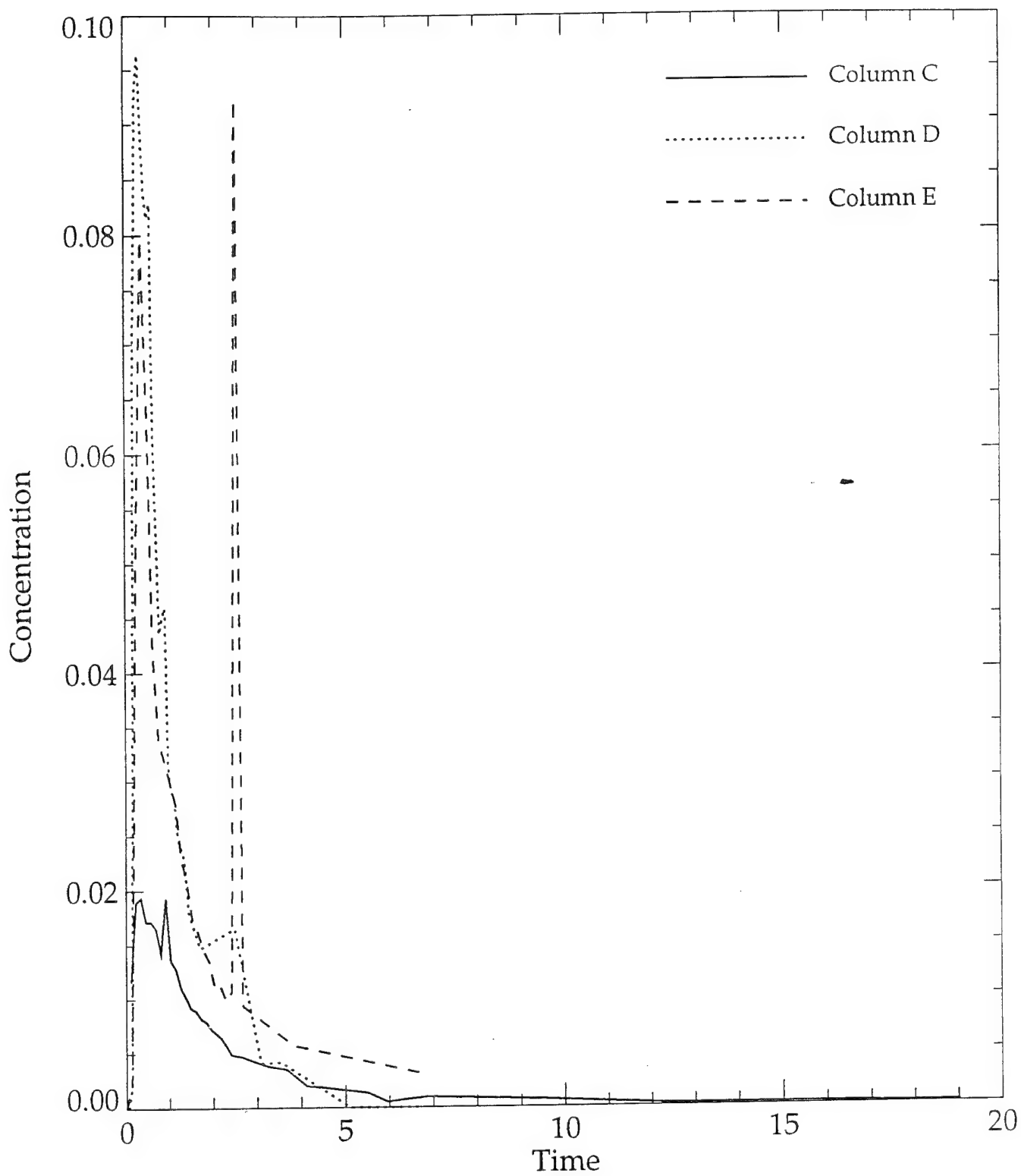
Figure D-21. Bromide concentrations vs. time from Port 21, column tests, C, D, and E.
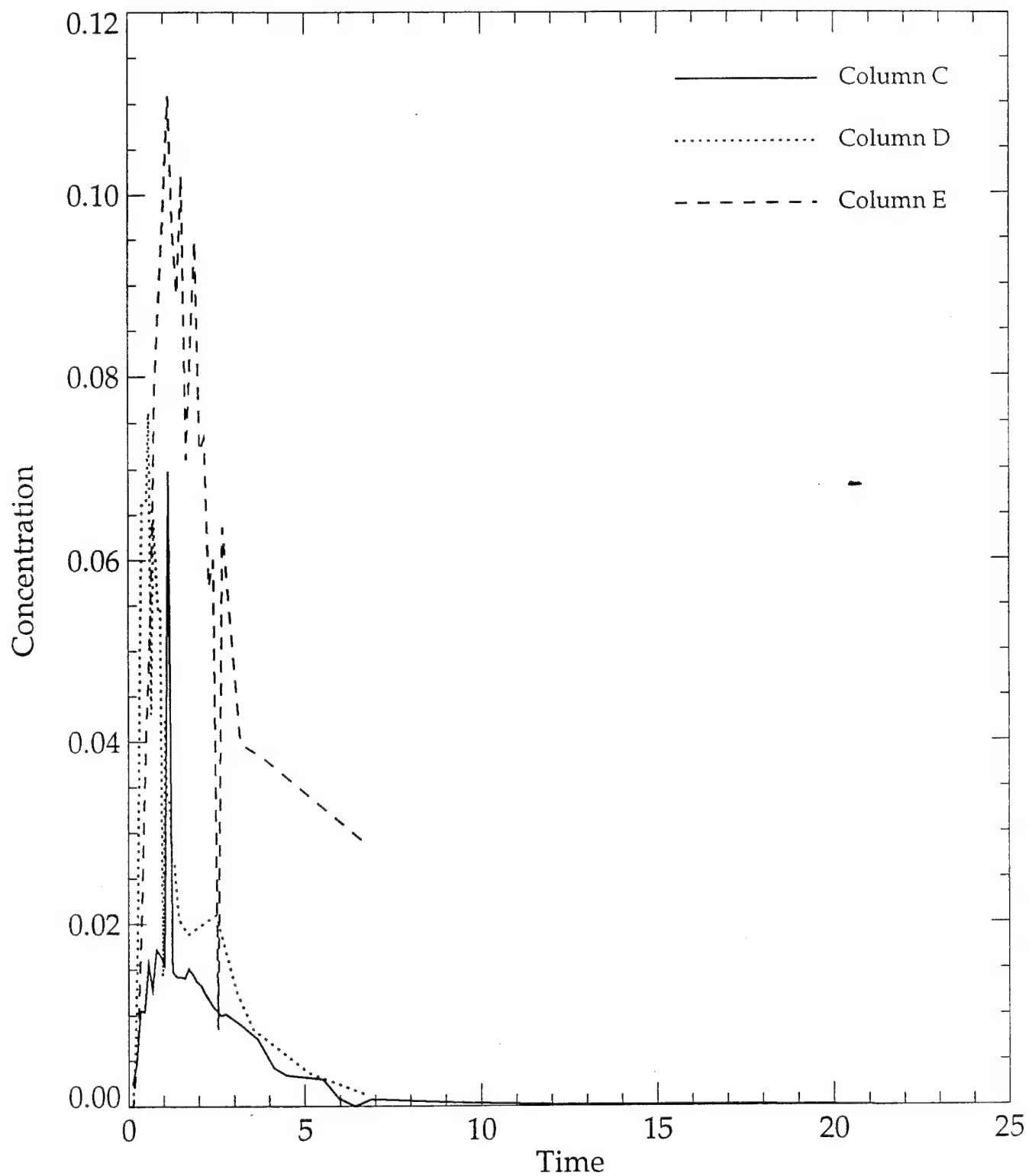
Figure D-22. Bromide concentrations vs. time from Port 22, column tests, C, D, and E.
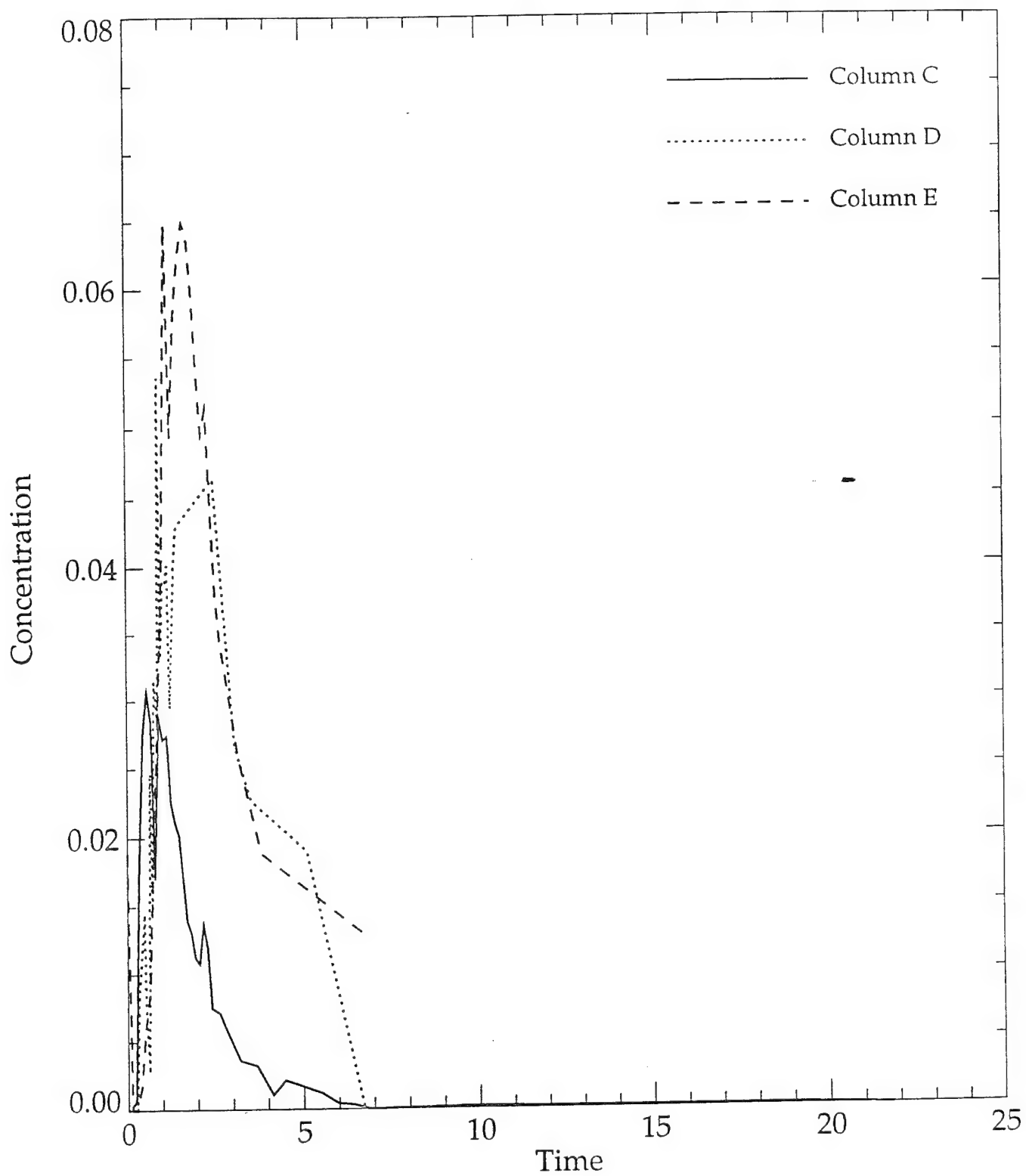
Figure D-23. Bromide concentrations vs. time from Port 23, column tests, C, D, and E.
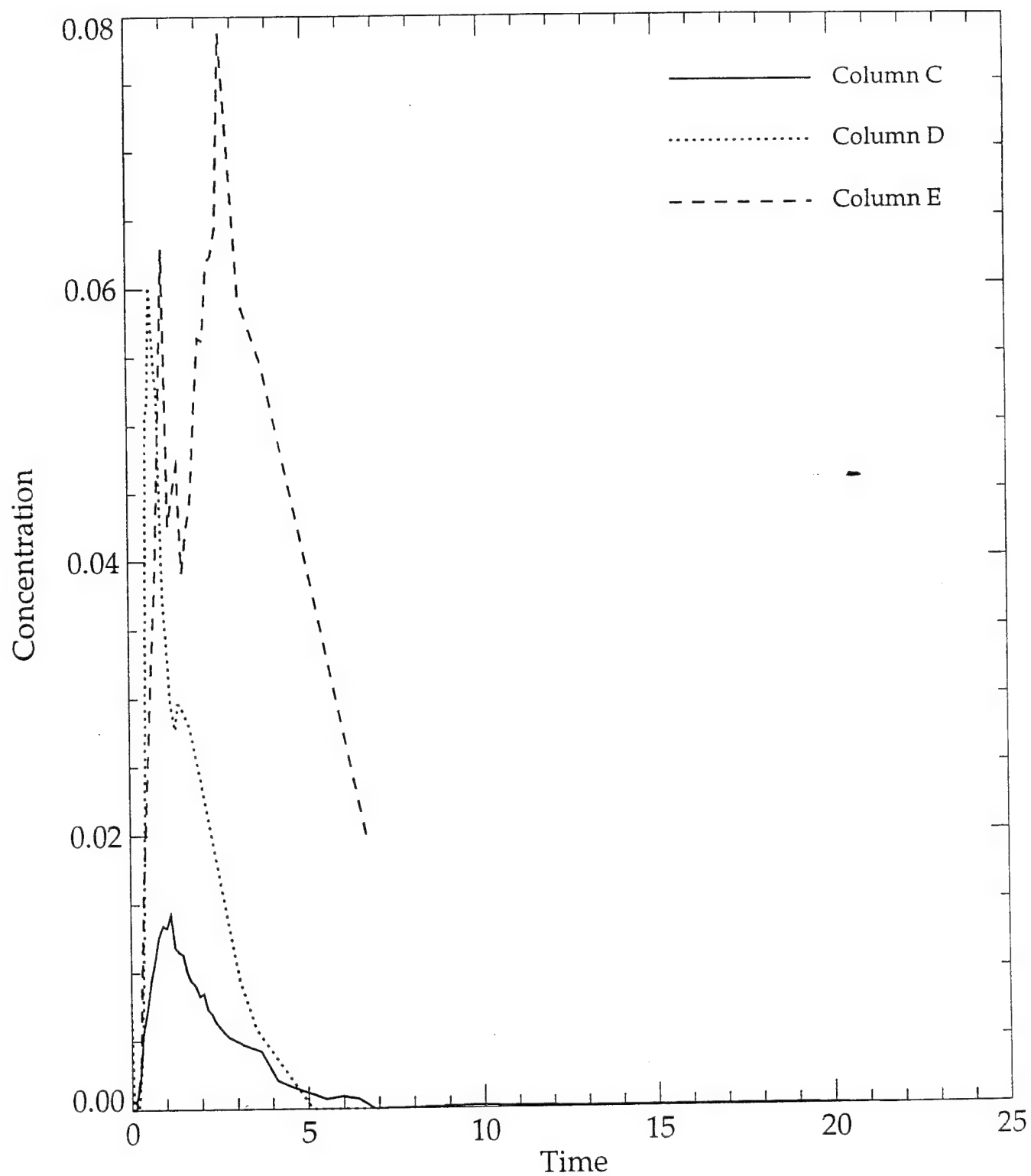
Figure D-24. Bromide concentrations vs. time from Port 24, column tests, C, D, and E.

Figure D-25. Bromide concentrations vs. time from Port 25, column tests C, D,. and E.
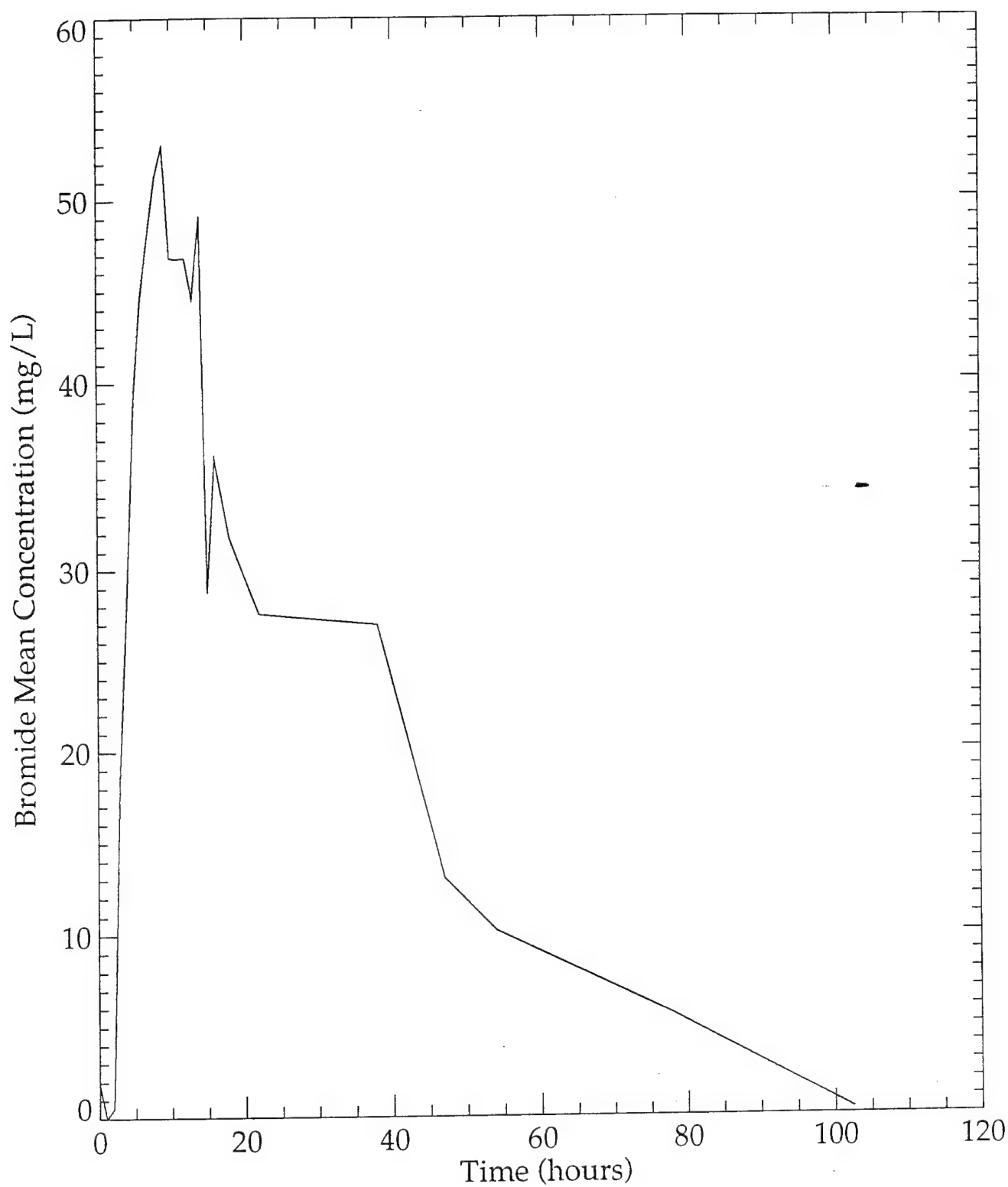
Figure D-26. Mean bromide concentration from ports 1-4 vs. time, column test C.

Figure D-27. Mean bromide concentration from ports 5-8 vs. time, column test C.
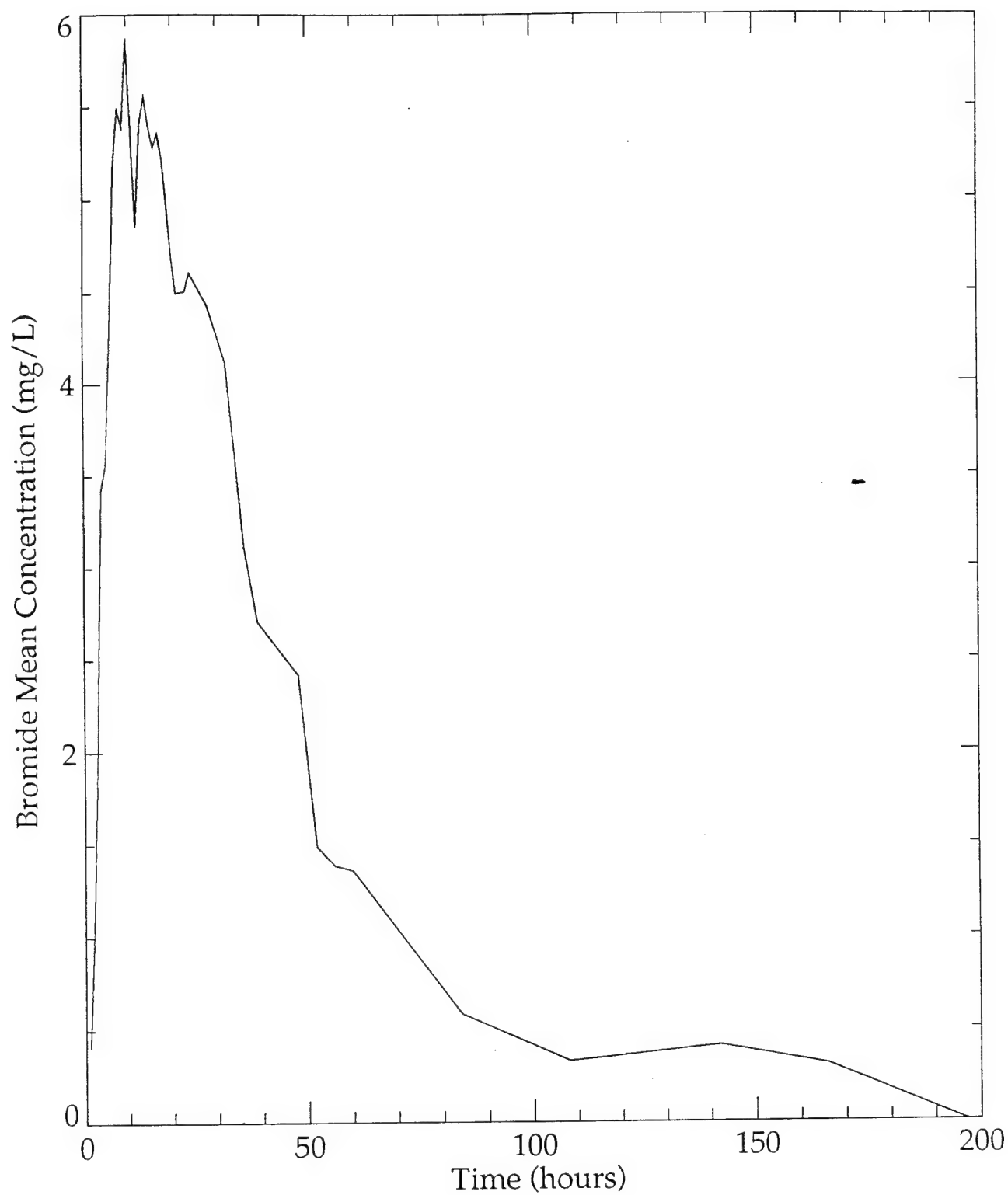
Figure D-28. Mean bromide concentration from ports 9-12 vs. time, column test C.

141
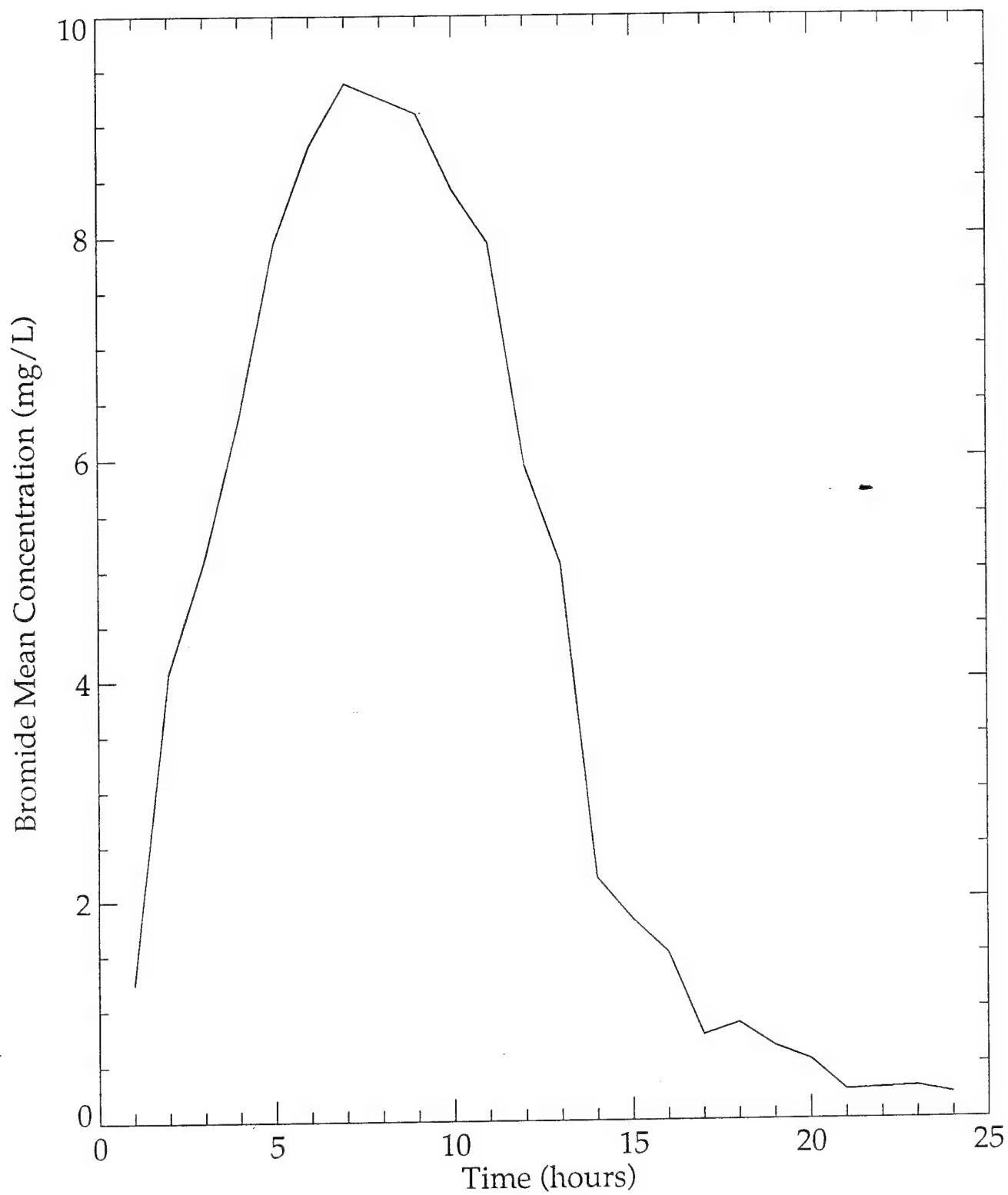
Figure D-29. Mean bromide concentration from ports 13-16 vs. time, column test C.
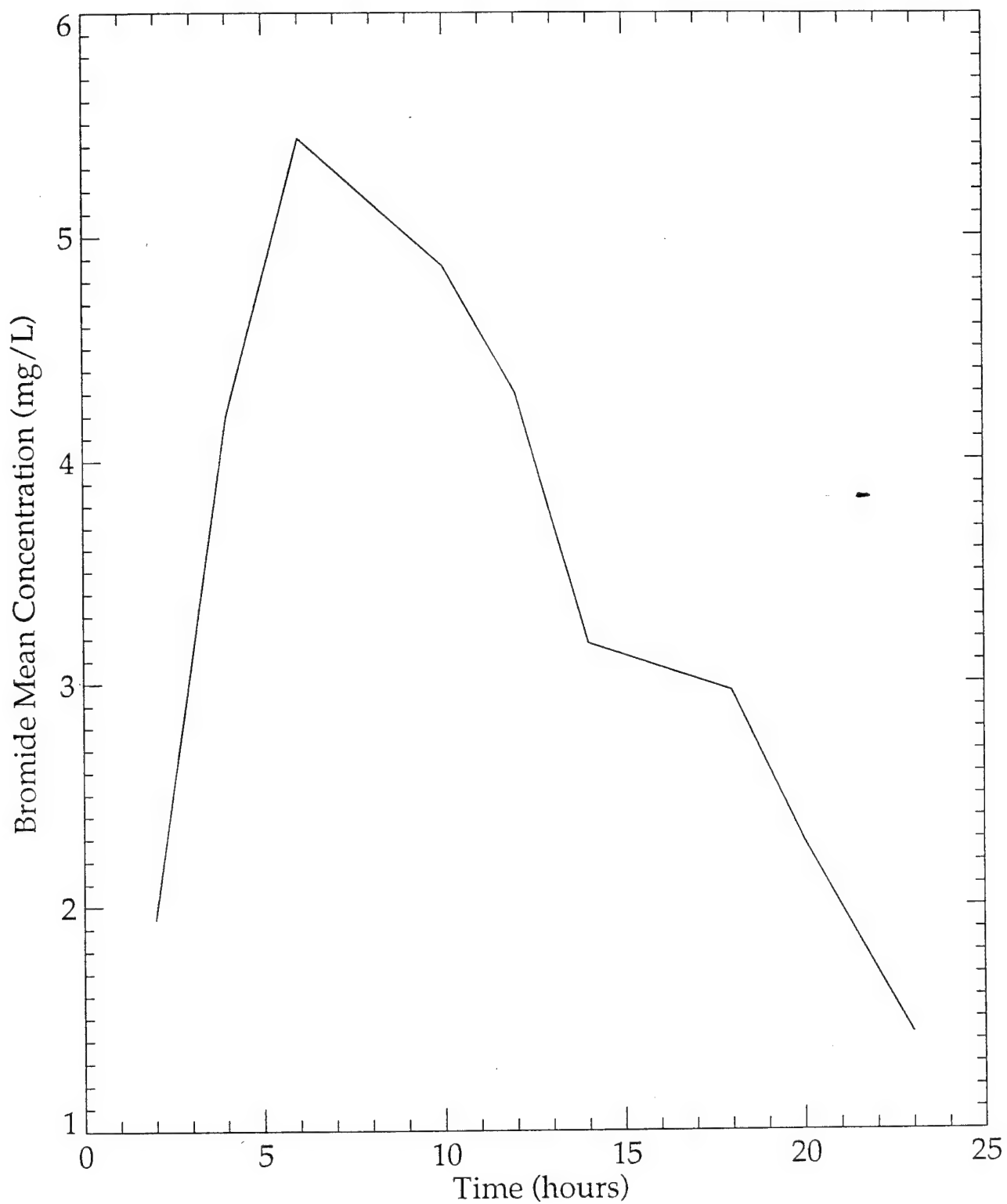
Figure D-30. Mean bromide concentration from ports 17-20 vs. time, column test C.
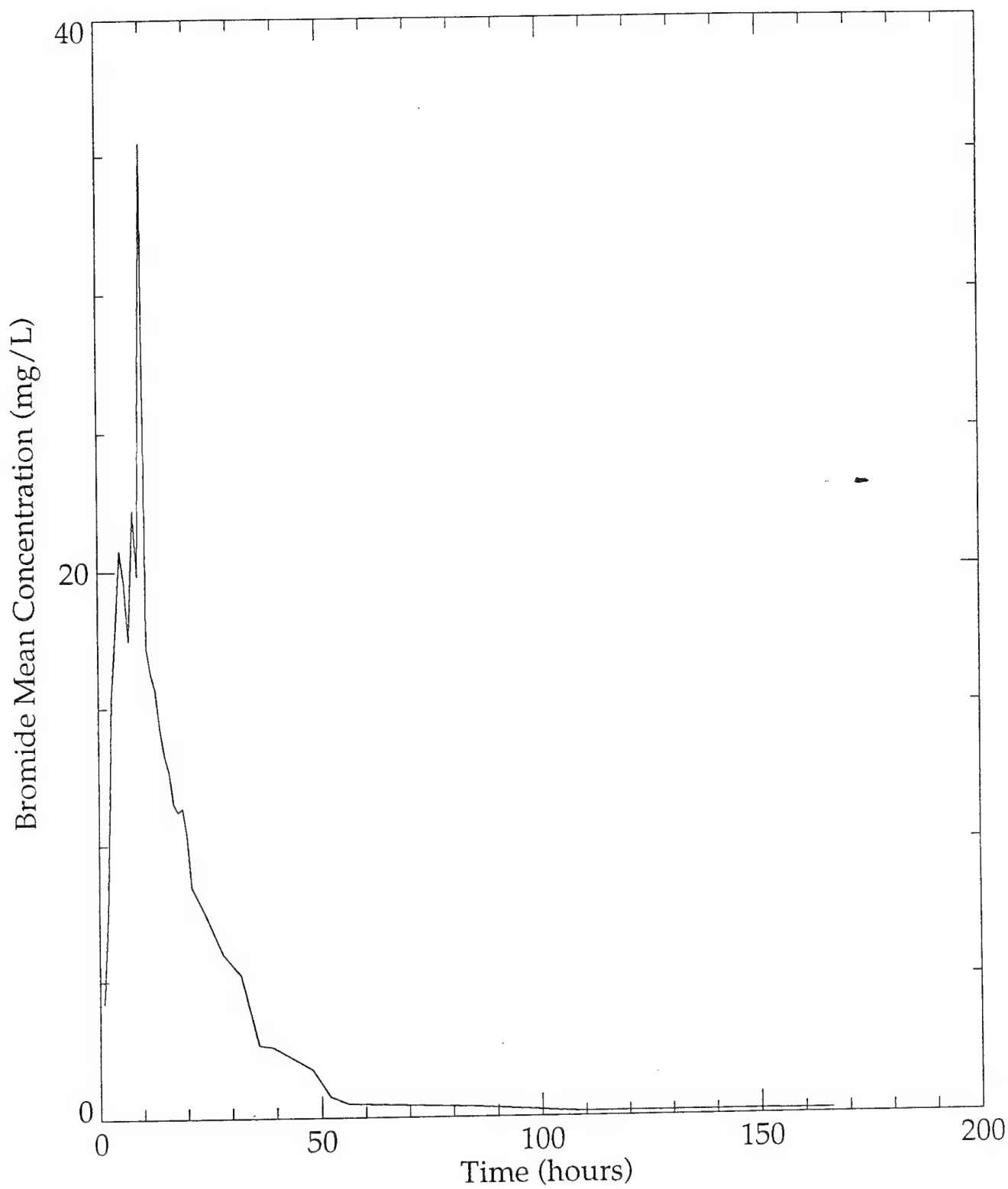
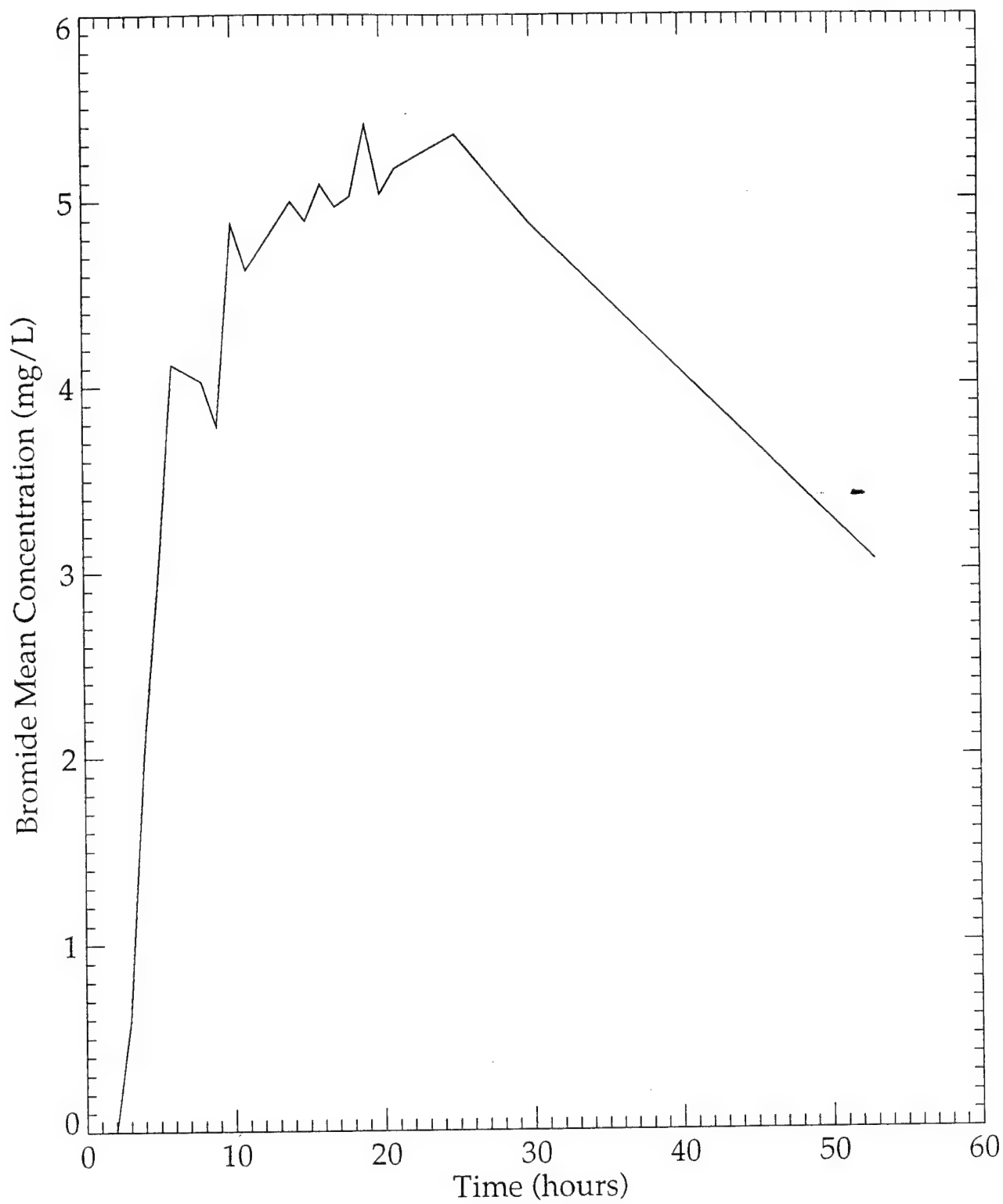Figure D-31. Mean bromide concentration from ports 21-24 vs. time, column test C.
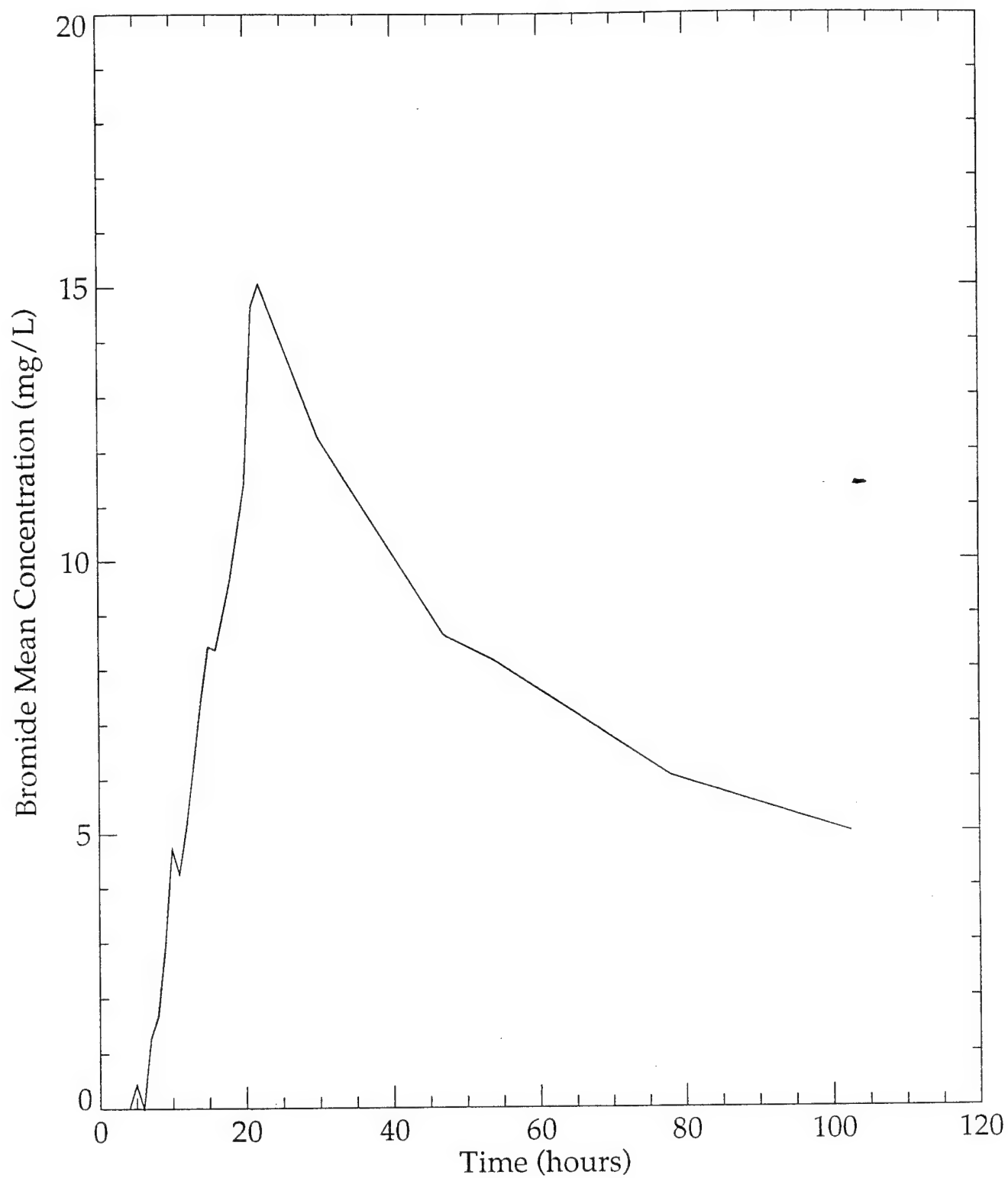
Figure D-32. Mean bromide concentration from ports 1-4 vs. time, column test D.
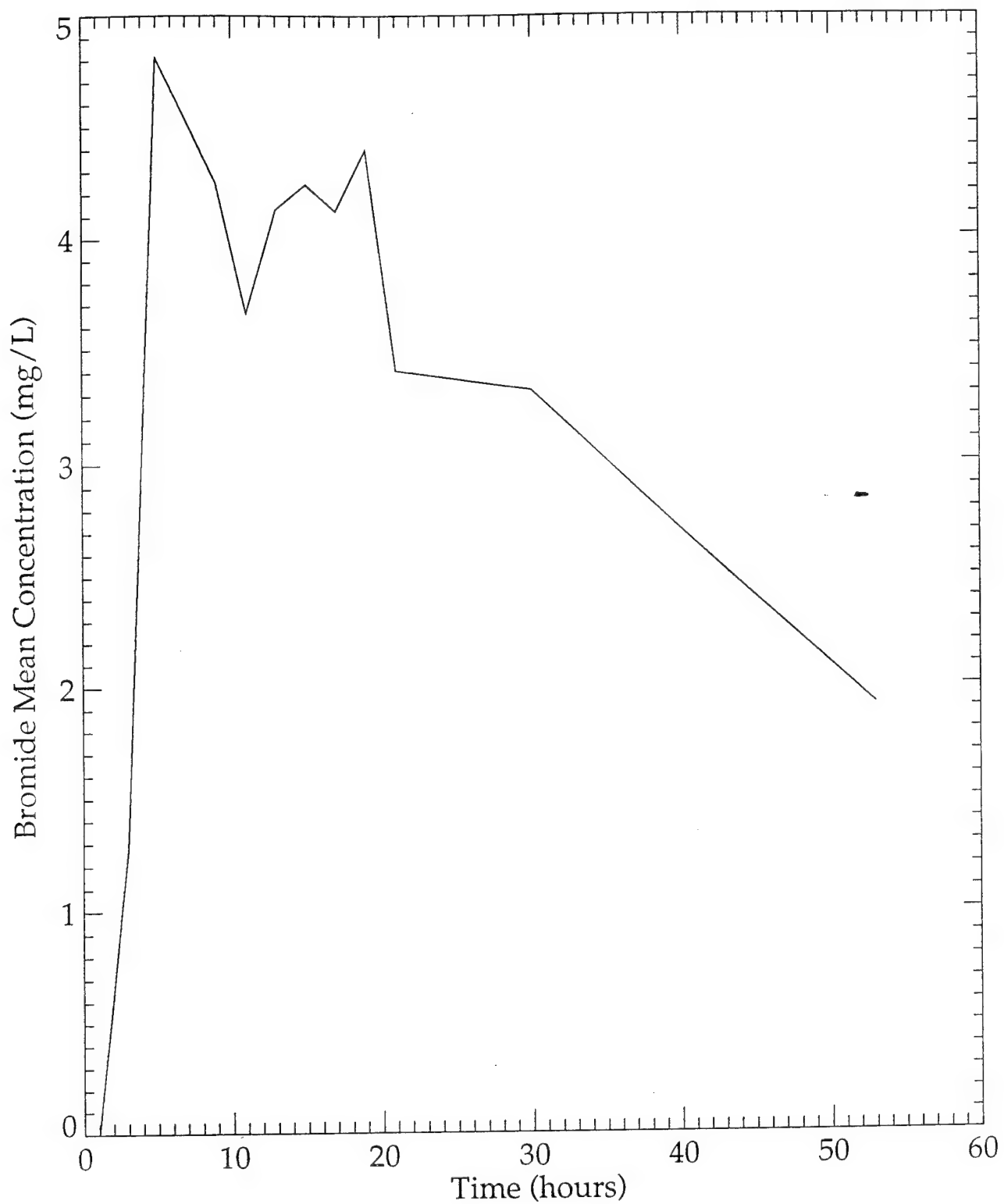
145
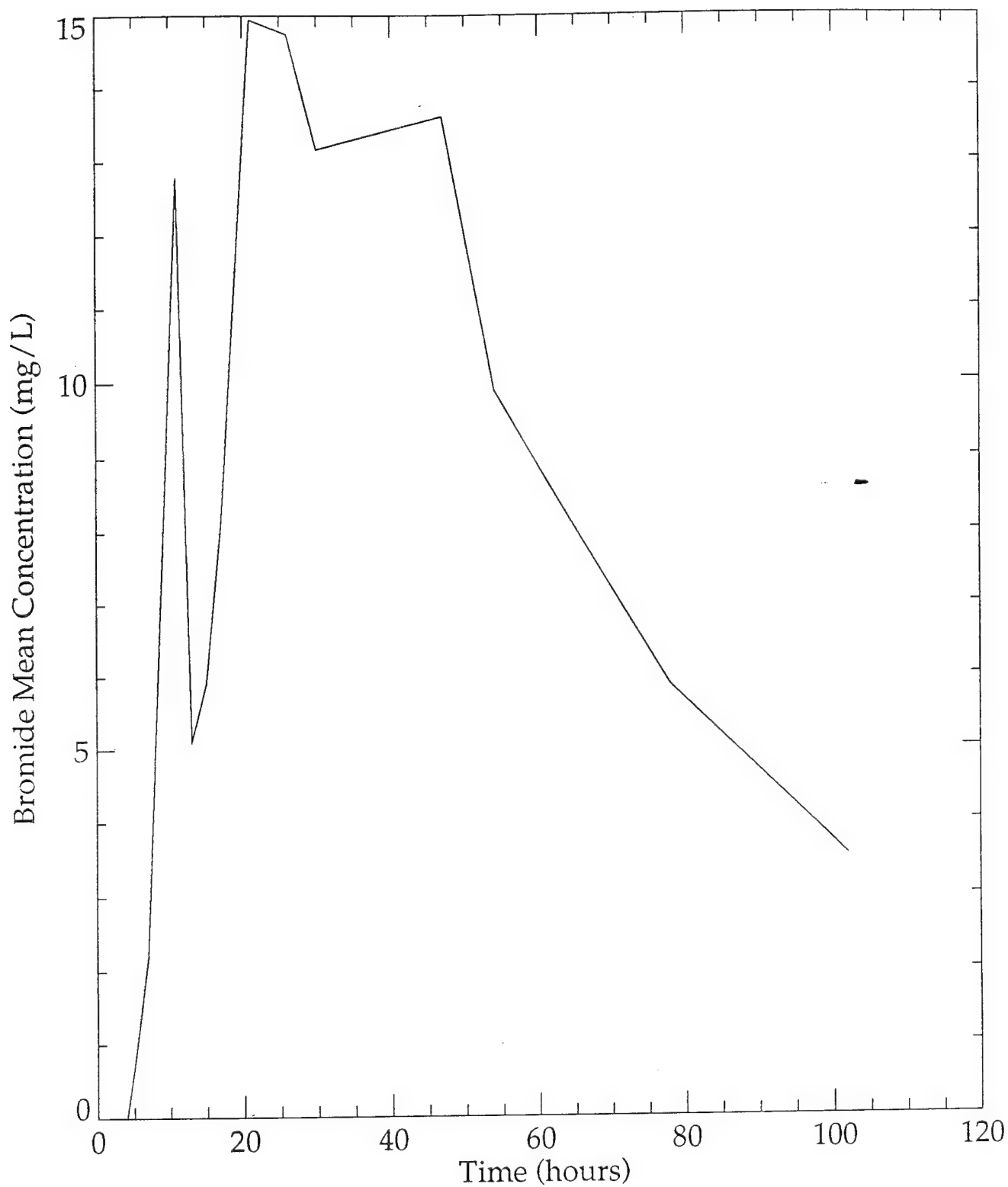
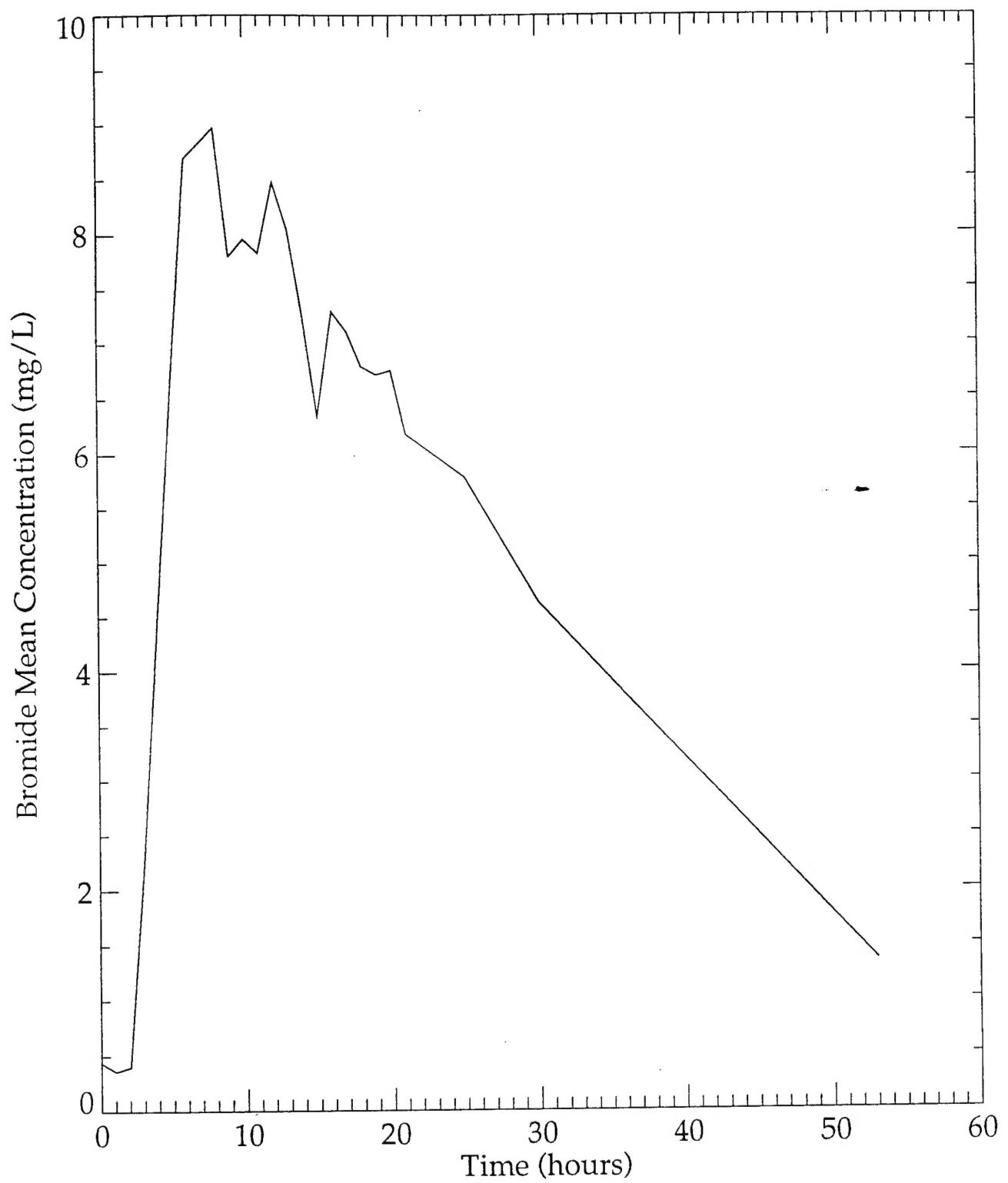Figure D-33. Mean bromide concentration from ports 5-8 vs. time, column test D.
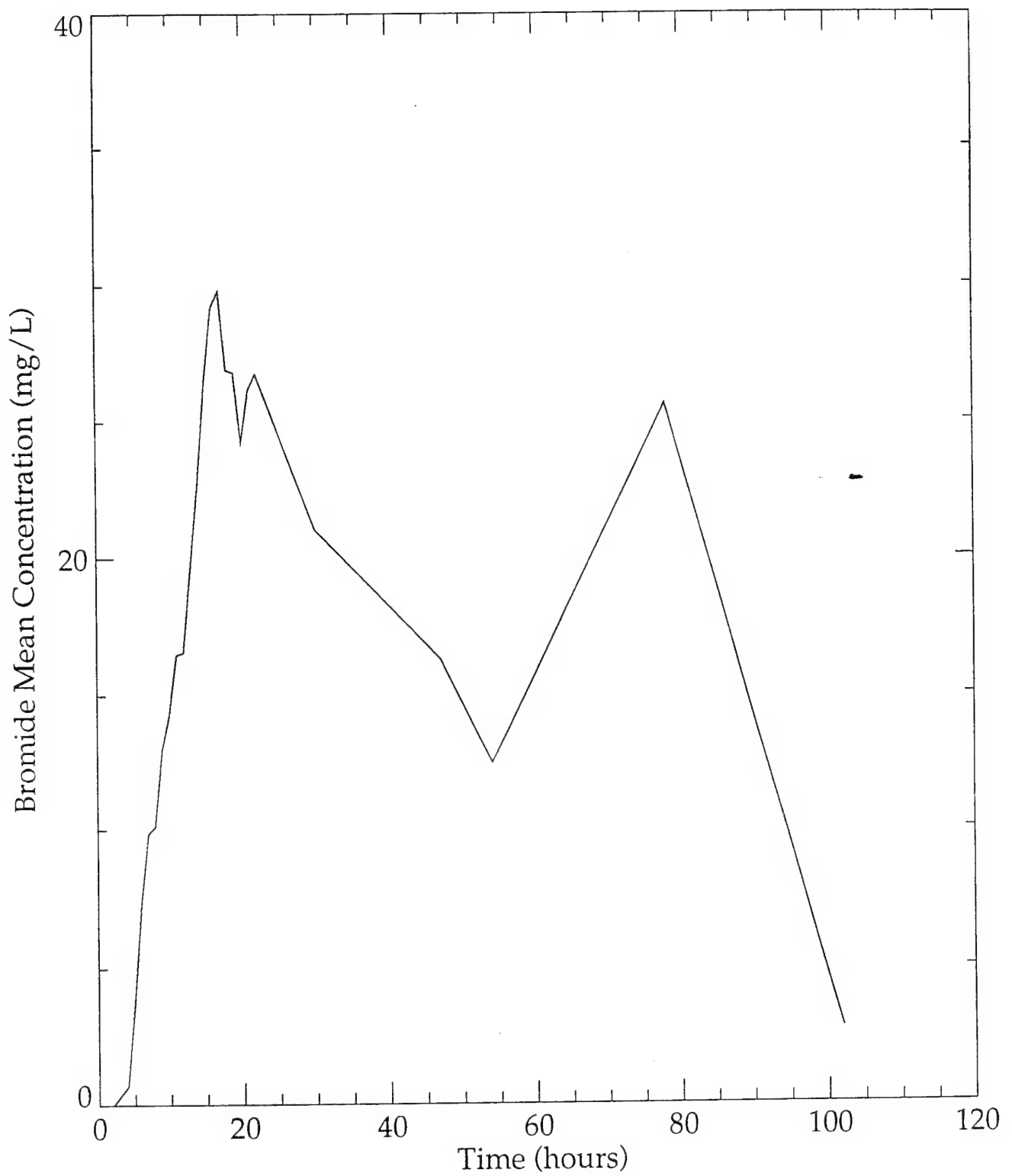
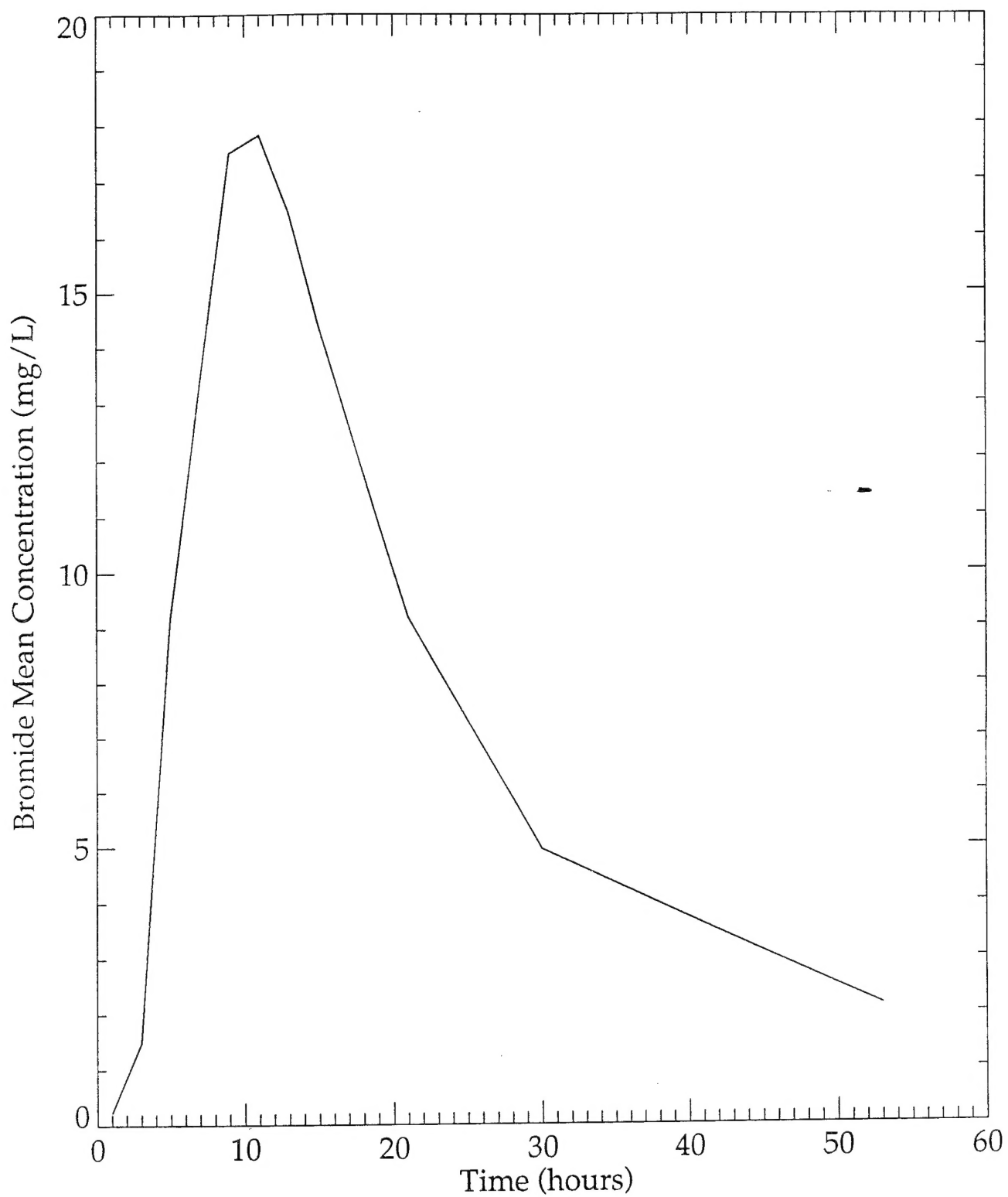Figure D-34. Mean bromide concentration from ports 9-12 vs. time, column test D.
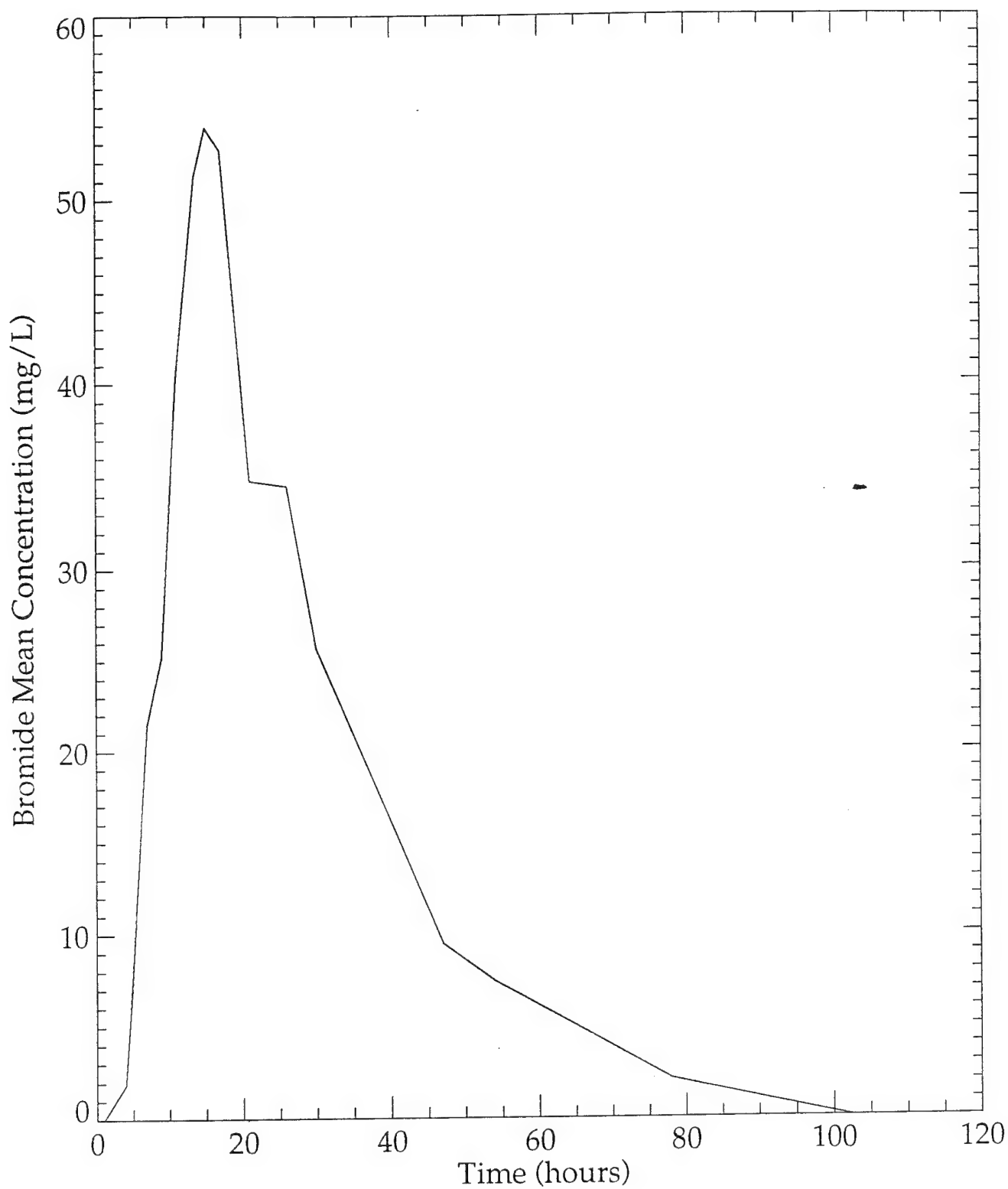
Figure D-35. Mean bromide concentration from ports 13-16 vs. time, column test D.
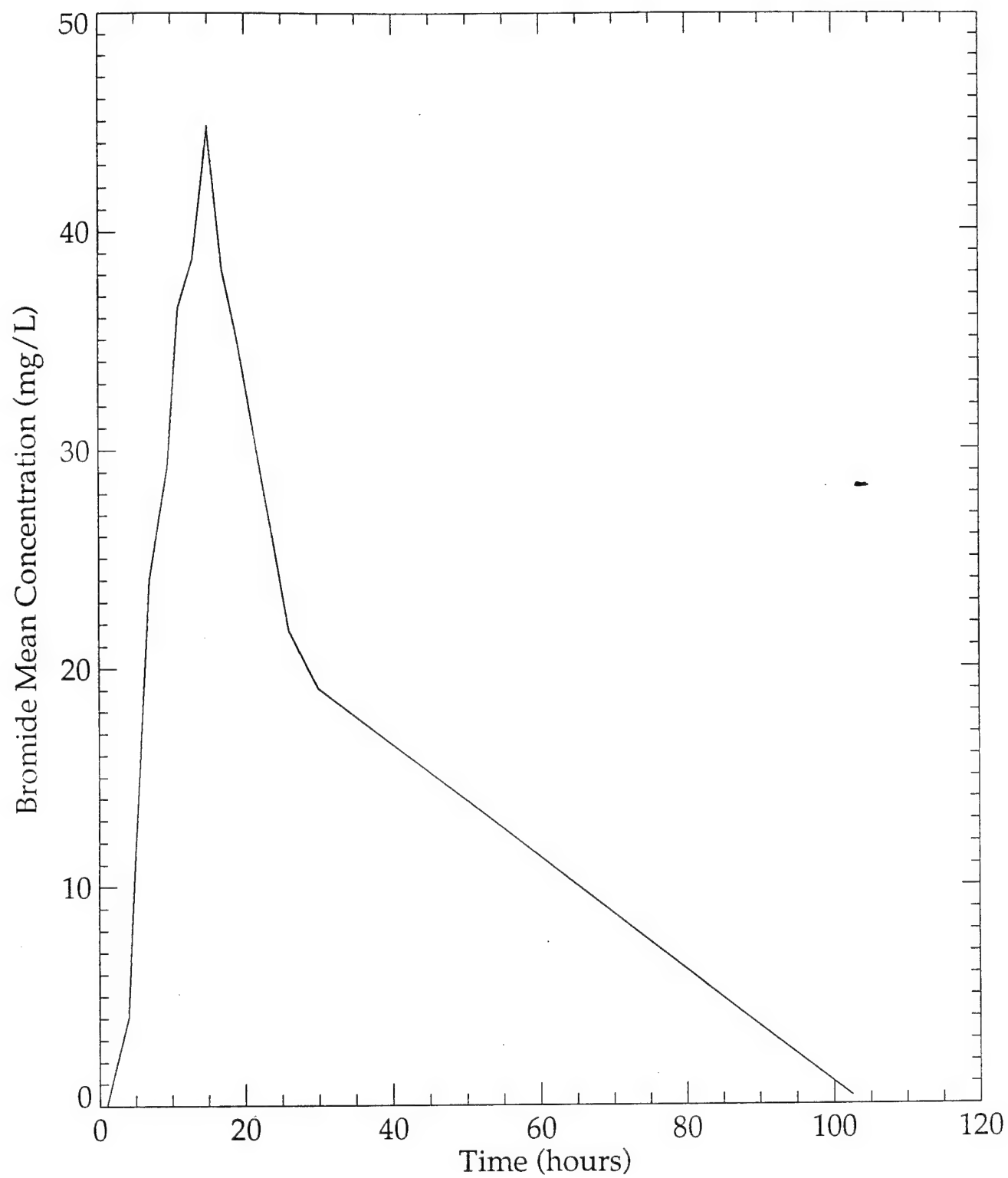
Figure D-36. Mean bromide concentration from ports 17-20 vs. time, column test D.

Figure D-37. Mean bromide concentration from ports 21-24 vs. time, column test D.

Figure D-38. Mean bromide concentration from ports 1-4 vs. time, column test E.

Figure D-39. Mean bromide concentration from ports 5-8 vs. time, column test E.

Figure D-40. Mean bromide concentration from ports 9-12 vs. time, column test E.

Figure D-41. Mean bromide concentration from ports 13-16 vs. time, column test E.
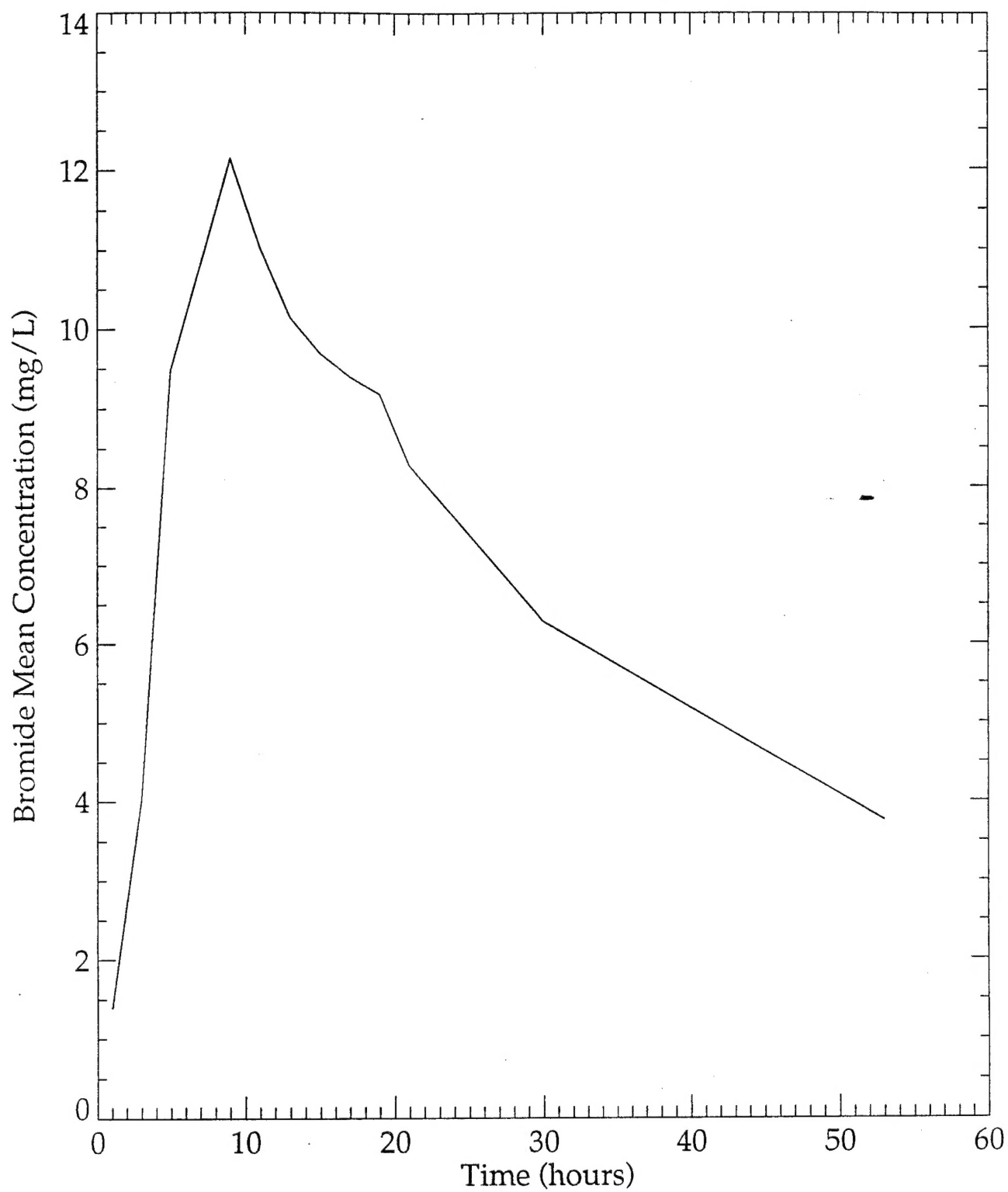
Figure D-42. Mean bromide concentration from ports 17-20 vs. time, column test E.
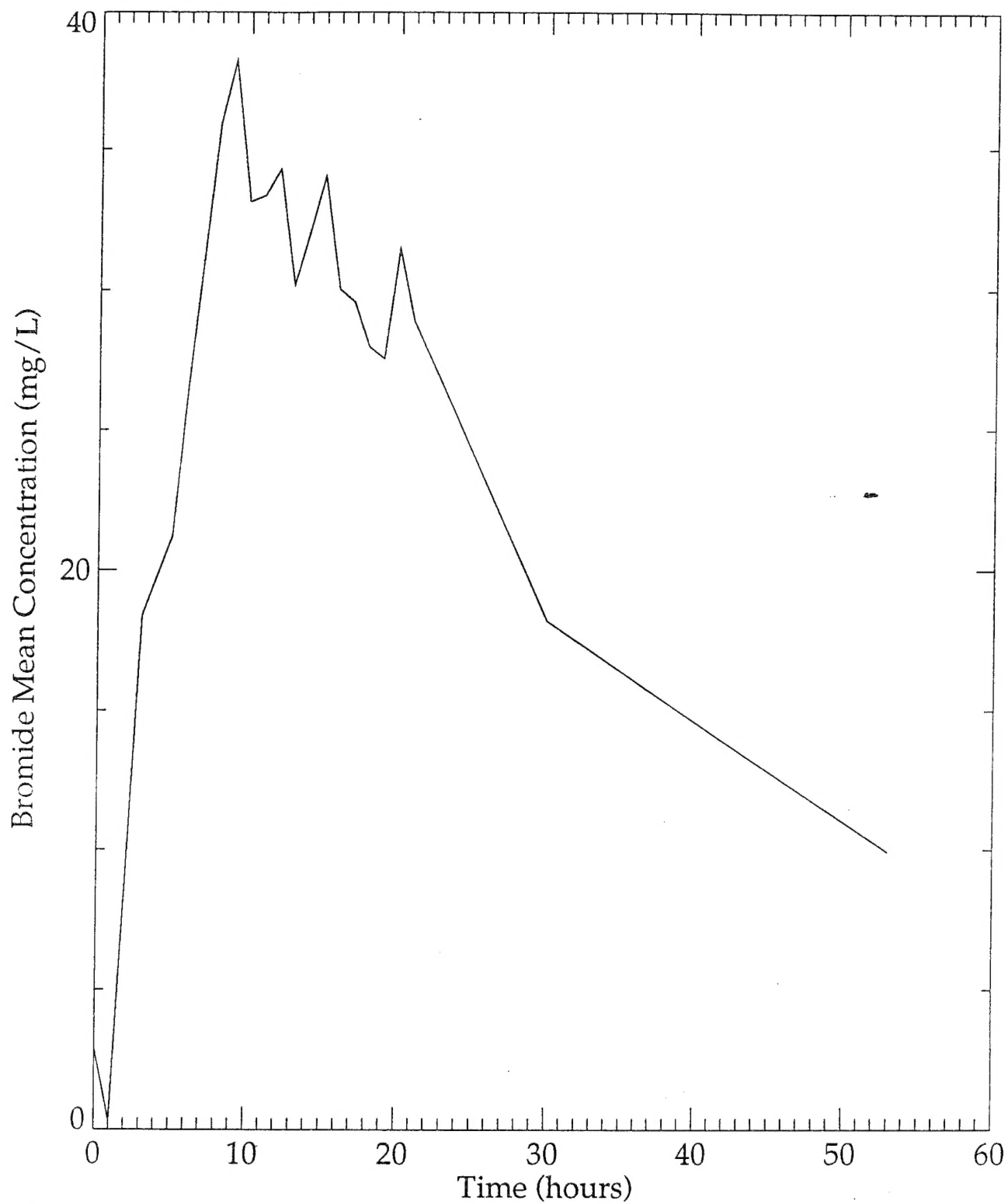
155

Figure D-43. Mean bromide concentration from ports 21-24 vs. time, column test E.